COMPUTATIONAL HARMONIC ANALYSIS ON PLATE-LIKE BASE PANEL OF AIR CONDITIONING OUTDOOR UNIT USING DIRECT METHOD

CHOON WEI FENG

FACULTY OF ENGINEERING
UNIVERSITY OF MALAYA
KUALA LUMPUR

2022

COMPUTATIONAL HARMONIC ANALYSIS ON PLATE-LIKE BASE PANEL OF AIR CONDITIONING OUTDOOR UNIT USING DIRECT METHOD

CHOON WEI FENG

RESEARCH REPORT SUBMITTED IN PARTIAL FULFLMENT OF THE REQUIREMENTS FOR THE DEGREE OF MASTER OF MECHANICAL ENGINEERING

**FACULTY OF ENGINEERING
UNIVERSITY OF MALAYA
KUALA LUMPUR**

2022

UNIVERSITY OF MALAYA

ORIGINAL LITERARY WORK DECLARATION

Name of Candidate: Choon Wei Feng

Matric No: S2016689

Name of Degree: Master of Mechanical Engineering

Title of Project Paper/Research Report/Dissertation/Thesis (“this Work”):

Computational Harmonic Analysis on Plate-Like Base Panel of Air Conditioning Outdoor Unit Using Direct Method

Field of Study: Finite Element Analysis, Vibration

I do solemnly and sincerely declare that:

(1) I am the sole author/writer of this Work;
(2) This Work is original;
(3) Any use of any work in which copyright exists was done by way of fair dealing and for permitted purposes and any excerpt or extract from, or reference to or reproduction of any copyright work has been disclosed expressly and sufficiently and the title of the Work and its authorship have been acknowledged in this Work;
(4) I do not have any actual knowledge nor do I ought reasonably to know that the making of this work constitutes an infringement of any copyright work;
(5) I hereby assign all and every rights in the copyright to this Work to the University of Malaya (“UM”), who henceforth shall be owner of the copyright in this Work and that any reproduction or use in any form or by any means whatsoever is prohibited without the written consent of UM having been first had and obtained;
(6) I am fully aware that if in the course of making this Work I have infringed any copyright whether intentionally or otherwise, I may be subject to legal action or any other action as may be determined by UM.

Candidate’s Signature Date:

Subscribed and solemnly declared before,

Witness’s Signature Date: 16/7/2022

Name: Ir. Dr. ALEX ONG ZHI CHAO

Designation: Assosiate Professor
Department of Mechanical Engineering
Faculty of Engineering
Universiti Malaya
50603 Kuala Lumpur

COMPUTATIONAL HARMONIC ANALYSIS ON PLATE-LIKE BASE PANEL OF AIR CONDITIONING OUTDOOR UNIT USING DIRECT METHOD

ABSTRACT

Harmonic response analysis is a useful tool to check for the structural response (acceleration) when subjected to constant harmonic excitation. By extracting the response of the desired spectrum from the structure by using finite element method, the potential resonance or peaks with high vibration can be observed. In HVAC industries, the source of vibration are from unit transportation, fan motor vibration and compressor vibration, engineers will have to design and test the components of the unit to ensure the component can withstand the vibration. This study focusses on the effect of transportation vibration against the base panel of an air-conditioning outdoor unit. To ensure all component can withstand road and ship transportation vibration, Daikin utilizes hydraulic shaker with a prefix harmonic vibration profile to represent actual transportation condition. FEA can be used during design stage of component to check the vibration integrity. Commercial FEA solver is usually expensive, with its licensing cost. The alternatives would be using open-source FEA solver such as Code_Aster®. Usage on Code_Aster® will lead to extensive saving in licensing cost. To ensure the method of an open-source solver is valid, simulation results from Code_Aster® will be compared against commercial solver (Altair Optistruct®) currently use in Daikin. Modal and harmonic response analysis will be constructed on both solvers, with similar boundary condition and properties and proper keyword. To further enhance the validity, two experiment will be done to verify the results from the simulations. EMA are used to check the modal parameters such as natural frequency and mode shapes of the base panel against the result from FEA. Shaker with harmonic excitation from 5Hz-100Hz will be used to excite the base panel, accelerometers will be used to collect the response such as acceleration from different location. Response from simulation and experiment can be use as comparison and verification. After the validation process through experiment, Code_Aster® modeling technique can be integrated into design workflow of DRDM with confidence. When comparing Code_Aster® with Altair Optistruct®, the frequency difference are only within 1.89% and the MAC plot in all 8 modes are near to 1. This shows that the settings used are correct in Code_Aster®. The results validation for normal mode in Code_Aster® with EMAshows that mode 1, 2, 3, 5 and 7 are present and comparable, mode 4 and mode 6 are missing from EMA. This might be due to localized mode which is not captured by accelerometer. The maximum error on frequency against EMA is only 12.6%. Experiment harmonic response analysis can capture the peaks of resonance and the shapes are comparable to FEA although the magnitude in FEA is higher. Improvement can be made in FEA by using element with actual material data in weld and screw area to reduceoverall stiffness. More accelerometers can be used to measure the response on the panel to capture localized mode in multiple DOF, actual damping coefficient from EMA can beinputted into FEA to generate an accurate response.

Keywords: Vibration FEA, Code_Aster®, Open-source, EMA, Harmonic response

ANALISIS HARMONIK KOMPUTASI PADA PANEL ASAS SEPERTI PLAT UNIT LUAR PENYAMAN DINGIN MENGGUNAKAN KAEDAH TERUS

ABSTRAK

Analisis tindak balas harmonik ialah alat yang berguna untuk memeriksa tindak balas struktur (pecutan) apabila tertakluk kepada pengujaan harmonik yang berterusan. Dengan mengekstrak tindak balas spektrum yang dikehendaki daripada struktur dengan menggunakan kaedah unsur terhingga, potensi resonans atau puncak dengan getaran tinggi boleh diperhatikan. Dalam industri HVAC, sumber getaran adalah daripada pengangkutan unit, getaran motor kipas dan getaran pemampat, jurutera perlu mereka bentuk dan menguji komponen unit untuk memastikan komponen itu boleh menahan getaran. Kajian ini memberi tumpuan kepada kesan getaran pengangkutan terhadap panel asas unit luar penghawa dingin. Untuk memastikan semua komponen boleh menahan getaran pengangkutan jalan dan kapal, Daikin menggunakan penggoncang hidraulik dengan profil getaran harmonik awalan untuk mewakili keadaan pengangkutan sebenar. FEA boleh digunakan semasa peringkat reka bentuk komponen untuk memeriksa integriti getaran. Penyelesai FEA komersial biasanya mahal, dengan kos pelesenannya. Alternatifnya akan menggunakan penyelesai FEA sumber terbuka seperti Code_Aster®. Penggunaan pada Code_Aster® akan membawa kepada penjimatan yang meluas dalam kospelesenan. Untuk memastikan kaedah penyelesai sumber terbuka adalah sah, hasil simulasi daripada Code_Aster® akan dibandingkan dengan penyelesai komersial (Altair Optistruct®) yang sedang digunakan dalam Daikin. Analisis tindak balas modal dan harmonik akan dibina pada kedua-dua penyelesai, dengan keadaan dan sifat sempadan yang serupa dan kata kunci yang betul. Untuk meningkatkan lagi kesahan, dua eksperimen akan dilakukan untuk mengesahkan keputusan daripada simulasi. EMA digunakan untuk menyemak parameter modal seperti frekuensi semula jadi dan bentuk mod panel asas terhadap hasil daripada FEA. Shaker dengan pengujaan harmonik dari

5Hz-100Hz akan digunakan untuk menguja panel asas, pecutan akan digunakan untuk mengumpul tindak balas seperti pecutan dari lokasi yang berbeza. Maklum balas daripada simulasi dan eksperimen boleh digunakan sebagai perbandingan dan pengesahan. Selepas proses pengesahan melalui eksperimen, teknik pemodelan Code_Aster® boleh disepadukan ke dalam aliran kerja reka bentuk DRDM dengan yakin. Apabila membandingkan Code_Aster® dengan Altair Optistruct®, perbezaan frekuensi hanya dalam 1.89% dan plot MAC dalam semua 8 mod adalah hampir kepada 1. Ini menunjukkan bahawa tetapan yang digunakan adalah betul dalam Code_Aster®. Pengesahan keputusan untuk mod biasa dalam Code_Aster® dengan EMA menunjukkan bahawa mod 1, 2, 3, 5 dan 7 hadir dan setanding, mod 4 dan mod 6 tiada daripada EMA. Ini mungkin disebabkan olehmod setempat yang tidak ditangkap oleh pecutan. Ralat maksimum pada kekerapan terhadap EMA hanya 12.6%. Analisis tindak balas harmonik eksperimen boleh menangkap puncak resonans dan bentuknya setanding dengan FEA walaupun magnitud dalam FEA lebih tinggi. Penambahbaikan boleh dibuat dalam FEA dengan menggunakanelemen dengan data bahan sebenar dalam kawasan kimpalan dan skru untukmengurangkan kekakuan keseluruhan. Lebih banyak pecutan boleh digunakan untuk mengukur tindak balas pada panel untuk menangkap mod setempat dalam berbilang DOF,pekali redaman sebenar daripada EMA boleh dimasukkan ke dalam FEA untuk menjanatindak balas yang tepat.

Kata kunci: Getaran FEA, Code_Aster®, Sumber terbuka, EMA, Respons harmonik

ACKNOWLEDGEMENTS

Firstly, I would like to take this opportunity to acknowledge and send my sincere gratitude toward my supervisor, Assoc. Prof. Ir. Dr. Alex Ong Zhi Chao, which provided my endless support and guidance on the field of vibration and FEA. Dr. Ong has given a lot of suggestion and improvement idea whether it's on the area of experimental vibration and FEA or on the feedback and correction toward the final report writing. Throughout the project along with his expertise and knowledge in the field of industrial vibration and FEA, a lot of the technical problem can be solved rather easily. The project is made possible with his guidance.

Secondly I would like to express my appreciation towards the colleague(s) in Daikin Research & Development Malaysia Simulation section (2022), especially NVH team Mr. Syazwan, Mr. Shamsul, Dr. Azam and Senior Manager Mr. Low Lee Leong, for their visionary insights and providing valuable data on the company's product noise and vibration analysis for the usage of this project.

Thirdly, I would like to thanks to my course mate who provided me a huge source of motivation as we study, work, and complete the research project module together. Without their encouragement it will be lot harder to complete the project within given timeframe.

Finally, I would like to give my special and utmost gratitude towards my family members, close friends, and my hiking mates (The HikeMates). Thanks to them for the continuous love, support and understanding while I am undertaking my research and completing my report.

Each one of you has made this research project possible.

TABLE OF CONTENTS

Abstract iii

Abstrak v

Acknowledgements vii

Table of Contents viii

List of Figures xi

List of Tables xviii

List of Symbols and Abbreviations xix

List of Appendices xxi

CHAPTER 1: INTRODUCTION 1

1.1 Background of Study 1

1.2 Problem Statement 4

1.3 Objective 5

CHAPTER 2: LITERATURE REVIEW 6

2.1 Solving Vibration Problem Using FEA 6

2.1.1 Vibration and Equation of Motion 6

2.1.2 Finite Element Vibration Analysis 9

2.1.3 Application of Finite Element Vibration Analysis on Thin Panel and Air-conditioner Component 13

2.2 Code_Aster Usage and Open-Source Licensing 17

2.3 Experimental Modal Analysis and Modal Assurance Criteria 20

2.4 Vibration Analysis and Data Acquisition 24

2.5 Summary 27

CHAPTER 3: METHODOLOGY 29

3.1 Introduction.. 29

3.2 Finite Element Vibration Analysis... 30

3.2.1 Modal Analysis.. 31

3.2.1.1 Commercial Solver (Altair's Optistruct 2021) 31

3.2.1.2 Open-Source Solver (Code_Aster 2019) 46

3.2.2 Harmonic Response Analysis 62

3.2.2.1 Commercial Solver (Altair's Optistruct 2021) 62

3.2.2.2 Open-Source Solver (Code_Aster 2019) 66

3.3 Commercial vs Open-Source FEA Result Extraction and Comparison................. 76

3.3.1 Commercial Post Processor (Altair Hyperview)...................................... 76

3.3.1.1 Modal Analysis 76

3.3.1.2 Harmonic Response Analysis 80

3.3.2 Open-Source Post Processor (ParaView) 84

3.3.2.1 Modal Analysis 84

3.3.2.2 Harmonic Response Analysis 87

3.4 Experimental Vibration Analysis.. 92

3.4.1 Experimental Modal Analysis (EMA)... 92

3.4.2 Harmonic Response Analysis 96

CHAPTER 4: RESULTS AND DISCUSSION 100

4.1 FEA Results Comparison.. 100

4.1.1 Modal Analysis.. 100

4.1.2 Harmonic Response Analysis 104

4.2 FEA Results (Normal Mode) Validation with Experimental Modal Analysis ... 106

4.3 FEA Results (FRA) Validation with Vibration Signature Data Acquisition........ 112

CHAPTER 5: CONCLUSION AND RECOMMENDATION................................116

5.1 Conclusion 116

5.2 Future Recommendations 117

5.3 Sustainability..118

5.4 Complexity..119

5.5 Lifelong learning...119

References 121

Appendix A 124

Appendix B 127

LIST OF FIGURES

Figure 1.1: Daikin Malaysia. 2

Figure 1.2: Code_Aster® logo (EDF) 3

Figure 2.1: Single 'element' of a spring mass system. 7

Figure 2.2: The project will primarily focus on free vibration (modal analysis) and harmonic response analysis 9

Figure 2.3: Three phases of an analysis (Petyt, 2003). 10

Figure 2.4: 4 nodes rectangular (quad) shell element. 11

Figure 2.5: Mode shapes and natural frequencies of a simple rectangular plate 12

Figure 2.6: Frequency response function (FRF) of a simple rectangular plate 12

Figure 2.7: Mode shapes of multi-hole plate using shell element. First bending, 2nd bending and 3rd bending mode are shown here (Ye et al., 2021) 13

Figure 2.8: Velocity response distribution and critical location nodal FRF from propeller pulse load condition. 14

Figure 2.9: Nonlinear vibration analysis of a beam structure 15

Figure 2.10: Daikin Outdoor Unit. 16

Figure 2.11: Shaker Test (DRDM, 2019) 16

Figure 2.12: AsterStudy GUI for an ODU Base Panel. 18

Figure 2.13: Open-Source FEA software process 19

Figure 2.14: GNU logo 20

Figure 2.15: General EMA setup with impact hammer (Jimin He, 2011) 21

Figure 2.16: Impact hammer with various tip. 21

Figure 2.17: Typical FRF of a general accelerometer which can be measured up to 20 kHz before any significant distortion. (Jimin He, 2011) 22

Figure 2.18: Roving hammer method, by moving around impact hammer after each collection of data (M P et al., 2013) 23

Figure 2.19: 2D MAC plot, if diagonal value are almost 1, all the mode shapes (FEA vs EMA) can be considered similar (Pástor et al., 2012)..24

Figure 2.20: A DAQ system (Rao, 2011)..25

Figure 2.21: A general accelerometer, which consist of piezoelectric element...............26

Figure 2.22: Time domain and frequency domain representation of a periodic signal (Brandt, 2011) 27

Figure 3.1: Research project workflow. 30

Figure 3.2: Original 3D model from designer..32

Figure 3.3: Base panel and base panel leg after geometry cleanup.................................32

Figure 3.4: Base panel after mid-surfacing. 33

Figure 3.5: Base panel leg after mid-surfacing...34

Figure 3.6: Solid rectangular table 34

Figure 3.7: Complete model which include a base panel, 4 base panel leg and a rigid table. 35

Figure 3.8: A very simple solid mapped mesh...36

Figure 3.9: Meshing of base panel consists of tria and quad elements, with 2.5mm element size...37

Figure 3.10: Element quality criteria check. 38

Figure 3.11: A close view on the element quality, with good quality.............................38

Figure 3.12: Full model without bad quality element. 39

Figure 3.13: The actual shaker test...39

Figure 3.14: Connection between leg (with screw hole) and table using RBE2. 40

Figure 3.15: Spot welding representation by RBE2 between base leg and base panel. . 41

Figure 3.16: RBE2 apply on the bottom surface of the rigid table. The excitation and fixed constraint will be applied on the independent node (center node) 42

Figure 3.17: Material property input 43

Figure 3.18: PSHELL assigned to CQUAD and CTRIA element (panel and leg)..........44

Figure 3.19: PSOLID assigned to Hexa element (rigid table) 44

Figure 3.20: EIGRL card. 45

Figure 3.21: SPC, fix all DOF 45

Figure 3.22: Load step. 46

Figure 3.23: Import mesh element into Salome Meca 47

Figure 3.24: Mesh assembling. Aster_Study UI let us to select keyword and apply to the FE model interactively with automatic keyword creation. 48

Figure 3.25: Keyword for mesh assembly. 48

Figure 3.26: Assign properties using AFFE_MODELE 49

Figure 3.27: Assign DKT to base panel and leg 49

Figure 3.28: Assigning shell thickness 50

Figure 3.29: Thickness for base panel and leg 50

Figure 3.30: Keyword for assigning thickness 50

Figure 3.31: Material parameters for steel 51

Figure 3.32: Assigning the material defined to all the mesh elements 52

Figure 3.33: Keyword for defining material properties 52

Figure 3.34: Assigning of fix boundary condition and rigid body element. 53

Figure 3.35: Fix boundary condition on the base of rigid table 53

Figure 3.36: Fix on X, Y, Z DOF 54

Figure 3.37: Link between 4 legs and table, 4 legs and panel. 54

Figure 3.38: Keyword for defining boundary condition 54

Figure 3.39: Defining stiffness matrix and mass matrix 55

Figure 3.40: Assigning model, number of DOF, material and boundary condition to matrix assembly 56

Figure 3.41: Keyword for defining matrix 56
Figure 3.42: Load step creation. 57

Figure 3.43: Assign assembly matrix defined previously. 57

Figure 3.44: Result type and result extraction method. 58

Figure 3.45: List of specify frequency on searching modes, mass normalization and MUMPS solver 59

Figure 3.46: Keyword that used to define load step. 59

Figure 3.47: Set output results and location. 60

Figure 3.48: Set ouput results 60

Figure 3.49: Run analysis setting. 61

Figure 3.50: Run parameters 61

Figure 3.51: SPCD, single point constraint on the centered node 62

Figure 3.52: Excitation data in table format 63

Figure 3.53: RLOAD2, with harmonic load parameters 64

Figure 3.54: Frequency step result output definition. 64

Figure 3.55: Acceleration output request. 65

Figure 3.56: Harmonic response load step. 65

Figure 3.57: 160 nodes at the base of the table. which subjected to 4.81N harmonic load. 66

Figure 3.58: The harmonic load only acts upon Z direction. 67

Figure 3.59: The keyword for load assignment. 67

Figure 3.60: Define excitation function. 68

Figure 3.61: Define function parameters 69

Figure 3.62: 5Hz to 500Hz, with 4.81N force 69

Figure 3.63: Keyword for harmonic load table definition 69

Figure 3.64: Matrix assembly parameters 70
Figure 3.65: Harmonic load matrix. 70

Figure 3.66: Matrix assembly keyword. 71

Figure 3.67: DYNA_VIBRA keyword....72

Figure 3.68: Load input parameters....72

Figure 3.69: Damping definition....73

Figure 3.70: Keyword for harmonic load step....73

Figure 3.71: Result output....74

Figure 3.72: Keyword for result output....74

Figure 3.73: As same as modal analysis, rmed is the result file generated. 75

Figure 3.74: Result output file....75

Figure 3.75: Hyperview interface....77

Figure 3.76: Switch between modal results....77

Figure 3.77: Contour panel....78

Figure 3.78: Example of a mode shape result....78

Figure 3.79: Switch to multi-window mode....79

Figure 3.80: multi-window mode with different mode shapes....79

Figure 3.81: Export as GIF file and save to desired location. 80

Figure 3.82: Acceleration response. 81

Figure 3.83: Play the acceleration animation contour....81

Figure 3.84: Data panel. 82

Figure 3.85: Select node and create FRF curve....82

Figure 3.86: Example of the FRF....83

Figure 3.87: Export FRF as csv at desired location....83

Figure 3.88: Paraview user interface....84

Figure 3.89: Applying mode shape result....85

Figure 3.90: Warp by Vector filter....85

Figure 3.91: Changing contour preset. 86

Figure 3.92: Animation keyframe 86

Figure 3.93: Save the animation file a desired location........ 87

Figure 3.94: Load response results 88

Figure 3.95: Interactive select points tool 88

Figure 3.96: Center node 89

Figure 3.97: Selection over time filter 90

Figure 3.98: FRF data for acceleration and displacement. 90

Figure 3.99: Export scene 91

Figure 3.100: Example of csv FRF data from specified node 91

Figure 3.101: M3 screw to secure the base panel on top of acrylic sheet. 93

Figure 3.102: M3 screw to secure the base panel on top of acrylic sheet. 93

Figure 3.103: Fully secured and tightened screw location. 94

Figure 3.104: 21 points marking 94

Figure 3.105: EMA setup. 95

Figure 3.106: Example of an EMA FRF to be curve fit 96

Figure 3.107: Shaker with base panel 97

Figure 3.108: Accelerometer attachments location 98

Figure 4.1: Mode shape (mode 1 – mode 4) from Code_Aster® 2019. 101

Figure 4.2: Mode shape (mode 1 – mode 4) from Altair's Optistruct®. 101

Figure 4.3: Mode shape (mode 5 – mode 8) from Code_Aster® 2019. 102

Figure 4.4: Mode shape (mode 5 – mode 8) from Altair's Optistruct®. 102

Figure 4.5: MAC correlation between mode shapes from both solvers 103

Figure 4.6: Acceleration FRF (log scale) from both solvers 104

Figure 4.7: Displacement FRF (log scale) from both solvers 105

Figure 4.8: Harmonic response from Code_Aster® 2019 near 137Hz 105

Figure 4.9: Harmonic response from Altair's Optistruct® near 137Hz 106

Figure 4.10: Point 11 accelerometer FRF.. 107

Figure 4.11: Point 10 accelerometer FRF.. 107

Figure 4.12: Point 12 accelerometer FRF.. 108

Figure 4.13: Mode 1 comparison between Code_Aster® and EMA............................ 108

Figure 4.14: Mode 2 comparison between Code_Aster® and EMA............................ 109

Figure 4.15: Mode 3 comparison between Code_Aster® and EMA............................ 109

Figure 4.16: Mode 5 comparison between Code_Aster® and EMA............................ 110

Figure 4.17: Mode 7 comparison between Code_Aster® and EMA............................ 110

Figure 4.18: Response from experimental sweep analysis 113

Figure 4.19: Experimental response from refine measurement at peak. 114

Figure 4.20: Response from Code_Aster®. 115

Figure 5.1: Full unit transportation simulation by using Code_Aster® (future FEA method development) 118

LIST OF TABLES

Table 3.1: Material and physical properties of the FE model 43

Table 4.1: Percentage difference between results from two solvers.............................. 103

Table 4.2: Frequency difference between Code_Aster® 2019 and EMA. 111

Table 4.3: MAC correlation between Code_Aster® 2019 and EMA. 111

Table 4.4: Damping coefficient for each mode from EMA. 115

LIST OF SYMBOLS AND ABBREVIATIONS

�	:	Mass
$\ddot{x}$	:	Acceleration
�	:	Damping
$\dot{x}$	:	Velocity
x	:	Displacement, single degree of freedom
�	:	Stiffness
�	:	External force
A	:	Amplitude
ω	:	Frequency
λ	:	Eigenvalue
� ��	:	Determinant
�	:	Time
�	:	Displacement
φ	:	Eigenvector
CAD	:	Computer aided design
CAE	:	Computer aided engineering
CAM	:	Computer aided manufacturing
DAQ	:	Data acquisition
DFT	:	Discrete Fourier Transform
DOF	:	Degree of freedom
DRDM	:	Daikin Research and Development Malaysia
EDF	:	Électricité de France
EMA	:	Experimental modal analysis
FE	:	Finite element

FEA	:	Finite element analysis
FEM	:	Finite element model
FFT	:	Fast Fourier Transform
FRA	:	Frequency response analysis
FRF	:	Frequency response function
HPC	:	High performance cluster
HVAC	:	Heating, ventilation, and air conditioning
LAN	:	Local area network
MAC	:	Modal assurance criteria
MDOF	:	Multiple degree of freedom
ODE	:	Ordinary differential equation
RBE2	:	Rigid body element type 2
SDOF	:	Single degree of freedom

LIST OF APPENDICES

Appendix A: Code_Aster® 2019 Normal Mode Analysis Command File 117

Appendix B: Code_Aster® 2019 Harmonic Response Analysis Command File 118

CHAPTER 1: INTRODUCTION

1.1 Background of Study

Daikin Malaysia (Figure 1.1) is a leading HVAC manufacturer in Malaysia and Southeast Asia as well as around the globe. Their product is ranging from usual residential unit (wall-mounted), ceiling conceal/cassette unit, heavy duty unit such as rooftop and air handling unit (AHU) for commercial buildings. Daikin Malaysia consists of manufacturing plant and a research and development (R&D) center. The main purpose of Daikin R&D Malaysia (DRDM) is to develop and improved new HVAC models, research on new HVAC technologies, and solving quality issues faced by customers using engineering expertise and knowledge ("DRDM,"). Engineers must have a strong problem-solving skill to cater current technology trend and the complexity of a HVAC unit. Tools such as computer aided design (CAD), computer aided manufacturing (CAM) and computer aided engineering (CAE) are crucial for problem solving. Most common problem that engineers needed to solve during development stage are structural and fluid problems. Structural problems can be categorized into noise and vibration, durability and strength; while condensation, air flow, air drafting, and air borne noise are common fluid problem faced by engineers. CAE tools such as finite element analysis and computational fluid dynamics are among the powerful companion to solve structural and fluid problem respectively. The focus of this project is on predicting the frequency response of a bottom panel of a residential outdoor unit by using open-source FEA solver and experimental vibration analysis.

Figure 1.1: Daikin Malaysia.

FEA is a very powerful numerical tools for solving structural borne problems especially in the field of static, nonlinear static, dynamic and vibration. Traditional engineering hand calculation methods (whether its exact or numerical solution) can on solve for very simple 1D or 2D problem such as simple beam, trusses, frames. Finite element tools using discretization methods to discretize a very complex geometry such as bridge or engine block, to a smaller evenly sized 'element' with nodes (Moaveni, 2015). By applying suitable boundary condition and material properties, the software will solve for the deformation (static/dynamic) or modal and frequency responses (vibration) in that complex structure usually by using local modern computers or high-performance computing (HPC) server that runs in Linux or Windows (Sabet, Koric, Idkaidek, & Jasiuk, 2021).

Commercial FEA tools were used extensively by structural analyst. The yearly maintenance, licensing, and renewal cost for a commercial FEA tool (Altair's Hyperworks) is extremely high. To reduce the cost burden, open-source FEA tools is a good alternative. Code_Aster® (Figure 1.2) is an industrial proven FEA solver that used by many researchers, engineers, and universities. Code_Aster® consists of different kind of module (static, dynamic, modal, fatigue) to solve for different engineering phenomenon (EDF). It is an open-source software and is distributed under GNU General Public License (GPL), the most widely use free software license in the world (EDF, 2021c; GNU, 2021a), which means that the user is free to use the tools on any occasion, whether it is for research work, education, or even in our case, for business and commercial usage.

Although the programming language and algorithm in Code_Aster® is very sophisticated and stable, but due to its open-source nature, it is not as user friendly as many commercial software. Users need to understand the FEA code and keywords used by Code_Aster® to debug problem and errors. The documentation provided is not that complete as we have seen in commercial software. Since it is free, there is no global support team to assist on the problem we faced. It is an extremely challenging project, but the reward is enormous, since the annual software licensing cost in DRDM can be greatly reduce.

Figure 1.2: Code_Aster® logo (EDF).

To ensure the structural integrity of a HVAC outdoor unit during transportation, test engineer will mount the unit on a shaker table and vibrate the whole unit with 1G acceleration for 2 and half hours. To cater the test during pre-development and design stage, designer will seek consultation from structural analyst regarding the vibrational structural integrity. Structural analyst will then use FEA tools to predict the vibration responses of the unit by applying the shaker profile as an input excitation. Traditionally, commercial FEA software (Altair Optistruct®) will be use throughout the study and investigation. Before fully utilizing and implementing new FEA software into DRDM design workflow, the methodology, result and robustness of the software must be validated. One of the methods is to compare the results generated from commercial software with Code_Aster®. The boundary condition, mesh properties and material properties must be the same for both solvers. The result data must be output on the same exact location across two platform (ie, same nodal displacement or vonMises stress). For vibration FEA, all platforms will be using exactly same mesh file with same number of elements and nodes, the mode shapes and natural frequency of outdoor bottom panel will compare. The displacement, velocity, and acceleration FRF will be output from a single node (exact same node across both solver) and make comparison. To validate the FEA results, EMA and vibration signature data acquisition was carried out. EMA was performed on the panel, the mode shape and natural frequency was extracted, by using Modal Assurance Criteria (MAC) as a similarity indicator to the result from FEA. During the vibration signature test, an accelerometer was attached on to the bottom panel to capture the responses while the panel is subjecting to shaker excitation. The FRF from both FEA and experiment will be compared.

1.2 Problem Statement

An important aspect while designing a HVAC unit is its structural integrity to be able to withstand the vibration from transportation by lorry or ship. Designers and test engineers needed to ensure all the unit is free from structural failure during transportation process. One of the mandatory tests for all the newly developed unit is shaker test. After a HVAC unit prototype was fabricated, the unit will place on a shaker table which produce a 1G vertical acceleration for 2 and a half hours, sweeping from 5-95Hz, to mimic actual transportation (sea and road) condition. The unit must survive the test without any form of structural failure. During design stage, designers will seek consultation from structural analyst regarding vibration failure response, FEA can be used to predict the vibration response of the structure when subjecting to 1G acceleration. By using frequency response analysis in FEA, structural analyst can simulate the vibration condition during transportation process (shaker process), and usually it is done by using commercial FEA tools. This study will focus on frequency response analysis on bottom panel of a HVAC outdoor unit by using Code_Aster®. The research project will act as a preliminary study and pioneering the possibilities for the utilization of open-source FEA tools in DRDM. To ensure that Code_Aster® is robust and accurate, the results generated will be compared to commercial FEA software (Altair Optistruct®) and experimental vibration analysis (EMA and vibration signature test) results.

1.3 Objective

1. To develop finite element (FE) modal analysis and harmonic response analysis method for plate-like base panel of air conditioning outdoor unit using Code_Aster® (i.e. an open-source FE software).

2. To compare the accuracy of FE modal analysis and harmonic response analysis results of an air-conditioning outdoor unit panel between the methods developed in open-source FE software (Code_Aster®) with commercial FE software (e.g. Altair Optisruct®).

3. To experimentally validate the FEA results and its assumptions in term of boundary condition, material properties, and mesh properties with vibration tests, i.e., Experimental Modal Analysis (EMA) by using impact hammer and harmonic response testing by using electrodynamic shaker system.

CHAPTER 2: LITERATURE REVIEW

2.1 Solving Vibration Problem Using FEA

FEA is a crucial tool to solve for vibration problems during or after design stage of a component. It can be used to predict or obtain the dynamic behavior and characteristics of a machine, structure before completing any form of experiment. Users only needed to input the CAD file, material properties, perform meshing and provide an accurate boundary condition to the model, the mode shape and natural frequencies, frequency response function (harmonic response analysis) or a full spectrum of power spectral density (PSD, for random vibration) can be output, thus giving engineers a sense of the overall vibration characteristics of the structure. In this section, few important elements will be discussed and reviewed such as the dynamic equation of motion, finite element vibration analysis and finally its application and research from other scholar around the world.

2.1.1 Vibration and Equation of Motion

The most important aspect for vibration analysis is the dynamic equation of motion. The equation tells us the motion of a vibrating element with respect of time. As derived from the Newton 2nd law of motion, the general dynamic equation of a single degree of freedom (SDOF) spring-mass system can be given by ("Formulation of the Equations of Motion," 2010):

$$M\ddot{x} + C\dot{x} + Kx = F \tag{2.1}$$

Which is a 2nd order nonhomogeneous ordinary differential equation,

where:

M = Mass of a particle

c = Damping coefficient

k = Spring constant

x = Displacement (the subscript represents the 1st and 2nd derivative, velocity, and acceleration respectively).

f = External force or excitation to the system

The inertia force $m\ddot{x}$, damping force $c\dot{x}$ and stiffness kx are in equilibrium with external force f, and can be represented in a spring mass system as shown in Figure 2.1.

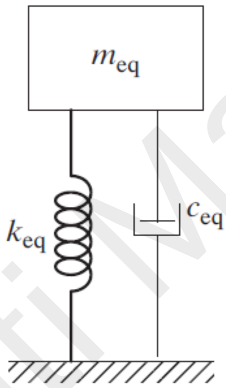

Figure 2.1: Single 'element' of a spring mass system.

Vibration analysis can be categorized as two major group, free vibration and forced vibration. Free vibration as named, there is no external force or damping acts upon the system, the dynamic equation of motion become:

$$m\ddot{x} + kx = 0 \tag{2.2}$$

The general solution is:

$x = A$ � ��� (2.3)

$$\ddot{x} = -\omega^2 A \sin(\omega t) \tag{2.4}$$

Substitute equation 2.3 and 2.4 to 2.2, with $\omega^2 = \lambda$, and rearranging:

$$([K] - \lambda[M])\{X\} = 0 \tag{2.5}$$

Is an eigen system of a linear dynamic equation. For a solution that is non-trivial ie, finding the determinant will solve the equation:

$$\det([K] - \lambda[M]) = 0 \tag{2.6}$$

Where is λ eigenvalues (natural frequency) and (Bai-Mao, Van-Xuan, Xiang-Hong, & Qian) is eigenvectors (mode shapes), and, the natural frequency, $\omega = \sqrt{\lambda}$ can be solved.

The idea of SDOF can be extended to multiple DOF (MDOF), by utilizing matrix algorithms:

$$\det\left(\begin{bmatrix} k_{11} & \cdots & k_{1n} \\ \vdots & \ddots & \vdots \\ k_{n1} & \cdots & k_{nn} \end{bmatrix} - \begin{bmatrix} \lambda_1 \\ \vdots \\ \lambda_n \end{bmatrix} \begin{bmatrix} m_{11} & 0 & 0 \\ 0 & \ddots & 0 \\ 0 & 0 & m_{nn} \end{bmatrix}\right) \begin{bmatrix} X_1 \\ \vdots \\ X_n \end{bmatrix} = 0 \tag{2.7}$$

The second category are forced vibration, which the external force acting as an excitation to the system and cannot be ignored as shown in equation 2.1. Given a harmonic force acting on a spring-mass system, equation 2.1 become:

$$m\ddot{x} + c\dot{x} + kx = F \sin(\omega t) \tag{2.8}$$

The steady state response can be obtained by solving the equation directly in exponential form:

$$m\ddot{x} + c\dot{x} + kx = F e^{i(\omega t)} \tag{2.9}$$

The solution for the above nonhomogeneous 2nd ODE:

$$\{x(t)\} = \{X(\omega)\} e^{i\omega t} \tag{2.10}$$

$$\{\dot{x}(t)\} = j\omega\{X(\omega)\}e^{j\omega t} \tag{2.11}$$

$$\{\ddot{x}(t)\} = -\omega^2\{X(\omega)\}e^{j\omega t} \tag{2.12}$$

Substitute equation 2.10, 2.11, 2.12 into equation 2.9 yield:

$$-\omega^2[M]\{X(\omega)\} + j\omega[C]\{X(\omega)\} + [K]\{X(\omega)\} = \{F(\omega)\} \tag{2.13}$$

Rearranging:

$$x = [K - \omega^2 M + j\omega C]^{-1} F e^{j\omega t} \tag{2.14}$$

In this approach, equation 2.14 are solved directly, to compute the inverse of coefficient matrix (hence, direct method), which are computationally expensive and requires more memories for multi component complex system. For a relatively simple single component, the solution across the spectrum can be obtained (more accurate) and does not require as much computational resources. Figure 2.2 shows the general approach of dynamic analysis.

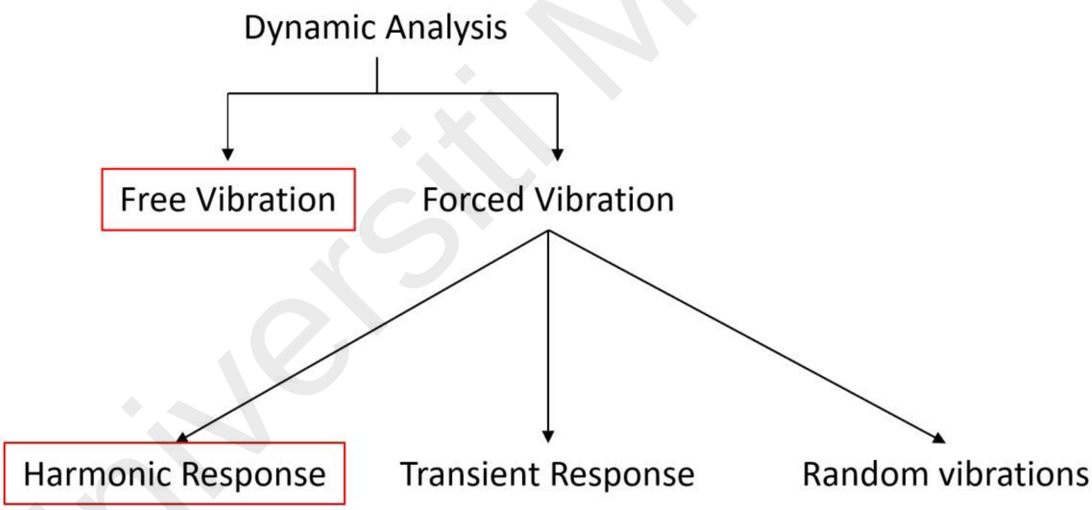

Figure 2.2: The project will primarily focus on free vibration (modal analysis) and harmonic response analysis.

2.1.2 Finite Element Vibration Analysis

For a very complex geometry (2D or 3D), FEA was used to solve for free vibration and forced vibration problem. The system can simply span from few DOF to millions of

DOF. To conduct an FEA, the following simple procedure is required (N.S Gokhale, 2008):

- Segregate CAD geometry into finite number of mesh (collection of elements and nodes).
- Define material and physical properties.
- Apply loads and boundary conditions.
- Defining systems of equations at nodes (normal modes, harmonic response etc.).
- Solving the system of equations at nodes (ie., displacement).
- Postprocessing (calculate further desired result from displacement, ie. Stress, strain, acceleration).

The procedure can be categorized into three phases, as shown in Figure 2.3, namely pre-processing (define material, physical properties, boundary etc.), solving and post-processing.

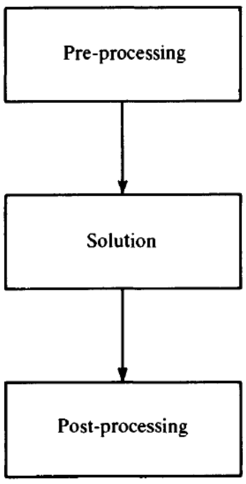

Figure 2.3: Three phases of an analysis (Petyt, 2003).

A 4 nodes quad shell element is typically used for a sheet metal FEA, which consists of 6 DOF (translation x, y, z, rotation rx, ry, rz) at each node. The normal modes, natural frequencies and responses at each node are than calculated via suitable equation and shape functions.

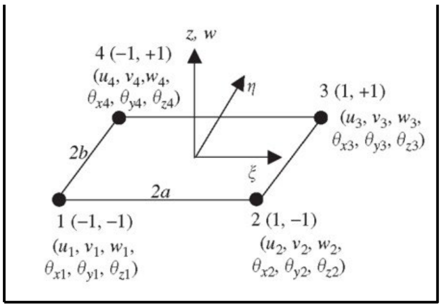

Figure 2.4: 4 nodes rectangular (quad) shell element.

The algorithm used to solve for modal analysis for both Altair Optistruct® and Code_Aster® are Lanczos method (EDF, 2021d), which is an iterative numerical method devised by Cornelius Lanczos. It is very efficient computationally for solving eigenvalues and eigenvectors of a large sparse matrices (Paige, 1980). Direct method (Newmark) is used to solve for harmonic response problems for both solvers, solving

$[K - \omega^2$�$+$ �$\omega C]^{-1}$ term at each timestep (Petyt, 2003).

Post processing part is where the crucial data and results are surfaced. The mode shapes and natural frequencies of free vibration of the structure will be normalized (usually to mass) are represented in contour form in Figure 2.5.

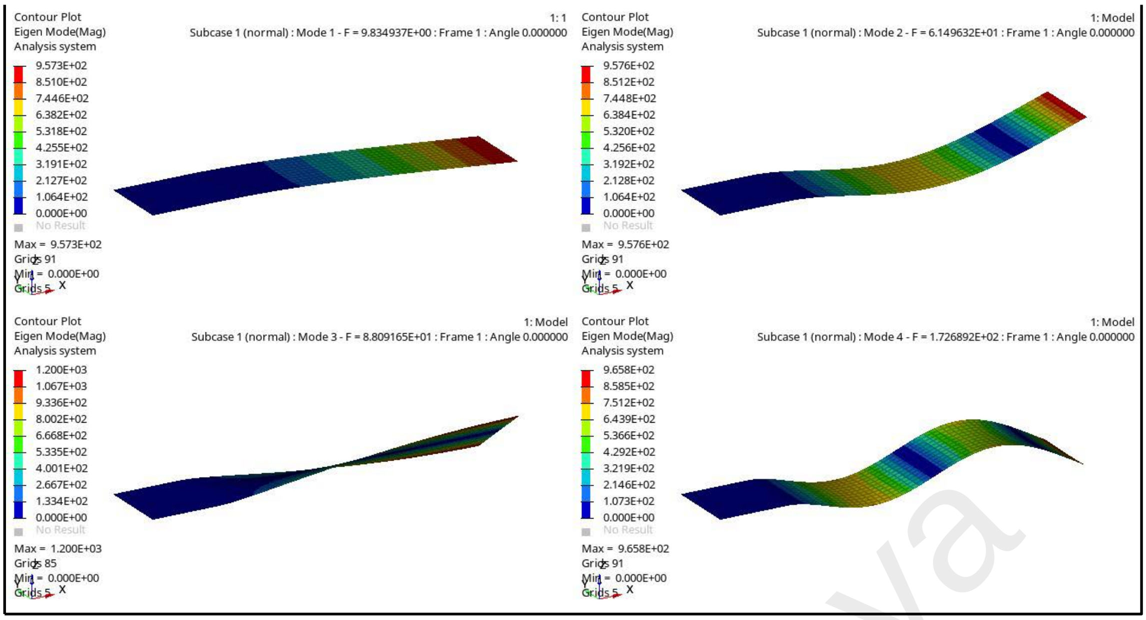

Figure 2.5: Mode shapes and natural frequencies of a simple rectangular plate.

For harmonic response, an actual response such as displacement, acceleration, and velocity (even stress, strain) can be outputted and plot against the whole frequency spectrum of interest (FRF) as shown in Figure 2.6. These results are usually compared to real world experimental data.

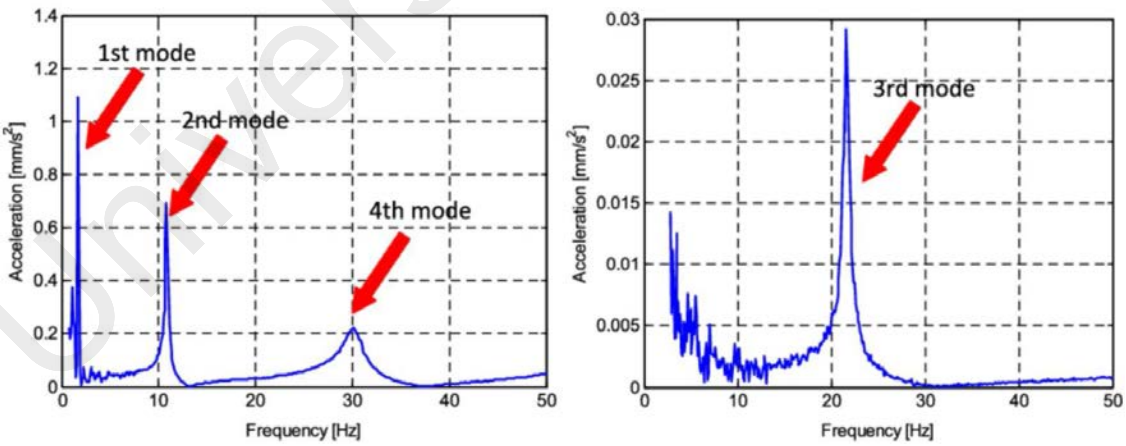

Figure 2.6: Frequency response function (FRF) of a simple rectangular plate.

2.1.3 Application of Finite Element Vibration Analysis on Thin Panel and Air-conditioner Component

Various study and literature have been presented on the finite element vibration analysis on thin panel. Multi DOF shell (plate) element was used in the study of free vibration with various boundary condition and the modes and natural frequency are compared with several literature with high accuracy (Gupta, 1985). The study in (Ye, Su, & Yang, 2021) also showed that using FEA with shell element achieving in high accuracy for free vibration and forced harmonic response analysis of a multi hole plate structure as shown in Figure 2.7.

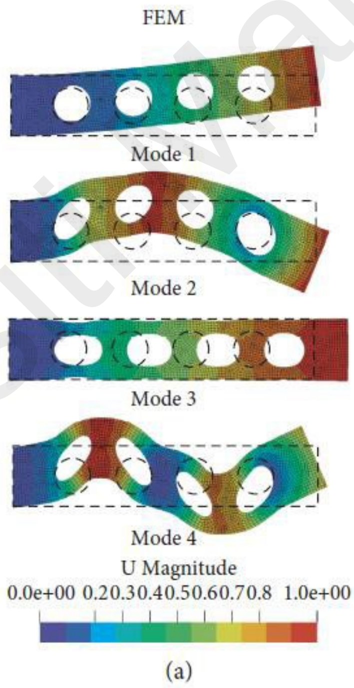

Figure 2.7: Mode shapes of multi-hole plate using shell element. First bending, 2nd bending and 3rd bending mode are shown here (Ye et al., 2021).

(M. Sergio, 2015) use shell element to model whole structure of a ship vessel (Figure 2.8) to estimate its modes and natural frequency. Response analysis was carried out via several load excitation condition. The response from the vessel is than compared to marine vibration standard to ensure its safety. From several study above, modal analysis is essential prior to response analysis, to ensure the dynamic behavior of the whole structure is accurate by using FEA and rectangular shell element for thin panel.

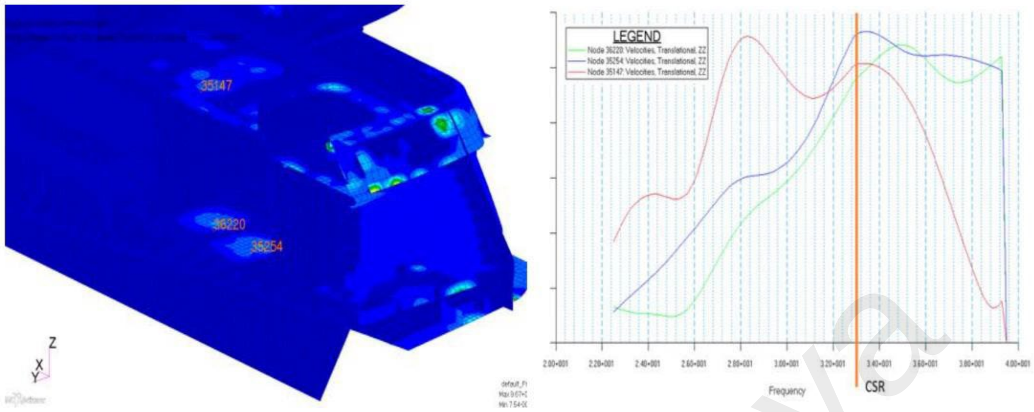

Figure 2.8: Velocity response distribution and critical location nodal FRF from propeller pulse load condition.

Several academic and industrial studies used open-source FEA solver such as Code_Aster® to carry out vibration analysis, the results generated is very high in accuracy and reliable. Code_Aster® originally developed by EDF and used by the company on thermonuclear structural analysis until present day. EDF must ensure its nuclear reactor is reliable in the long run thus, in 1989 EDF R&D has chosen to develop its own FEA solver for structural analysis and having two objectives in mind, an efficient FEA solver for engineering study and with quality assurance reliability (Han, Dominique, & Jiesheng, 2019). (Antonutti, Peyrard, Incecik, Ingram, & Johanning, 2018) is using Code_Aster® on dynamic simulation to a floating wind turbine, (Shen, 2021) used Code_Aster® on nonlinear vibration analysis in a thin structure and using Code_Aster® to develop the guideline for ship structure finite element analysis, the results are shown in Figure 2.9. This showed that the vibration analysis results from Code_Aster® is highly reliable and ready for industrial applications.

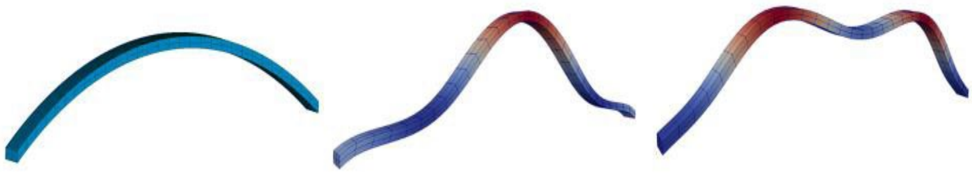

Figure 2.9: Nonlinear vibration analysis of a beam structure.

There are many researchers and engineers using FEA to solve for vibration issue on an air-conditioner unit, such as using modal analysis and harmonic response analysis (FEA, EMA, FRA) to solve for piping resonance problem (M.H. Fouladi, 2014; S.H. Lee, 2012). An air-conditioning outdoor unit consists of many components as shown in Figure 2.10, are particularly prone to vibration and noise problem. The source of vibration of an outdoor unit is from the following:

i) Fan Motor
ii) Transportation
iii) Compressor

Typically, fan motor excitation is small unless it is amplified by unbalanced fan, which rarely happens. Our focus on this project is on transportation vibration (vertical shaker test) on base panel component.

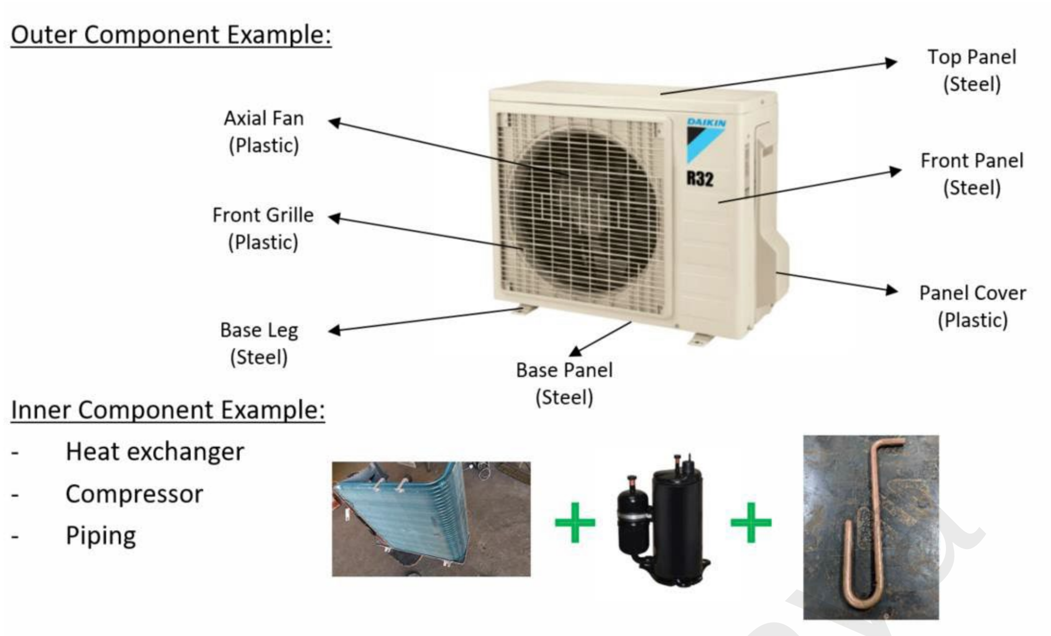

Figure 2.10: Daikin Outdoor Unit.

Transportation excitation is very important design aspect for a consumer product such as air conditioning. This study (V. Chonhenchob, 2010) shows that typical road and sea transportation PSD span from 5Hz to 100Hz. In Daikin Malaysia, the related road condition PSD are converted to constant 1G excitation from 5Hz to 100Hz, which is rather conservative. A shaker is used to mimic this condition, and all unit must survive without any structural failure (DRDM, 2019), the general test setup is shown in Figure 2.11.

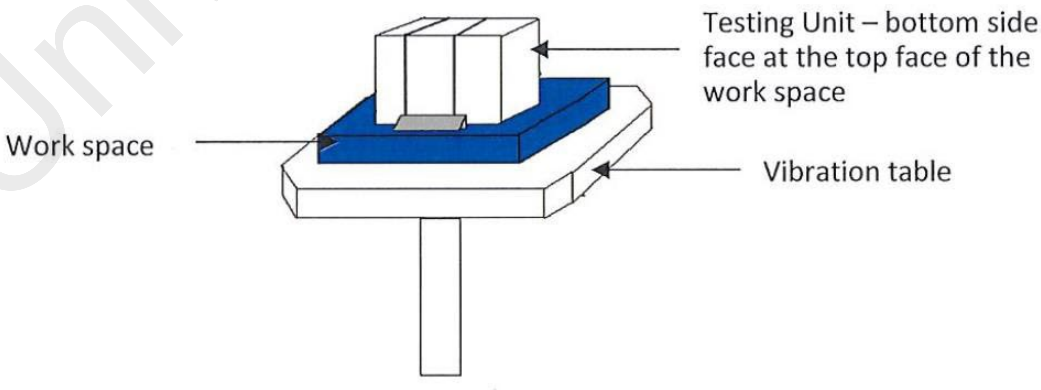

Figure 2.11: Shaker Test (DRDM, 2019).

This physical test can be simulated via harmonic response FEA. The study of the vibration response by compressor excitation (Venugopal, Pinninti, & Komaraiah, 2014) shows that by using harmonic response FEA, one can predict the vibration amplitude of a structure and can be validated via vibration signature test, which will be discuss in section 2.5. Similar approaches will be used for our bottom panel, but constant vertical load of 1G will be the excitation source.

2.2 Code_Aster® Usage and Open-Source Licensing

Code_Aster®, acronym for Analysis of Structures and Thermomechanics for Studies and Research is a FEA software develop by EDF (Electicite De France) R&D Department. There are several FEA modules that solves for different problems such as: linear static, nonlinear static, linear dynamics, nonlinear dynamic, thermodynamics, and Multiphysics etc (Durand, 2007). Due to its complex capabilities and open-source nature, the user interface is somewhat unfriendly, thus making the learning curve very steep for beginners. Salome Meca is a pre-processing open-source platform environment that consists of several module such as SMESH (mesh generator), GEOM (CAD generator), AsterStudy (Code_Aster® GUI), ParaVis (Postprocessor). The development of AsterStudy (Code_Aster® GUI module that integrated in Salome Meca) had eased the usage of Code_Aster®, the GUI is shown in Figure 2.12. It consists of several graphical user interface on boundary condition set-up, material properties assignment, mesh properties assignment etc.

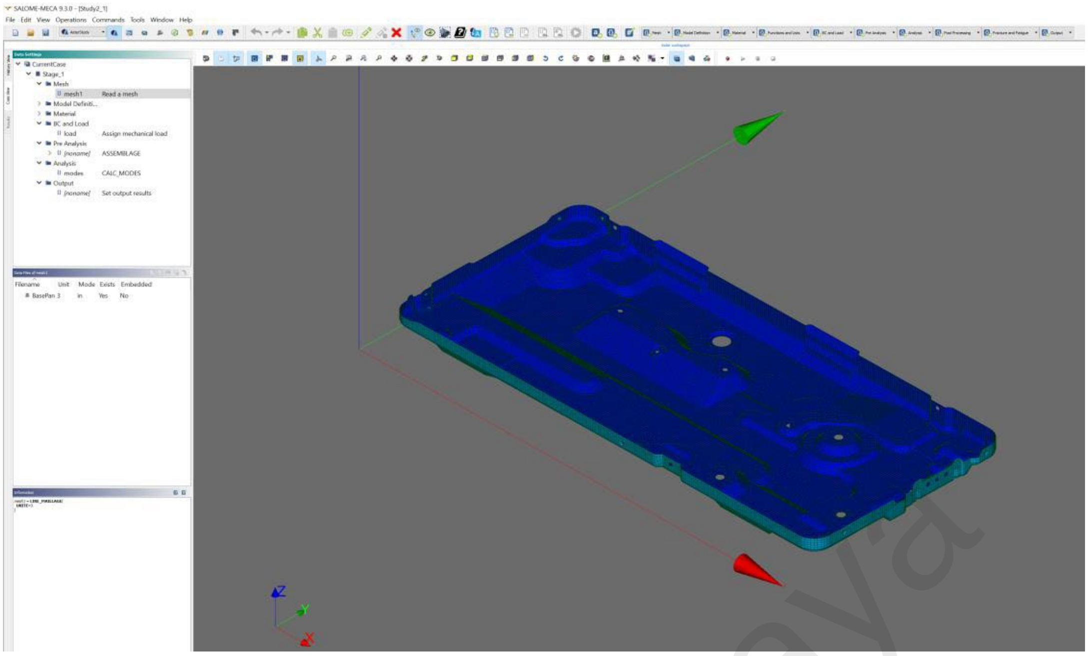

Figure 2.12: AsterStudy GUI for an ODU Base Panel.

Code_Aster® and Salome-Meca® are originally developed and provided for Linux environment only, and in year 2018, it starts to release the official version for 64-bit Windows operating system, and eligible for Windows 7, 8, 8.1, and 10 (EDF, 2021a). This study will primarily be using the Windows version of Code_Aster® for pre- and post-processing. For a very large model vibration analysis, a high-performance cluster (DRDM in house HPC) with CentOS (Linux) will be used for background calculation. The source code for Code_Aster® was written in 1M lines of FORTRAN, 10k lines of C and 200k lines in Python and integrated with some of the advanced algorithm and library for FEA solving such as MUMPS, PETSC, BLAS, LAPACK, MPI etc. (EDF, 2021b). Code_Aster® settings is configured by a series of command file (.comm), and act as an input file to the solver. Users can edit the .comm file via any text editors, or by using Aster_Study®, a GUI module integrated into Salome-Meca® (J.P.Aubry, 2021). All the results will be stored as. rmed, a binary file, and it's readable by ParaView® (an open-source post processor) for post-processing. Figure 2.13 shows the general software for this project, all of them are open source, except for Microsoft's Excel®.

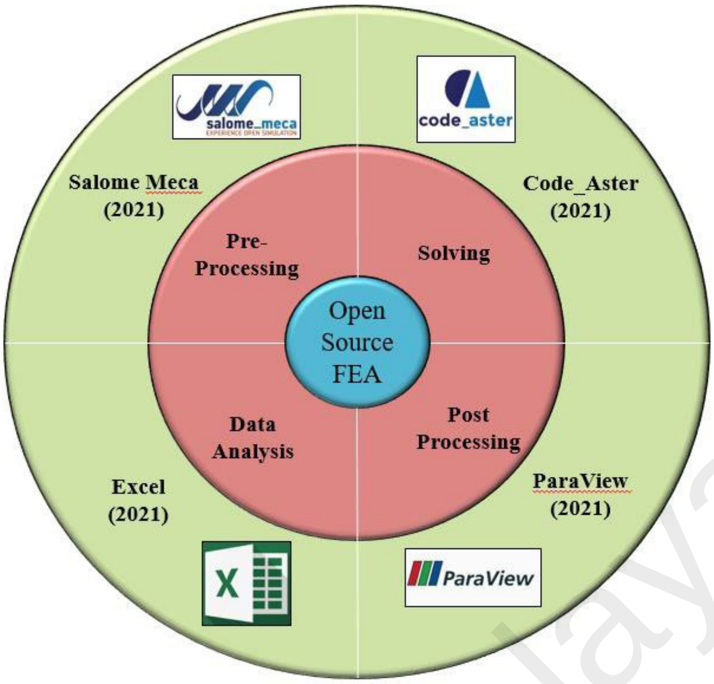

Figure 2.13: Open-Source FEA software process.

Both Code_Aster® and Salome-Meca® is distribute under GNU General Public License (GPL, Figure 2.14), the most widely use free software license in the world. GNU stands for "GNU not Unix!" (design like Unix, without Unix code), is a free software operating system initiated by Richard Stallman, during his year at MIT Artificial Intelligence Lab (Stallman, 1983). The objective of the GNU Project was to promotes and enable user worldwide to have a "free software". The definition of "free software" are as below (GNU, 2021b):

- The freedom to run the program as you wish, for any purpose (freedom 0).
- The freedom to study how the program works and change it so it does your computing as you wish (freedom 1). Access to the source code is a precondition for this.
- The freedom to redistribute copies so you can help others (freedom 2).

- The freedom to distribute copies of your modified versions to others (freedom 3). By doing this you can give the whole community a chance to benefit from your changes. Access to the source code is a precondition for this.

To protect the rights of the owner/user of a free software, the software will be distributed under GPL. GPL licensed software have these traits, which commonly known as “copyleft”, as opposed to the definition of copyright:

- To grant the rights to ensure any users will have the freedom to distribute copies.
- To grant legal permission to modified source code whenever they want.
- Patents cannot be used to render the program non-free.
- Freedom of usage for commercial or non-commercial used.

ParaView are using BSD license (another free software license), which are somewhat a subtle different than a GPL. BSD allowed software to be eventually commercialized with minimal legal issues (FreeBSD, 2021).

Figure 2.14: GNU logo.

2.3 Experimental Modal Analysis and Modal Assurance Criteria

Experimental modal analysis is the process of determining the dynamic characteristics such as natural frequencies, mode shapes, damping factor, of a structure. By establishing the relationship between vibration response at one location and excitation at the same or another location as a function of frequency (frequency response function, FRF) by using modal data. The measured FRF data constitute a column of the FRF matrix. Again, the data should suffice theoretically. With sufficient data, numerical analysis will derive modal parameters by ways of curve fitting (Jimin He, 2011). Figure 2.15 shows the general setup of EMA, which consists of a hammer, DAQ, and accelerometer attached onto the structure.

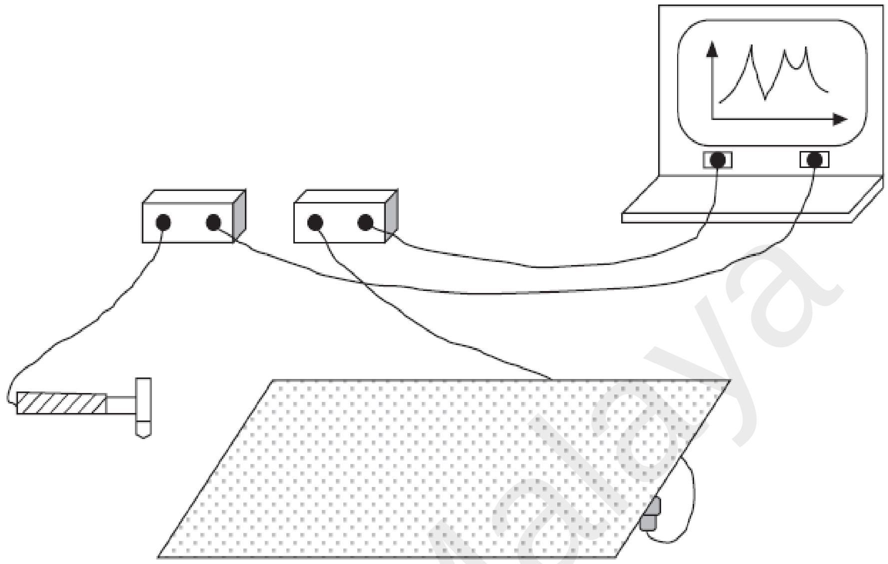

Figure 2.15: General EMA setup with impact hammer (Jimin He, 2011).

The excitation method typically uses a force transducer ‘hammer’ exciting the structure via a force impulse with sufficient amplitude and frequency band, depend on the hardness of the tip used. The impact hammer and various tip are shown in Figure 2.16.

Figure 2.16: Impact hammer with various tip.

An accelerometer was also used to collect the response data from the structure (acceleration and frequency), thus the FRF of an accelerometer should be uniformly flat on frequency band of interest so that no amplitude measurement from the structure is distorted (Jimin He, 2011). The FRF of a general accelerometer is shown in Figure 2.17, which does not have any peak before 20 kHz.

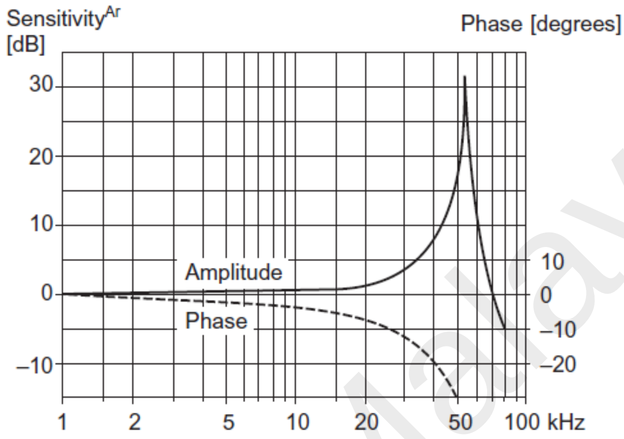

Figure 2.17: Typical FRF of a general accelerometer which can be measured up to 20 kHz before any significant distortion. (Jimin He, 2011).

EMA on a steel plate has done by many researchers. Roving hammer or roving shaker method was among the common one due to the convenience of the test, by fixing the location of accelerometer and striking the impact hammer on different location of the structure to collect the FRF, as shown in Figure 2.18 (M P, Yaacob, Abdul Majid, & Krishnan, 2013).

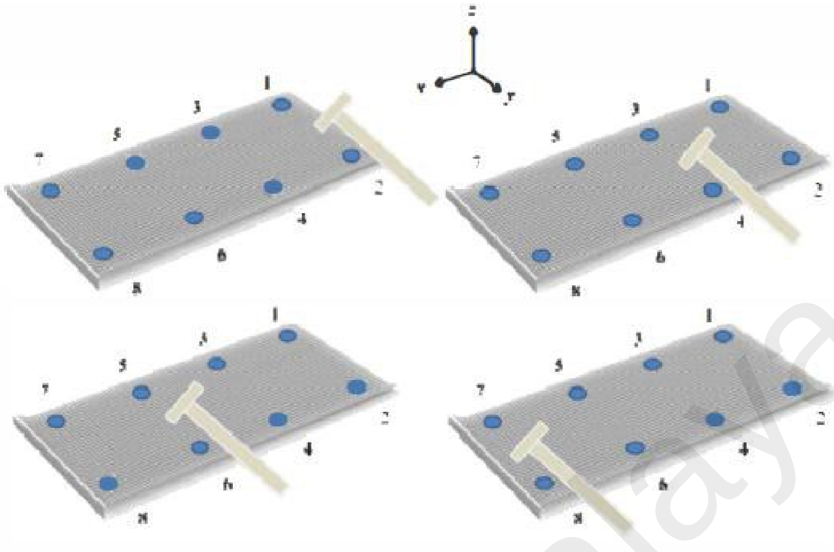

Figure 2.18: Roving hammer method, by moving around impact hammer after each collection of data (M P et al., 2013).

After collecting the FRF, the dynamic parameters of the structure can be extracted by using curve fitting method (least squared method, Dobson method, rational fraction polynomial method) (Jimin He, 2011).

To perform validation, modal assurance criterion (MAC) can be used as a statistical indicator between the similarity of EMA and FEA mode shapes. MAC is a calculation of normalized scalar product of two sets of mode vectors in each node. The equation of MAC is insensitive to scaling, thus suitable for FEA EMA comparison. The equation is given by (Pástor, Binda, & Harčarik, 2012):

$$MAC(A,X) = \frac{\left|\{\varphi_A\}^T\{\varphi_X\}\right|^2}{\left(\{\varphi_A\}^T\{\varphi_A\}\right)\left(\{\varphi_X\}^T\{\varphi_X\}\right)} \tag{2.16}$$

Where $\{\Psi_A\}$ and $\{\Psi_X\}$ are the two sets of mode vectors respectively.

Although the vector of modes is complex, the MAC quantity is truly scalar and can span from 0 to 1, if two vectors are dissimilar (difference or independent between the two mode shapes), the MAC = 0. If the two vectors are in linear relationship (similar mode shape), the MAC is near to 1. The desired MAC value (diagonally = 1) is shown in Figure 2.19.

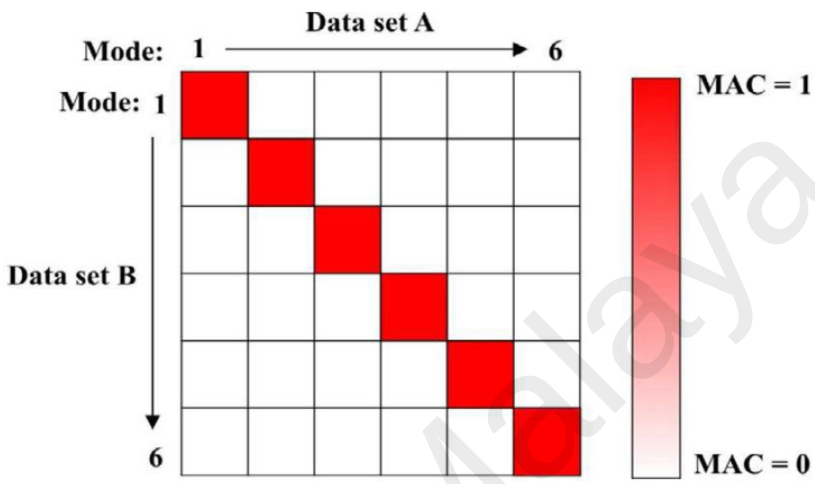

Figure 2.19: 2D MAC plot, if diagonal value are almost 1, all the mode shapes (FEA vs EMA) can be considered similar (Pástor et al., 2012).

Study from (Gülbahçe & Çelik, 2021) shows a good correlation (of the first four modes) between FEA and EMA of a plate like structure by using MAC as validation indicator. When using EMA as test validation against FEA, a good correlation in mode shape is those with MAC > 0.9 and with frequency error < 10% (G. Banwell, 2012).

2.4 Vibration Analysis and Data Acquisition

Vibration response from a structure such as displacement, velocity and acceleration are measured through a data acquisition system (DAQ), which consists of an exciter (typically a shaker), at least an accelerometer, FFT analyzer, and a signal conditioner connected to a personal computer via USB cable, or LAN cable.

Accelerometer is one of an important element to properly capture the vibration response. An accelerometer is an instrument that contain piezoelectric element that convert motion to potential difference (voltage), subjected to voltage sensitivity of difference piezoelectric, the output voltage will be different (Rao, 2011). The output voltage is then converted to acceleration signal via internal circuit and an amplifier, thus selecting a suitable accelerometer sensitivity is very important for getting an accurate response measurement. The acceleration data collected in time domain can be integrated to get velocity response, double integrating to get displacement response. The general setup of a harmonic response data acquisition is shown in Figure 2.20.

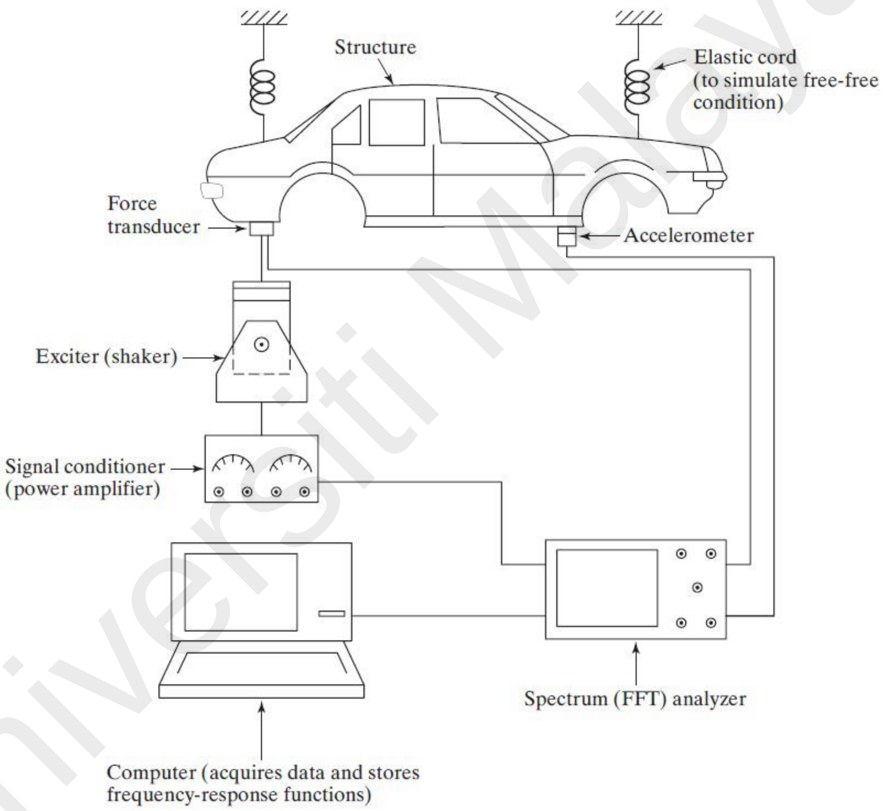

Figure 2.20: A DAQ system (Rao, 2011).

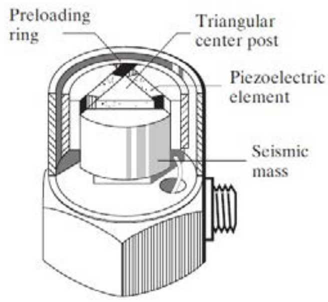

Figure 2.21: A general accelerometer, which consist of piezoelectric element.

All the signals are measure in time domain; it will be more useful if the data is analyzed in frequency domain for EMA and harmonic response analysis. Joseph Fourier, a French mathematician states that all periodic transient signal is a sum of infinite individual sinusoids, with respective amplitude, phase, and frequency, with the general equation given by (Brandt, 2011):

$$x_p(t) = \frac{a_0}{2} + \sum_{k=1}^{\infty} a_k \cos\left(\frac{2\pi k t}{T_p}\right) + \sum_{k=1}^{\infty} b_k \sin\left(\frac{2\pi k t}{T_p}\right) \tag{2.16}$$

Where a_k and b_k is a coefficient given by:

$$a_k = \frac{2}{T_p}\int_{t_1}^{t_1+T_p} x_p(t)\cos\left(\frac{2\pi k t}{T_p}\right)dt \quad k = 0,1,2,\ldots \tag{2.17}$$

$$b_k = \frac{2}{T_p}\int_{t_1}^{t_1+T_p} x_p(t)\sin\left(\frac{2\pi k t}{T_p}\right)dt \quad k = 1,2,3,\ldots \tag{2.18}$$

In real practice, the analysis is done by discrete Fourier transform (DFT) or fast Fourier transform (FFT), which is a nonparametric frequency analysis method. DFT is very different from general Fourier transform, which is a continuous integral form from minus infinity to infinity of a function. The DFT is computed from a sampled signal $x(n) = x(n\Delta t)$ with finite number of samples, N (or the blocksize) usually an integer power of 2, due to binary behavior of a digitalized device (such as PC or DAQ analyzer). The DFT,

$X(\text{�}) = X(\text{�}\Delta\text{�})$ of the sampled signal x(n) is defined as (Brandt, 2011) the following:

$$X(k) = \sum_{n=0}^{N-1} x(n)\cos\left(\frac{2\pi kn}{N}\right) - j\sum_{n=0}^{N-1} x(n)\sin\left(\frac{2\pi kn}{N}\right) \tag{2.19}$$

Which is the sum of real and imaginary parts, respectively. Most modern computers and DAQ analyzer use FFT as the default transformation algorithm, FFT is a much advance and efficient algorithm that improves from DFT. It uses Nlog2 (N) multiplications instead of N^2 for the DFT. Thus, for a sample size of N = 1024 will requires a computer to perform 2 million operations, whereas FFT only requires 30,000 operations, saving the computing cost by a factor of 68. Figure 2.22 shows a clearer overview of time domain and frequency domain of a periodic signal:

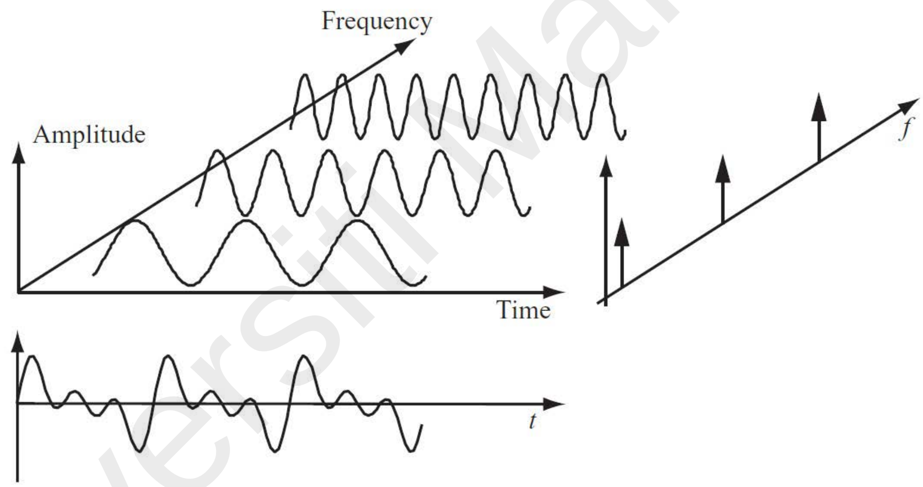

Figure 2.22: Time domain and frequency domain representation of a periodic signal (Brandt, 2011).

2.5 Summary

The reviewed literature suggests that there are many advantages to use FEA to predict the dynamic behavior and response of a plate like structure. Many researchers show that FEA vibration algorithms are sophisticated enough to solve for many vibrations problem and introduce into development and design flow. But very few of them is using open-source FEA solver, due to steep learning curve and unfriendly user interface. To ensure that the FEA boundary condition, material properties, element properties are correct, EMA (with roving hammer methodology) can be done to validate with the simulation results. MAC has been widely used by researchers to check the similarities of the mode shapes between FEA and EMA, or FEA and FEA, further enhance the numerical results accuracy and confidence. The harmonic vibration response (FRF) due to shaker excitation from both simulation and experiment should be similar if the parameters set in FEA are correct. With all the reviewed literature, there is lacking the detail study of dynamic response for air conditioning outdoor unit base panel. Current research project will refer the simulation and experimental methodology as discussed above and apply on the air conditioning outdoor unit base panel, particularly by using open-source FEA software.

CHAPTER 3: METHODOLOGY

3.1 Introduction

As discussed in previous chapter, FEA consists of three crucial steps, namely, preprocessing, solution (solving) and post-processing. Each step cannot afford to have a single mistake or else the solution would not run (ie with error) or the solution does not generate an accurate result to represent physical situation. As described by (DePalma, 2011), FEA results is only as good as its users, the solver can accept any values that the user provide such as material properties, mesh properties, boundary condition, input excitation etc, and will generate results if the solution converged, but the accuracy of the result heavily depends on the input given by the user. For example, a non-verified material properties or physical properties (thickness) input will cause difficulties in predicting the mechanical failure (yield, resonance, fatigue etc). Over constraint on the boundary condition will cause the model overly stiff, producing an inaccurate result. As such, FEA engineers must ensure that the input data is logical, precise, and accurate before attempting preprocessing workflow, always follow the “garbage in, garbage out principle”. Postprocessing is how the engineers interpret the results, by selecting the correct contour stresses or vectors, magnification or scaling for visualization, identifying the mode shapes can be contributed to the final representation of the simulation.

Once the result is generated and analyzed, experiment must be done to validate the model. EMA and harmonic response analysis are used for such cases. Verify the simulation results before using for design workflow is a very important procedure. In this chapter, three methods (FE modeling, commercial vs open-source software comparison, experimental vibration analysis) to tackle the objectives of the project will be discussed heavily, the result and validation will be discussed on the next chapter. Figure 3.1 shows the overall research workflow summary of this project of this project to achieve all the objectives within the given timeframe.

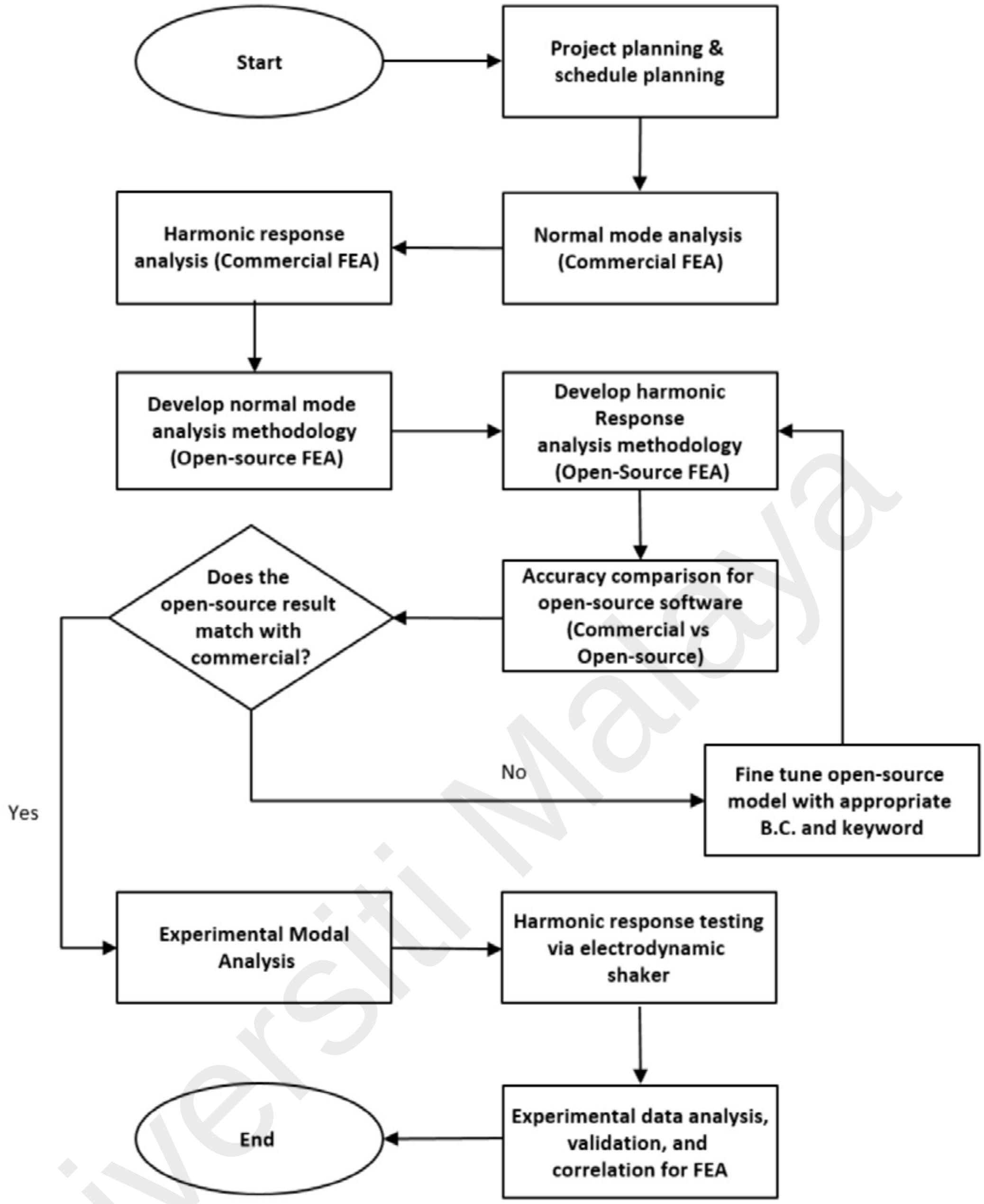

Figure 3.1: Research project workflow.

3.2 Finite Element Vibration Analysis

This subsection will consist of the general methodology of FEA on both modal analysis and harmonic analysis using the commercial software (Altair's Optistruct) and open-source software (Code_Aster®). The three stages of FEA will be heavily described throughout this section.

3.2.1 Modal Analysis

Modal analysis is the extraction of the natural frequencies and mode shapes of the component, by constructing finite element model and solving as discussed in chapter 2. Geometry cleanup, meshing, assigning properties and boundary conditions are among the general step of the analysis.

3.2.1.1 Commercial Solver (Altair's Optistruct® 2021)

Geometry cleanup is the first step for any FE modeling. While the designer passes the CAD to FE engineer, the CAD might not be ready for meshing for example, sharp vertices that causes element distortion while auto meshing, damaged surface, feature that are too small to be mesh (smaller than element size) etc. If the component is a thin panel (i.e. thickness is << than overall surface area), mid surfacing needed to be done in order to perform shell meshing. After geometry cleanup, a rigid table is drawn to represent the real shaker table. Meshing is performed afterward for both the panel and table. Material properties and physical properties (thickness) will be assigned to the respective component. Boundary condition and finally load step will be setup for the last step before solving.

The following are the detail steps for modal analysis:

Step 1: Unwanted component and feature defeaturing

The original CAD given by designers, consisting of every single component of the outdoor unit as shown in Figure 3.2.

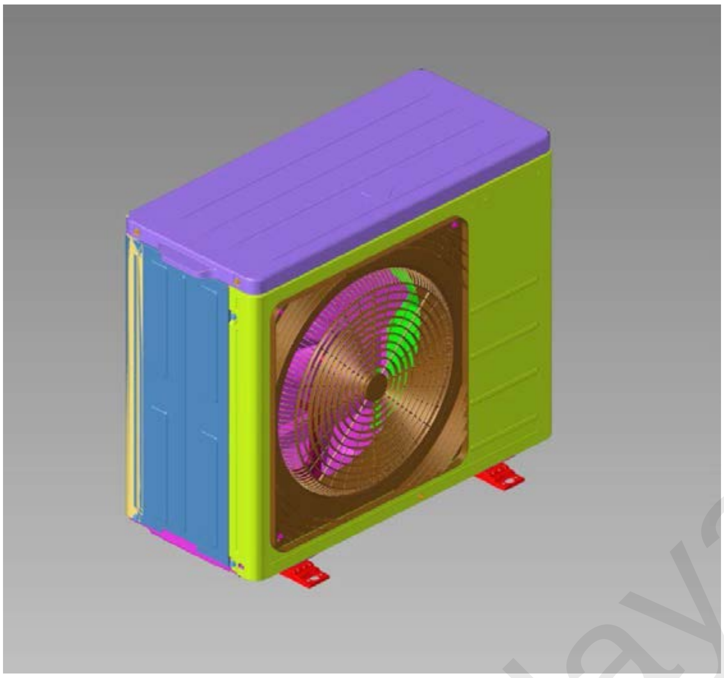

Figure 3.2: Original 3D model from designer.

Some small feature like logo, wire, PCB board can be deleted since it does not affect the result of the analysis. This research study only focusses on the base panel (Figure 3.3), thus other component will be removed.

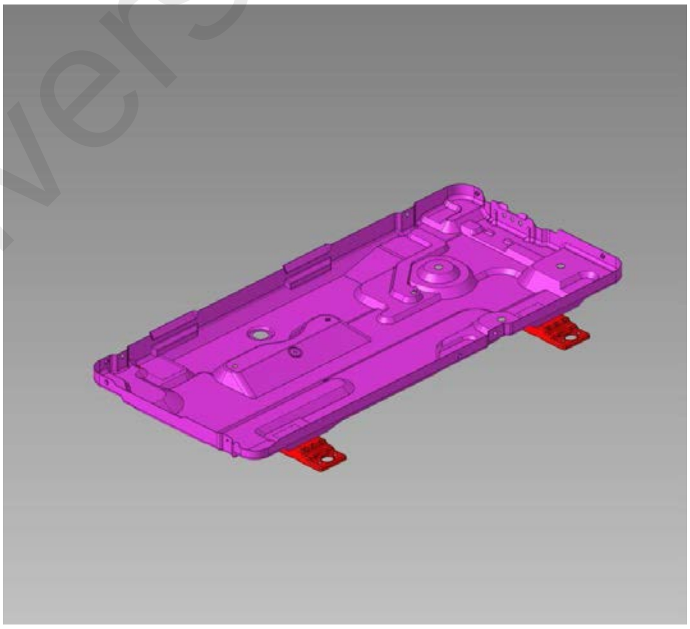

Figure 3.3: Base panel and base panel leg after geometry cleanup.

After the cleanup and defeaturing, only the base panel and base panel leg will be use in the analysis.

Step 2: Mid-surfacing

Since the thickness of the panel is very thin, it is more suitable to use shell element and assign the thickness in property section in the software rather than solid element, it will help to save computing cost and avoid elemental check error (very thin solid element has a very bad element quality that will be affecting the results). Thus, mid-surfacing is essential, by extracting the middle surface of a panel and base leg (Figure 3.4 & Figure 3.5).

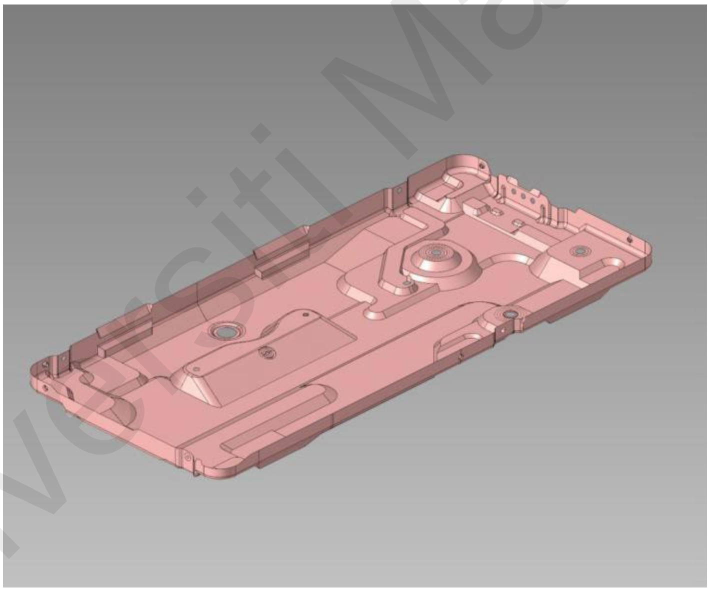

Figure 3.4: Base panel after mid-surfacing.

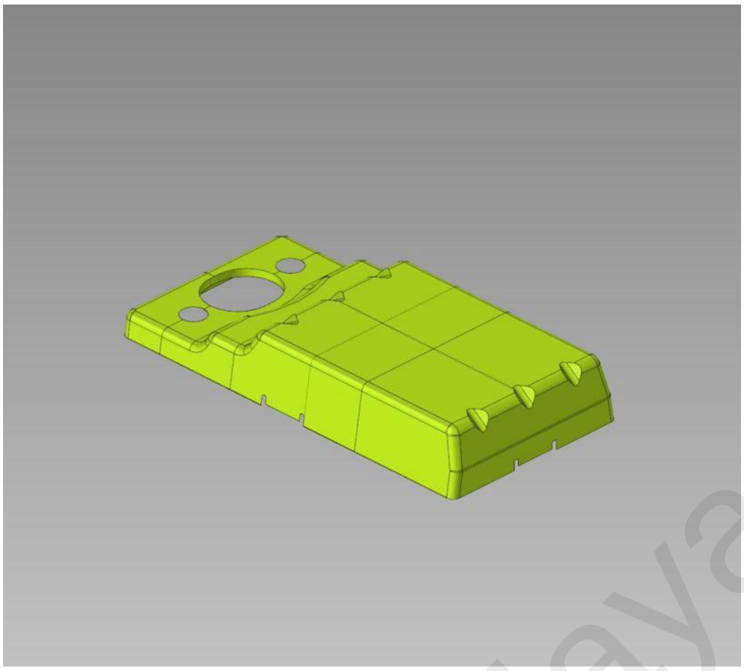

Figure 3.5: Base panel leg after mid-surfacing.

Step 3: Draw a rigid table that represents shaker table

A simple rectangular shaped 3D model (1000mm x 700mm x t10mm) is generated as shown in Figure 3.6 to represent the shaker table that act as the base excitation on the base panel. The base panel with base leg are place on top on the rigid table in Figure 3.7.

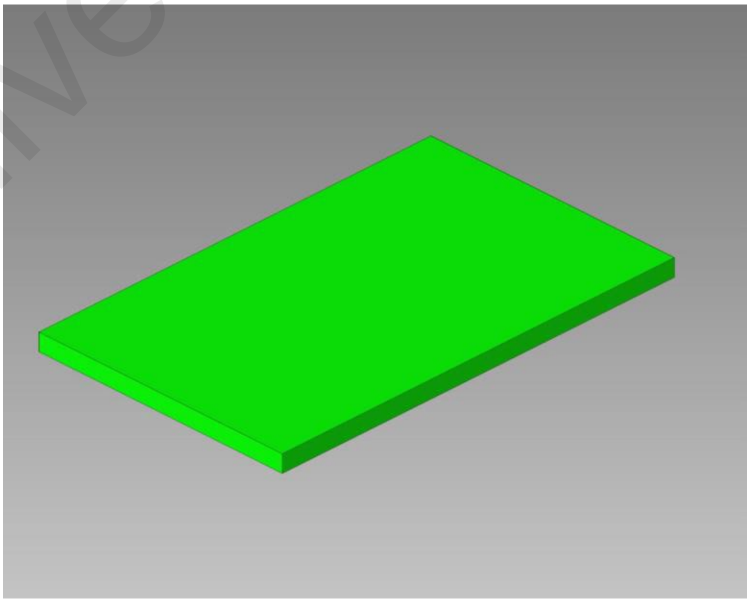

Figure 3.6: Solid rectangular table.

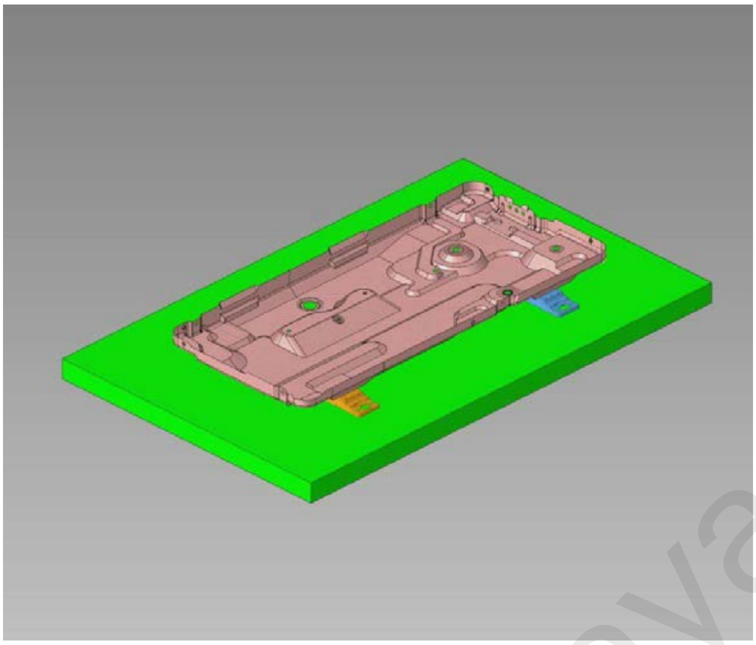

Figure 3.7: Complete model which include a base panel, 4 base panel leg and a rigid table.

Step 4: Meshing

The rigid table will be meshed by using 3D solid element (hexa 8) with 2.5mm average size since it is significantly thicker (not thin shell) as shown in Figure 3.7. While the base panel and base panel leg will be using shell element (CQUAD and CTRIA elements) with 2.5mm average size as shown in Figure 3.8.

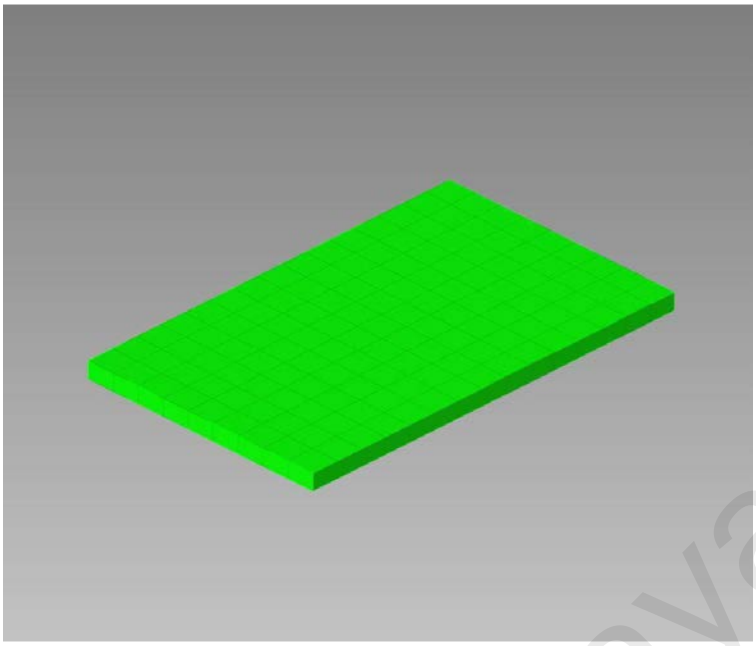

Figure 3.8: A very simple solid mapped mesh.

Auto mesh feature was used with the mixture of tria and quad element with 2.5mm average size (Figure 3.9).

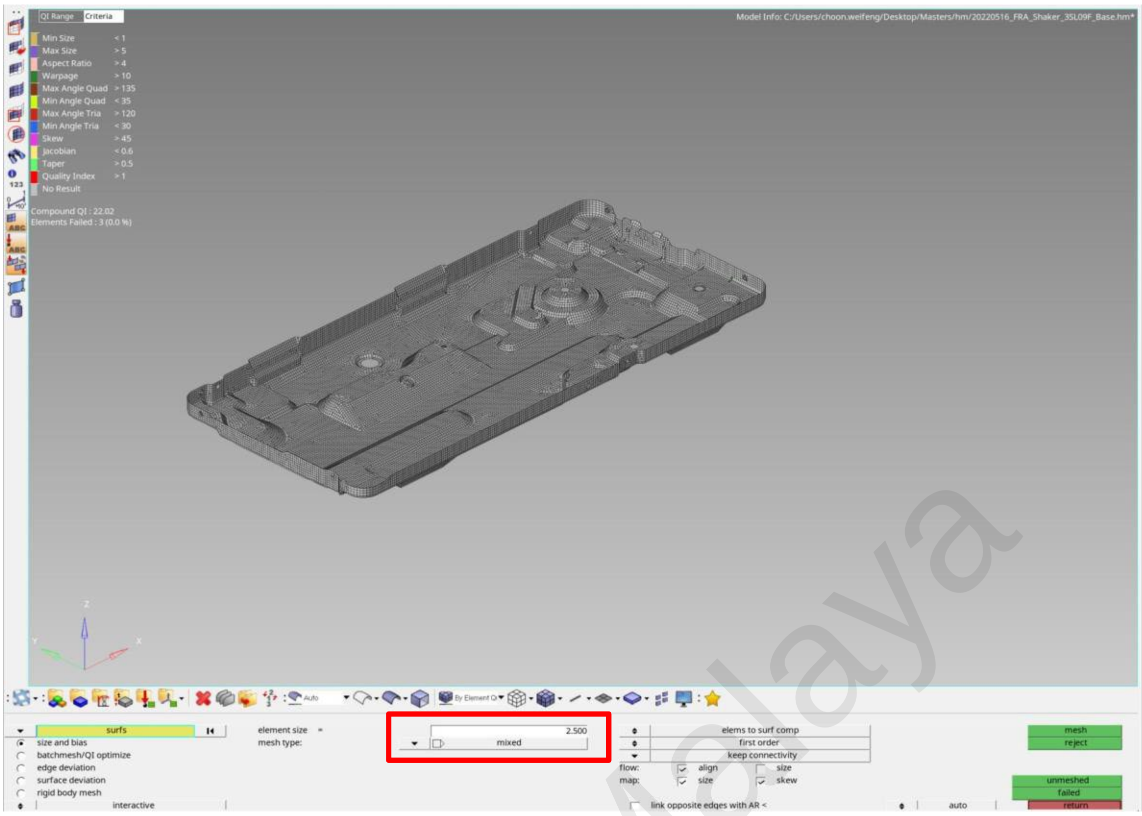

Figure 3.9: Meshing of base panel consists of tria and quad elements, with 2.5mm element size.

Step 5: Element quality check

Element quality assurance and checking is very important to ensure the result generated from FEA is reliable and free from significant numerical error. The element will be colored if the element exceeds the allowable criteria listed in Figure 3.10. The "no results" (white colored) should be presented on all the element if the model is free from bad quality element, as shown in Figure 3.11.

Figure 3.10: Element quality criteria check.

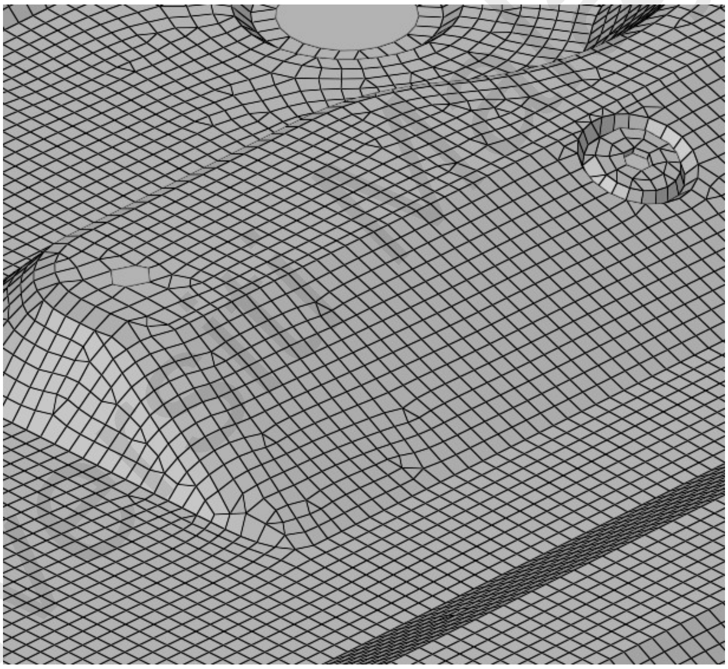

Figure 3.11: A close view on the element quality, with good quality.

Figure 3.13 shows the actual unit shaker test in DRDM, which is comparable to the FE model in Figure 3.12.

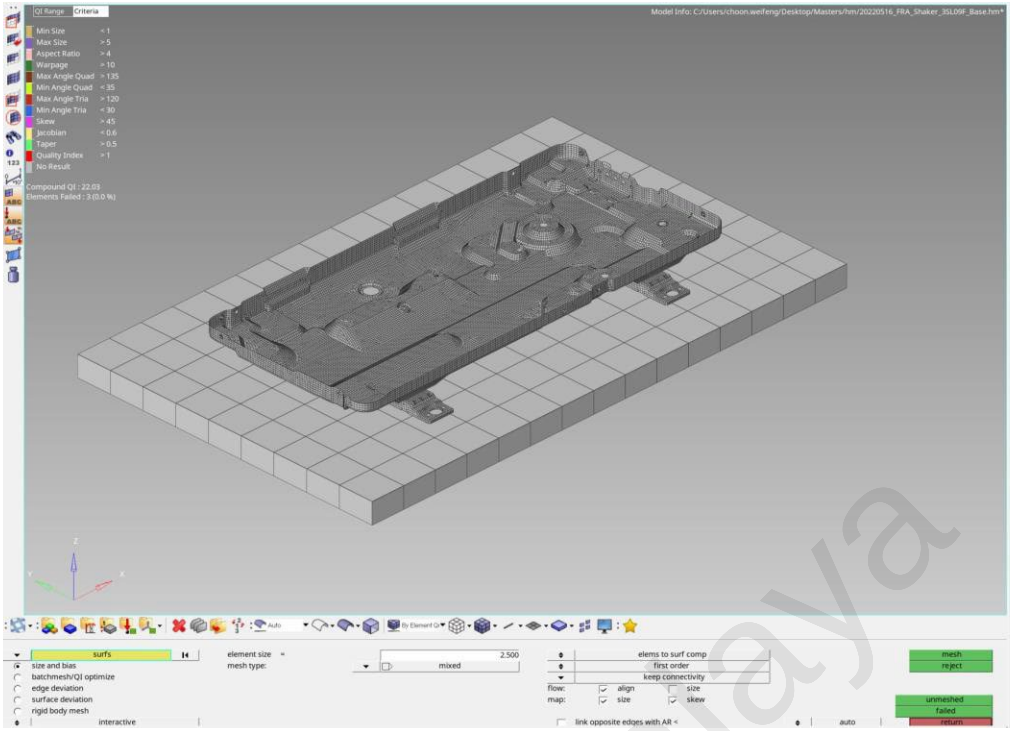

Figure 3.12: Full model without bad quality element.

Figure 3.13: The actual shaker test.

Step 6: Assigning rigid body element (RBE2)

A rigid body element type 2 (RBE2) is used to tie between components. If 2 nodes are connected via RBE2, the displacement of the dependent node will be like the independent nodes, thus it will move together as a ‘rigid’ part. RBE2 will be used to tie between the base panel and base panel leg to represent the physical model (spot welding). It will also be used to tie between the base panel leg and the rigid table, thus the base excitation from the table will transmit to the panel. The nodes in the base leg and rigid table are selected as shown in Figure 3.14, to create RBE2 and tie between the 2 components. In Figure 3.15, the spot weld connection between base panel and base leg are represented by RBE2 (blue colored).

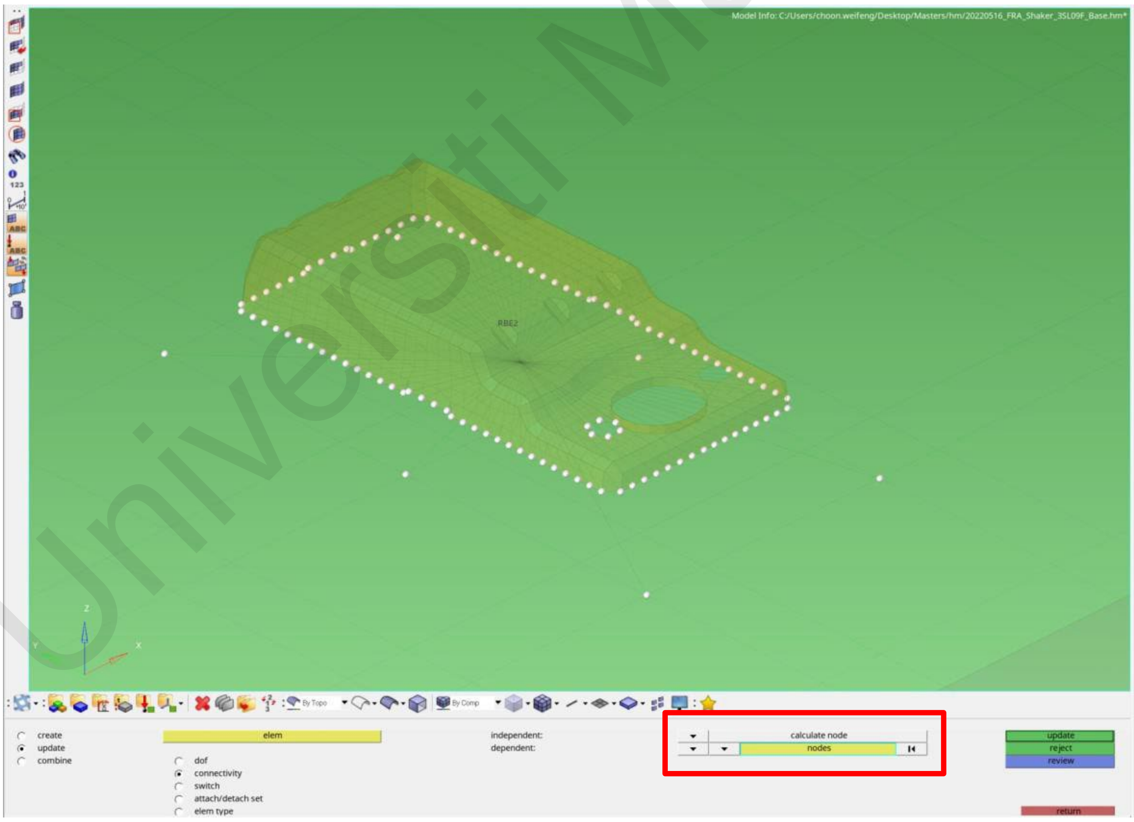

Figure 3.14: Connection between leg (with screw hole) and table using RBE2.

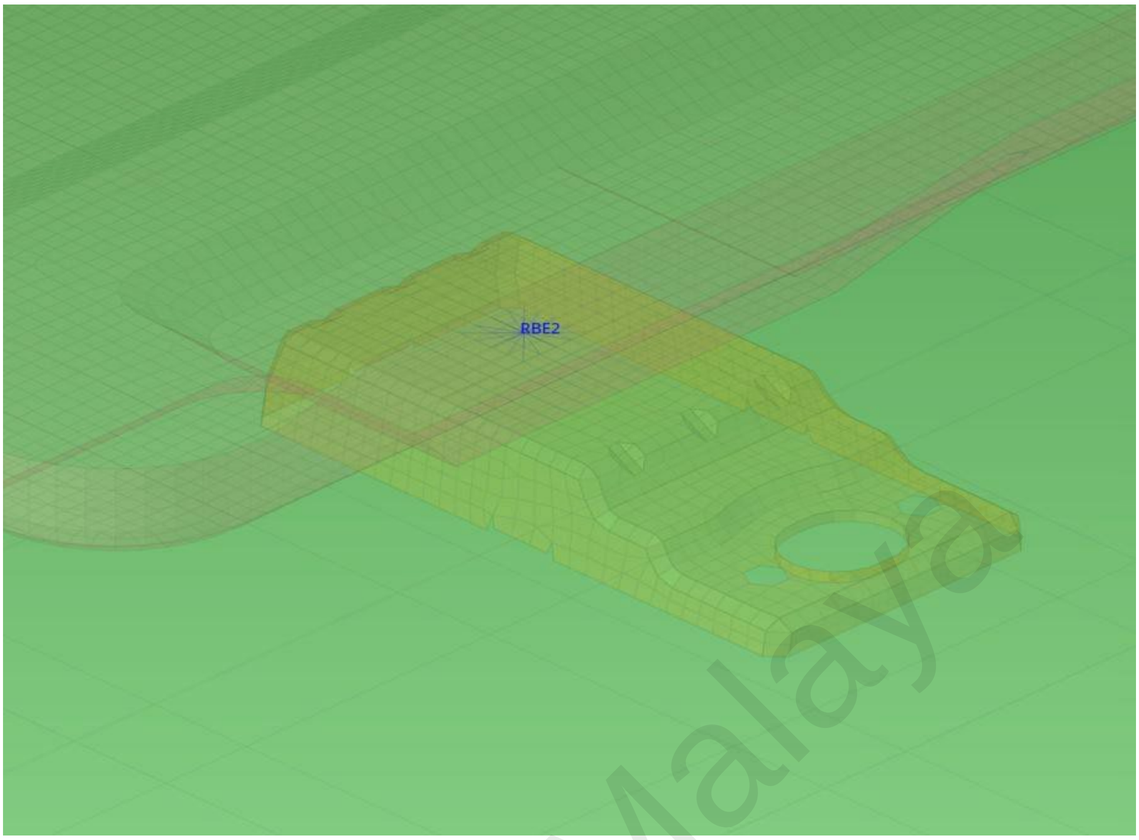

Figure 3.15: Spot welding representation by RBE2 between base leg and base panel.

RBE2 can also be used to stiffen the component. A RBE2 is connected to all the nodes at the bottom surface of the rigid table as shown in Figure 3.16 so that only a single constraint applies at the independent node (center of RBE2), the effect will be transmitted to all the dependent nodes (other nodes connected via RBE2 apart from center node).

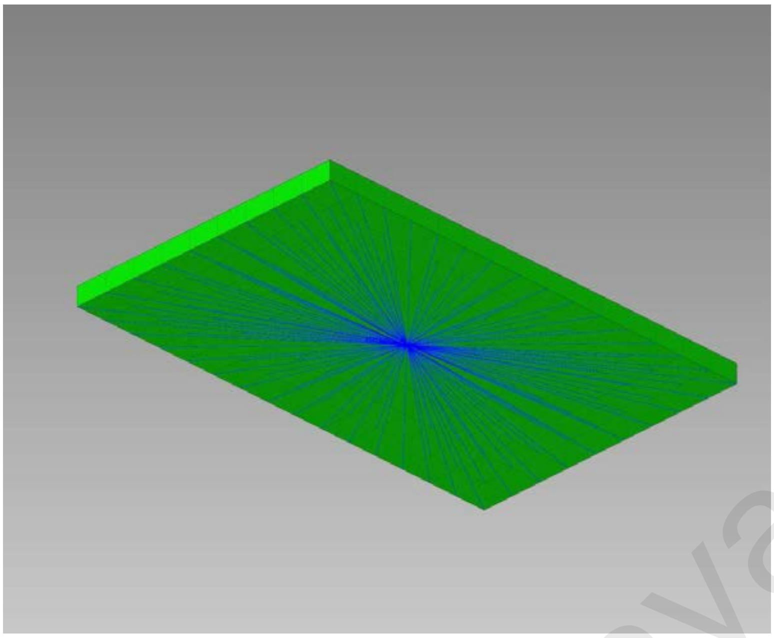

Figure 3.16: RBE2 apply on the bottom surface of the rigid table. The excitation and fixed constraint will be applied on the independent node (center node).

Step 7: Assigning material properties and physical properties.

Table 3.1 shows the material and physical properties associate to each component. The material data are acquired from in house tensile test at DRDM. Since modal and harmonic response analysis only require linear part of the data, only young's modulus, density and Poisson ratio are use in this study.

Table 3.1: Material and physical properties of the FE model.

	Young's Modulus (MPa)	Poisson Ratio	Density (ton/mm3)	Material	Thickness (mm)	Element Type
Base Panel	193,200	0.3	7.85e-09	Steel	0.80	CQUAD4. CTRIA3
Panel leg	193,200	0.3	7.85e-09	Steel	1.00	CQUAD4. CTRIA3
Rigid Table	193,200	0.3	7.85e-09	Steel	N/A	Solid (Hexa8)

The linear material is defined in the FE model via MAT1 card (linear material card) as shown in Figure 3.17.

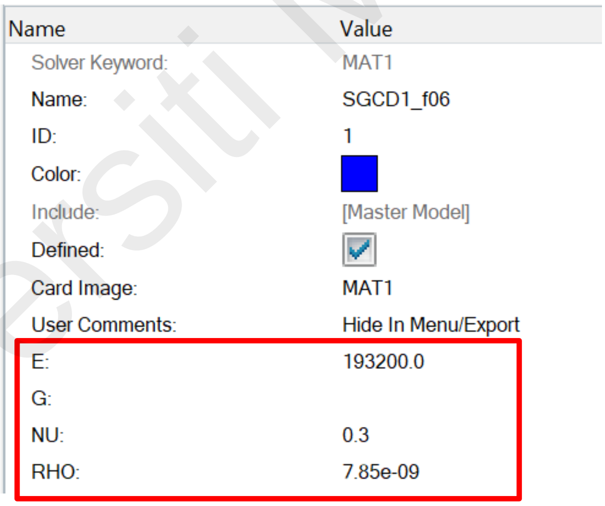

Figure 3.17: Material property input.

In Figure 3.18, the element for base panel and leg are assigned as shell (PSHELL) properties with respective thickness. The rigid table are assigned as solid element (PSOLID) as shown in Figure 3.19.

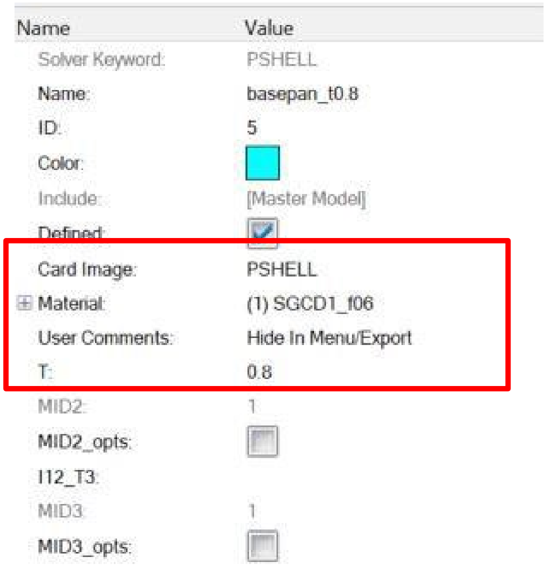

Figure 3.18: PSHELL assigned to CQUAD and CTRIA element (panel and leg).

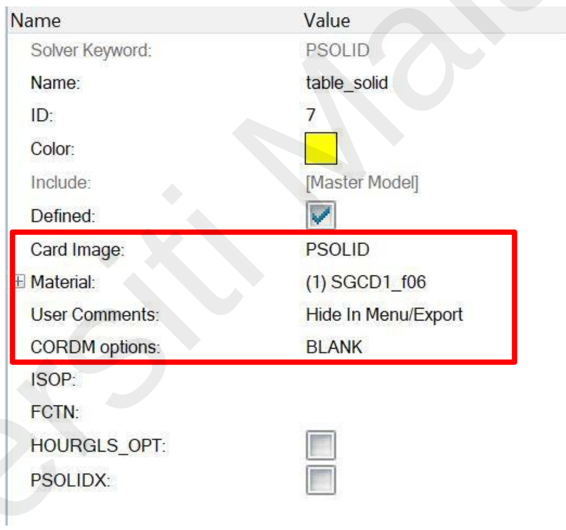

Figure 3.19: PSOLID assigned to Hexa element (rigid table).

Step 8: Create EIGRL card (Eigenvalue extraction card)

To extract mode shape (eigenvector) and natural frequency (eigenvalue) from the FE model, an EIGRL card in Figure 3.20 with a defined range of frequencies is created. The mode shape can be shown in a normalized way, either in mass normalization or displacement normalization. V1 represent the start frequency, V2 is the stop frequency. Thus, the modes and frequency result are from 0Hz – 500Hz range.

Figure 3.20: EIGRL card.

Step 9: Boundary conditions

The boundary conditions for modal analysis are simple, by just fixing 6DOF on the rigid table. In Altair Optistruct®, the keyword is called SPC (single point constraint), in which, users can select which DOF to fix on any nodes. There are total of 6 DOF fixed at the centered node as shown in Figure 3.21.

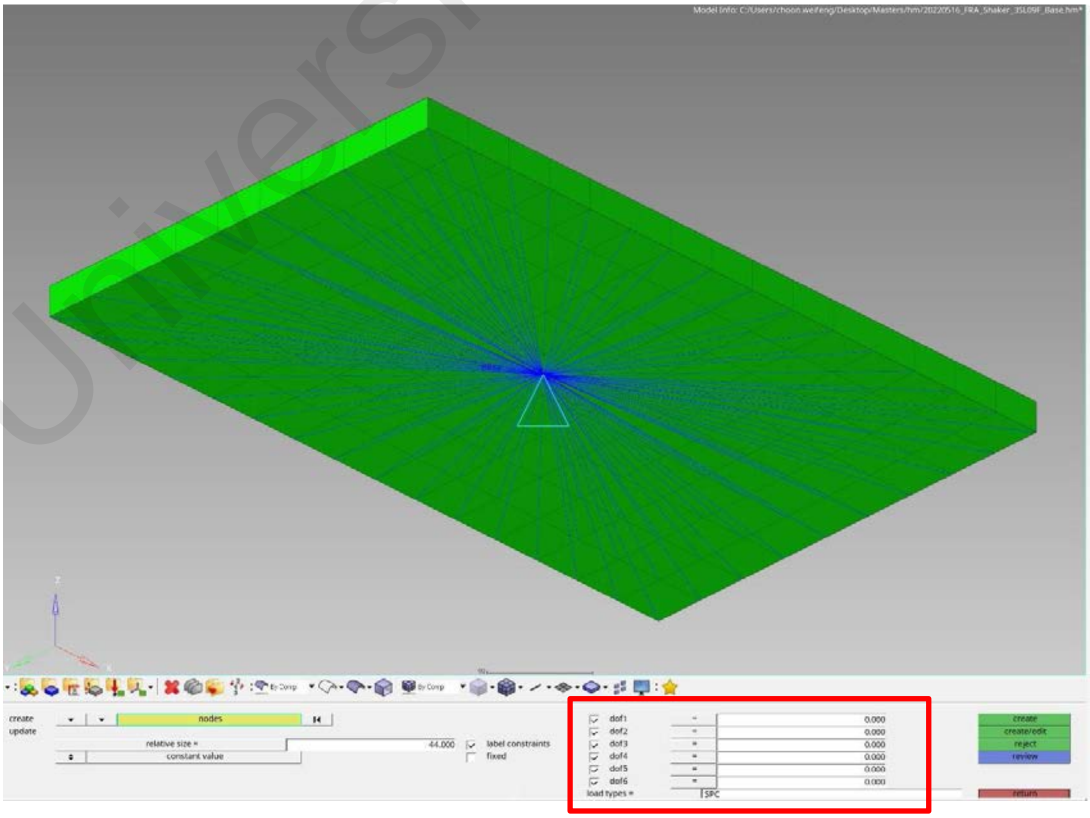

Figure 3.21: SPC, fix all DOF.

Step 10: Create load step

Figure 3.22 shows how to create a modal analysis load step by loading the SPC and EIGRL card to the respective field. The model is ready to be solve by a computer.

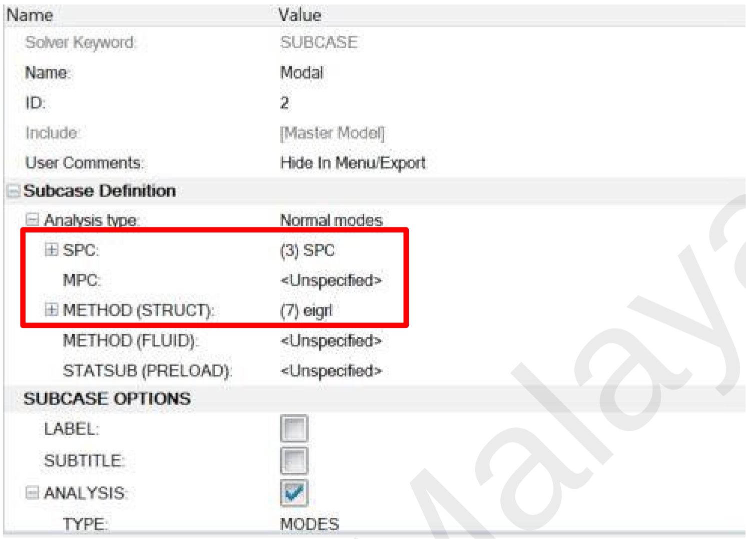

Figure 3.22: Load step.

3.2.1.2 Open-Source Solver (Code_Aster® 2019)

Open-source solver are not as straightforward as commercial solver, as it does not have the resources to improve on user interface and user friendliness. The keyword and settings must be study carefully on the documentation before applying to the model to avoid error and false results. The general step for modal analysis is quite like the commercial software, but the keyword is different. Each important keyword for modal analysis will be compared at the end of this section.

Step 1: Mesh import to Salome Meca module

The meshing steps are done in commercial software (Step 4 – 5 on previous section) since the mesh module at Salome Meca does not have a robust element quality check function and quality assurance function. The mesh file from Altair Optistruct® are export to NASTRAN file (.dat), (since Salome Meca® only reads NASTRAN mesh file) and import subsequently into Salome Meca® mesh module. Figure 3.23 shows the element in Salome Meca®, which imported from Altair Optistruct®, thus having the same node numbers and element shapes with Altair Optistruct® element.

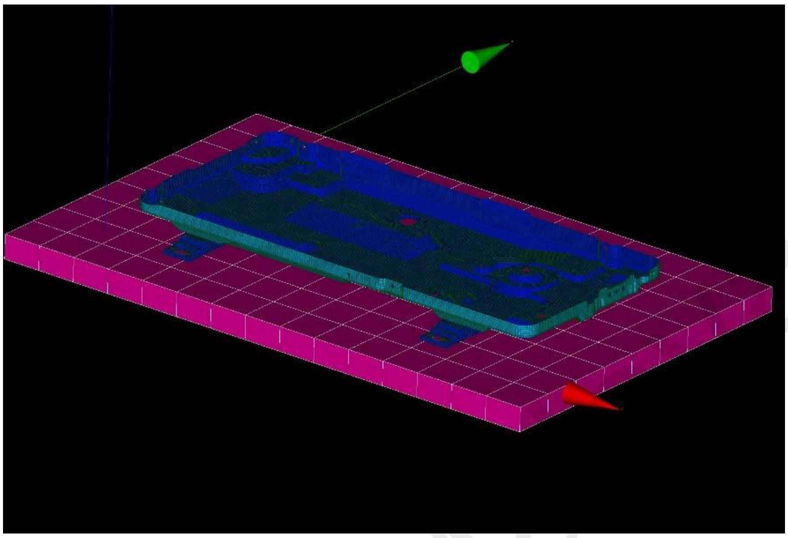

Figure 3.23: Import mesh element into Salome Meca.

Step 2: Mesh assembly for different part component

After importing the mesh, the component will be needed to assemble under one model for easier properties assignment, boundary conditions application and load step creation. To assemble different component mesh, keyword ASSE_MAILAGE was used. By selecting the component mesh 1 and mesh 2 (base panel and table), SUPERPOSE keyword were used to combine both mesh into a new name: ALL_MESH. The component mesh now is all under ALL_MESH component (Figure 3.24). Figure 3.25 is the keyword for mesh assembly.

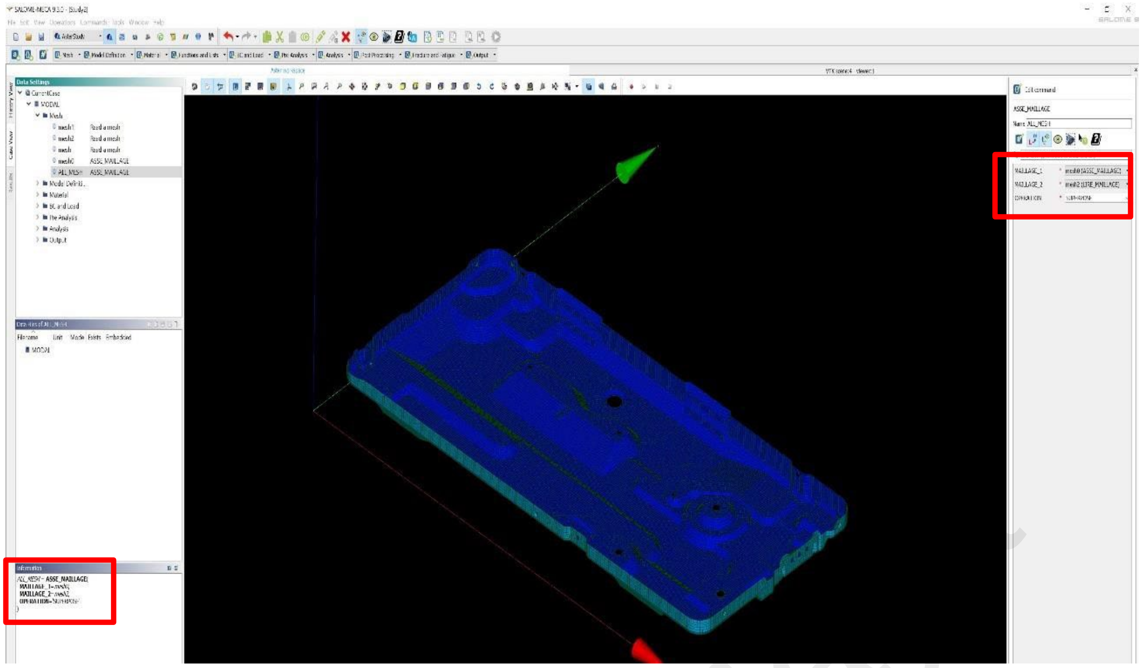

Figure 3.24: Mesh assembling. Aster_Study UI let us to select keyword and apply to the FE model interactively with automatic keyword creation.

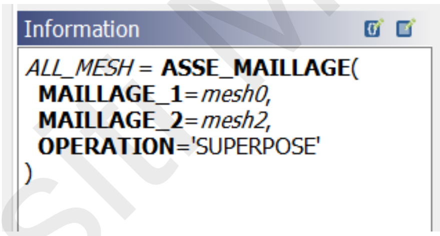

Figure 3.25: Keyword for mesh assembly.

Step 3: Assign finite element properties

By assigning finite element, the keyword is AFFE_MODELE (Figure 3.26). The shell properties are assigned to base panel and base panel leg while solid properties assigned to rigid table. Code_Aster® using keyword DKT as shell element as shown in Figure 3.27, the formulation is like CQUAD and CTRIA in NASTRAN and Altair Optistruct®.

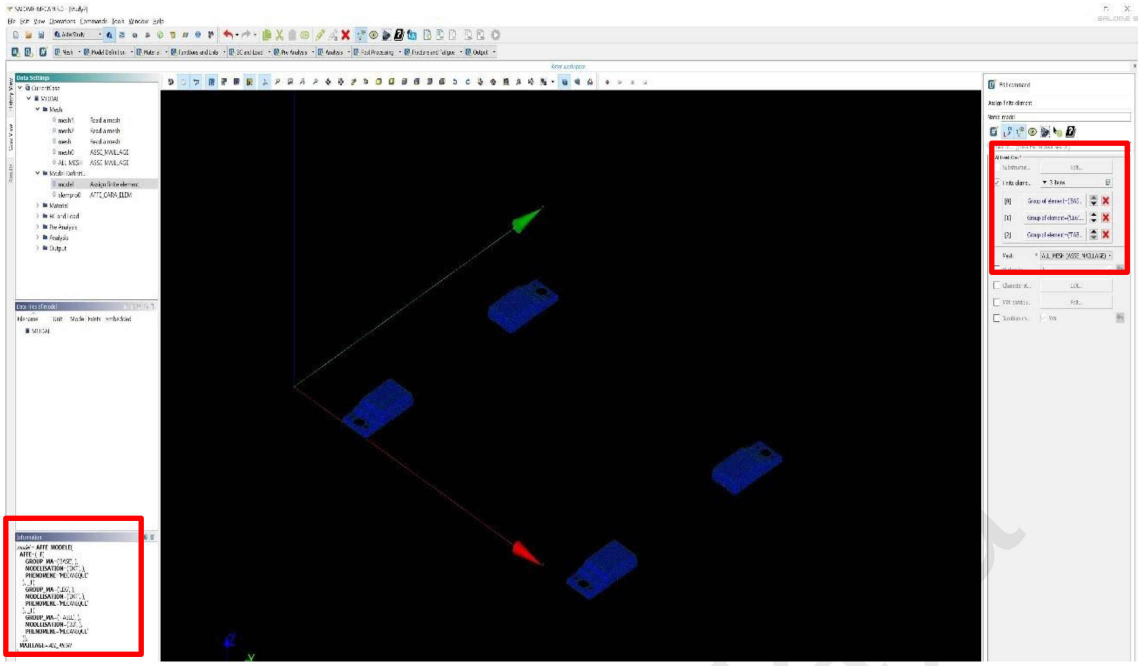

Figure 3.26: Assign properties using AFFE_MODELE.

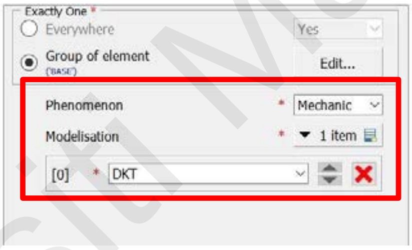

Figure 3.27: Assign DKT to base panel and leg.

To define thickness for shell element, AFFE_CARA_ELEM was used (Figure 3.28). COQUE is shell while EPAIS is thickness. 0.8mm for base panel leg and 1.00mm for base panel, as shown in Figure 3.29. The keyword for assigning shell element thickness is shown in Figure 3.30.

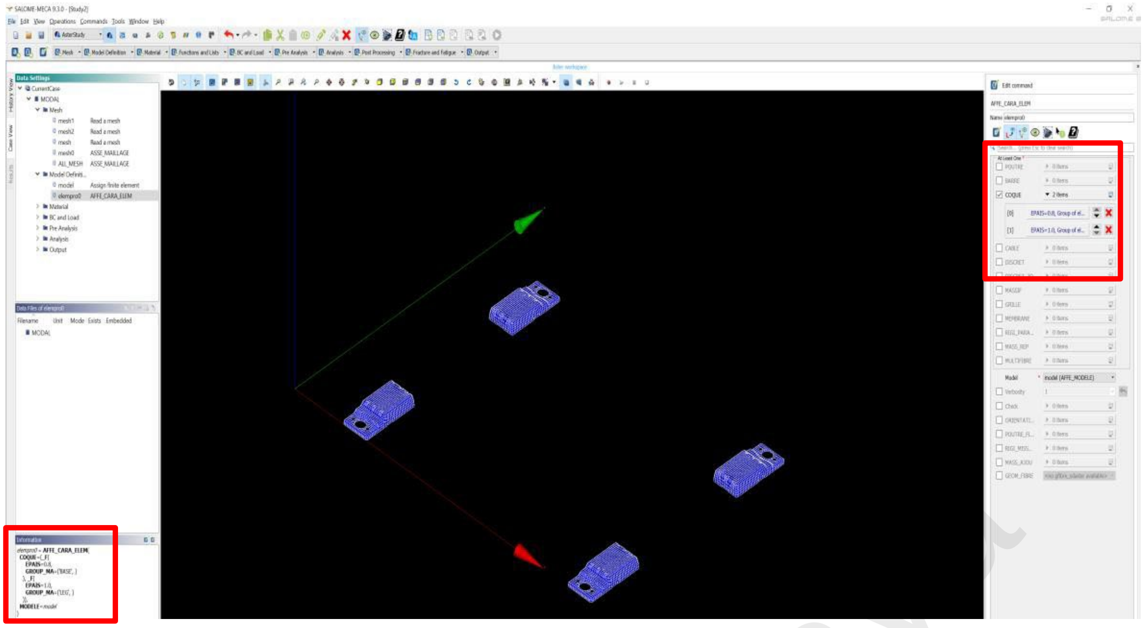

Figure 3.28: Assigning shell thickness.

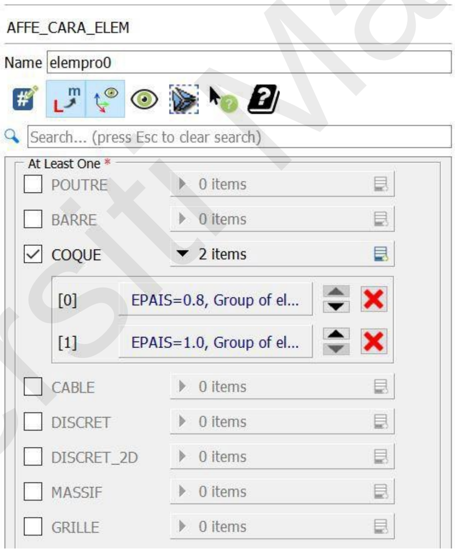

Figure 3.29: Thickness for base panel and leg.

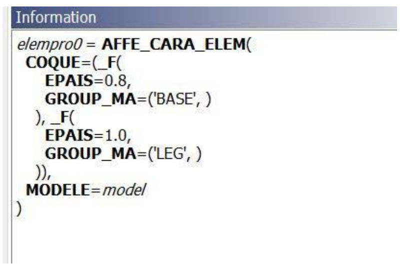

Figure 3.30: Keyword for assigning thickness.

Step 4: Assign material properties

DEFI_MATERIAU keyword is used to define the material and can be access from the GUI shown in Figure 3.31, E is for modulus of elasticity, NU is for poison ratio, and RHO is for density. The unit used here is same as in Altair Optistruct® which is mm, MPa and ton/mm3.

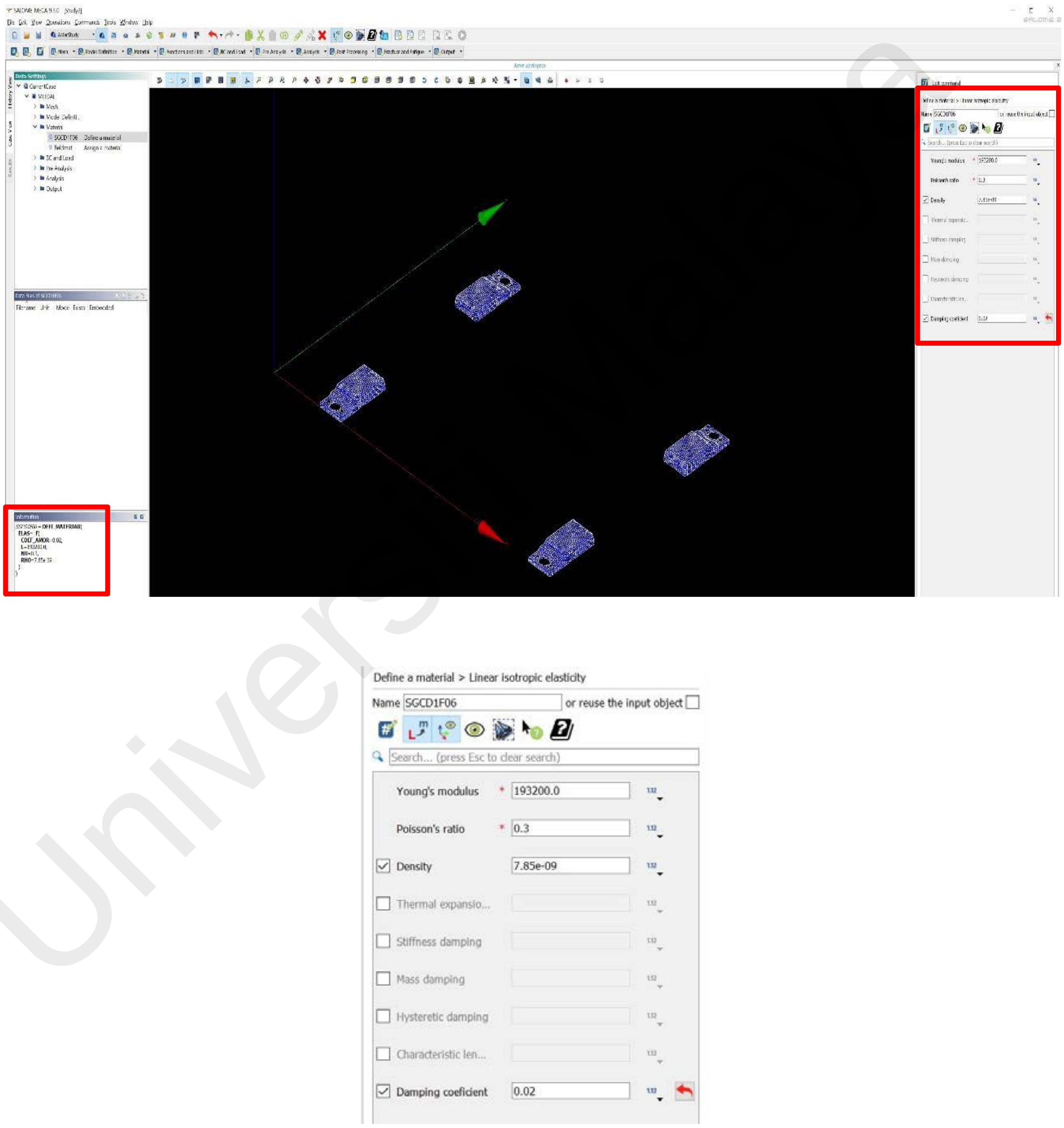

Figure 3.31: Material parameters for steel.

Figure 3.32 shows the material are assigning to all of the elements (“ALL_MESH”), while Figure 3.33 shows the keyword for assigning the material properties.

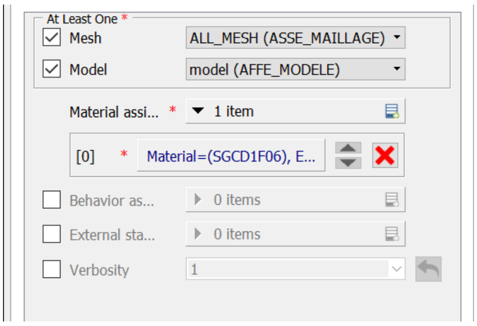

Figure 3.32: Assigning the material defined to all the mesh elements.

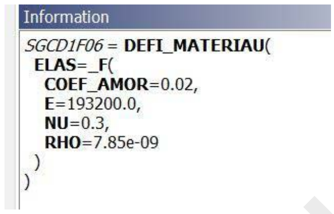

Figure 3.33: Keyword for defining material properties.

Step 5: Assign boundary condition and Rigid body element (RBE)

Boundary condition for modal analysis is straightforward, it only requires fixation point. Keyword AFFE_CHAR_MECA (DDL_IMPO = F(DX = 0.0, DY = 0.0, DZ = 0.0)) will be used as shown in Figure 3.34. Since the rigid table cannot be moved in X, Y, Z direction, displacement of 0 will be imposed (Figure 3.36) to all the nodes of base of rigid table as shown in Figure 3.35.

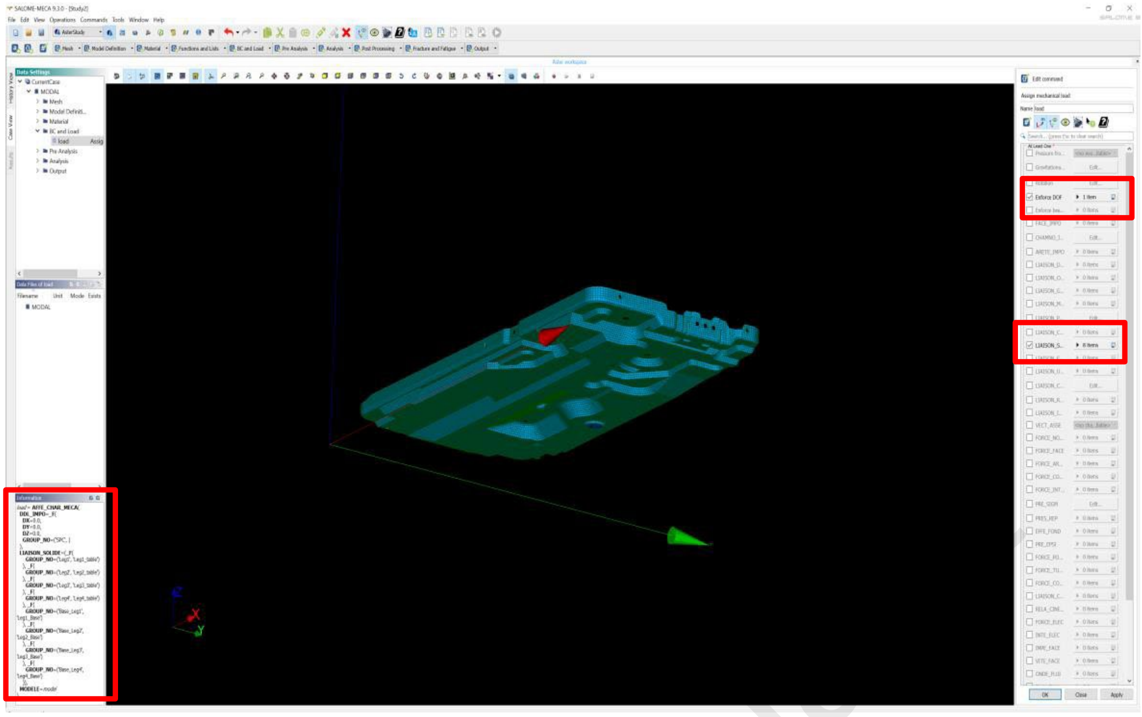

Figure 3.34: Assigning of fix boundary condition and rigid body element.

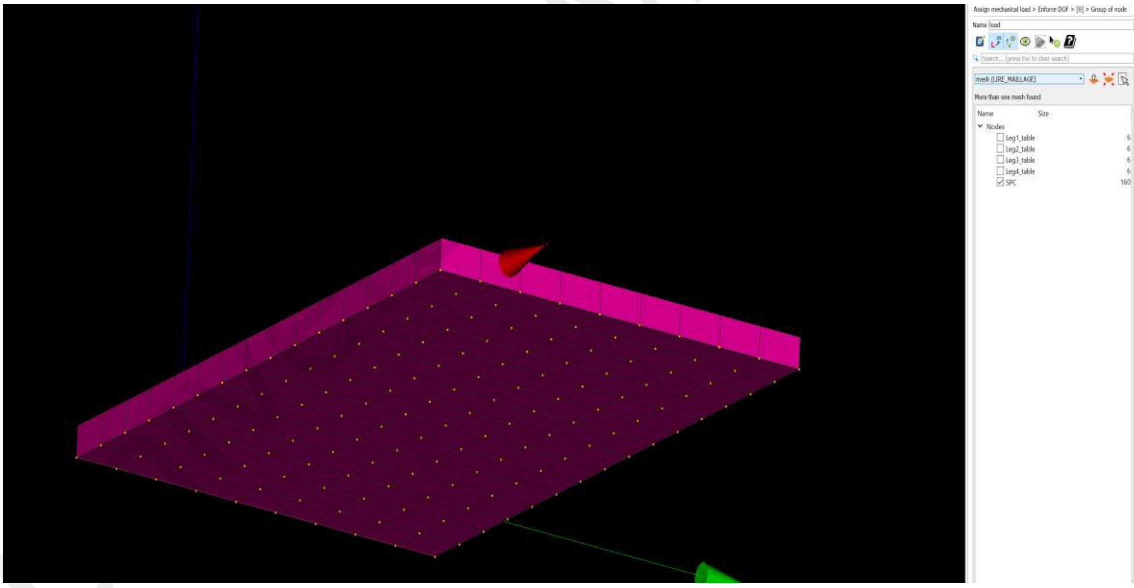

Figure 3.35: Fix boundary condition on the base of rigid table.

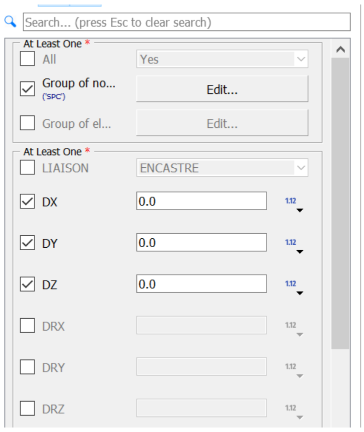

Figure 3.36: Fix on X, Y, Z DOF.

The rigid body element is used to connect between the base panel and leg, the leg, and the rigid table. Keyword LIASON_SOLIDE will be used as shown in Figure 3.37.

Figure 3.37: Link between 4 legs and table, 4 legs and panel.

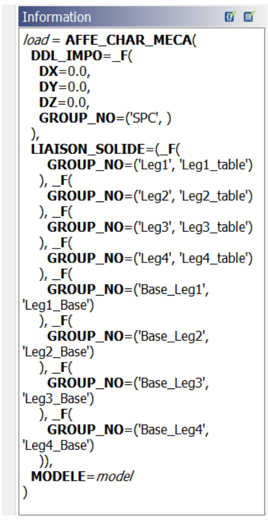

Figure 3.38: Keyword for defining boundary condition.

Step 6: Pre-analysis (stiffness matrix assembly)

In Code_Aster® modal analysis, the dynamic equation matrix (mass and stiffness) needed to define prior the analysis. ASSEMBLAGE (MATR_ASSE) keyword was used (Figure 3.39). The mesh mode, material and physical properties, and boundary condition were also assigned to the assembly matrix.

Figure 3.40 shows the assignment of the material field, element properties, and model to the assembly matrix (MATR_ASSE). Figure 3.41 is the keyword for defining assembly matrix.

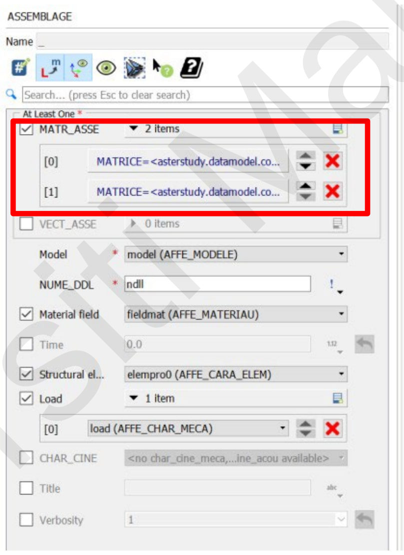

Figure 3.39: Defining stiffness matrix and mass matrix.

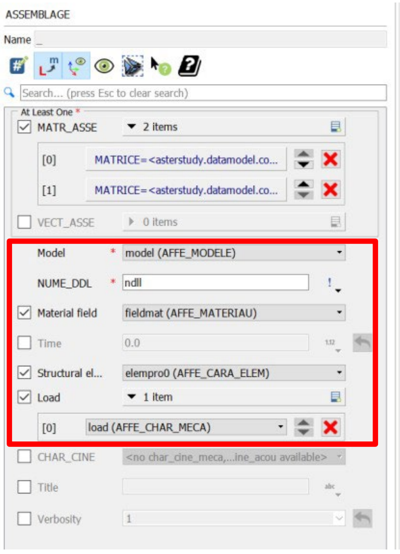

Figure 3.40: Assigning model, number of DOF, material and boundary condition to matrix assembly.

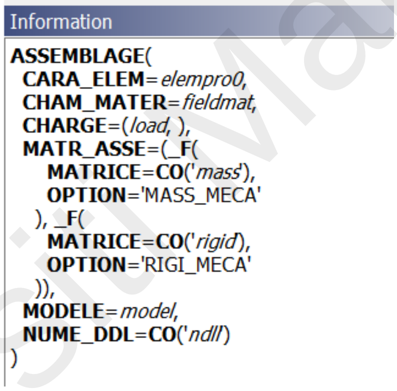

Figure 3.41: Keyword for defining matrix.

Step 7: Load step creation

Assigning the input file to include keyword for solving modes and natural frequency, by using Lanczos method. Like in the commercial solver, range of frequency need to be defined prior solving. Mass normalization on the mode shape vectors was chosen to ease the comparison between solvers. The keyword used here is CALC_MODES (Figure 3.42).

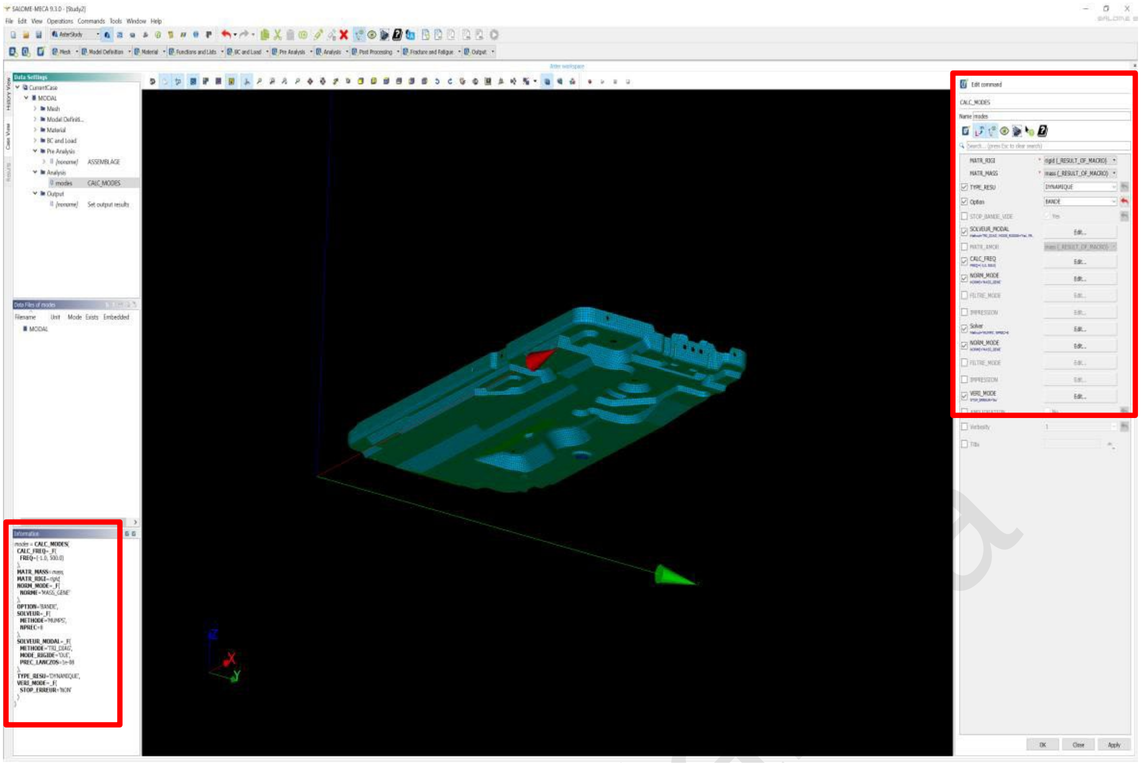

Figure 3.42: Load step creation.

Loading the matrix into the load step as shown in Figure 3.43, with MATR_RIGID (stiffness matrix) and MATR_MASS (mass matrix).

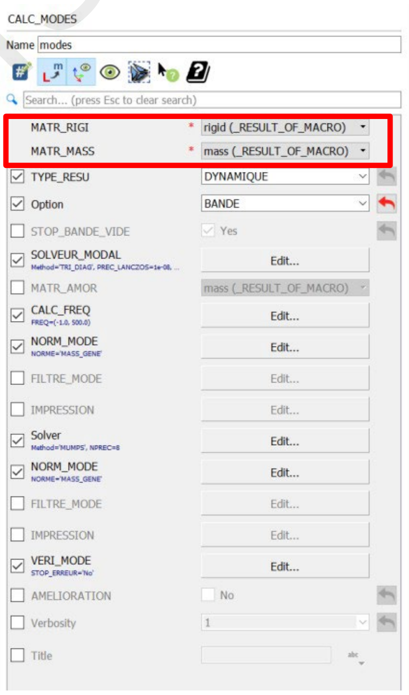

Figure 3.43: Assign assembly matrix defined previously.

Setting represented in Figure 3.44 such as TYPE_RESU = ‘DYNAMIQUE’ is to tell the solver that this is a dynamic analysis. OPTION = ‘BANDE’ was used to search a list of mode in the specify frequency range.

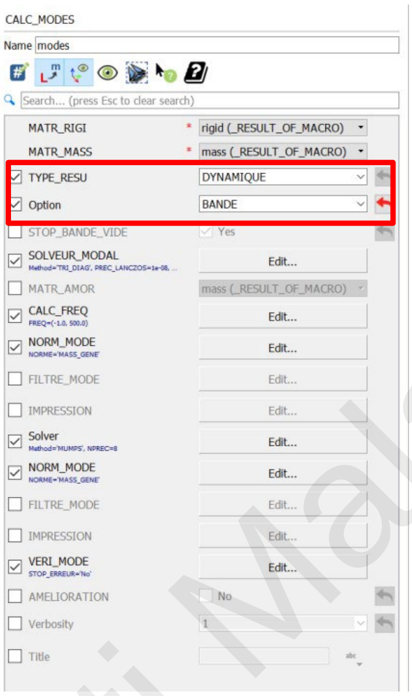

Figure 3.44: Result type and result extraction method.

Figure 3.45 shows the remaining parameters susch as CALC_FREQ, which represent the range of frequency that specify by users on modes searching. NORM_MODE = ‘MASS_GENE’ was used to normalize the mode shape vectors. MUMPS solver was used in this analysis.

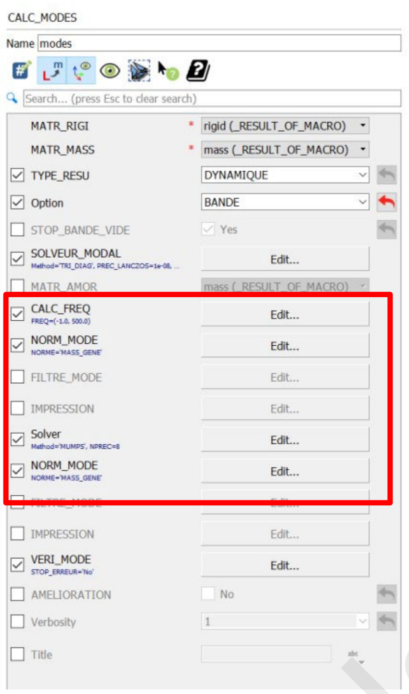

Figure 3.45: List of specify frequency on searching modes, mass normalization and MUMPS solver.

Figure 3.46 shows the keyword for assigning load step.

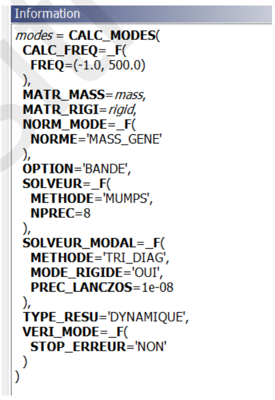

Information

```
modes = CALC_MODES(
  CALC_FREQ=_F(
    FREQ=(-1.0, 500.0)
  ),
  MATR_MASS=mass,
  MATR_RIGI=rigid,
  NORM_MODE=_F(
    NORME='MASS_GENE'
  ),
  OPTION='BANDE',
  SOLVEUR=_F(
    METHODE='MUMPS',
    NPREC=8
  ),
  SOLVEUR_MODAL=_F(
    METHODE='TRI_DIAG',
    MODE_RIGIDE='OUI',
    PREC_LANCZOS=1e-08
  ),
  TYPE_RESU='DYNAMIQUE',
  VERI_MODE=_F(
    STOP_ERREUR='NON'
  )
)
```

Figure 3.46: Keyword that used to define load step.

Step 8: Result output

IMPR_RESU keyword was used to save and export simulation results file to a specify location (Figure 3.47).

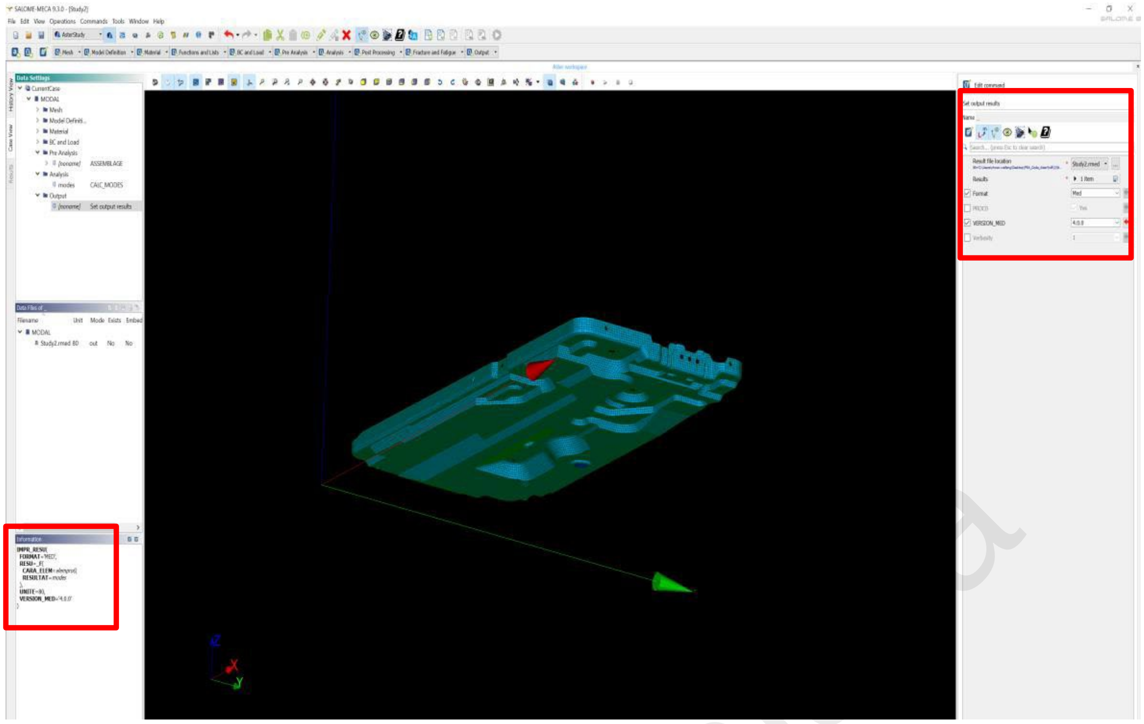

Figure 3.47: Set output results and location.

The format used was in .rmed (result med file) as med is the mesh file for Code_Aster®. The result file are save at same location with the model file and input file (.hdf and.comm). The settings are shown in Figure 3.48.

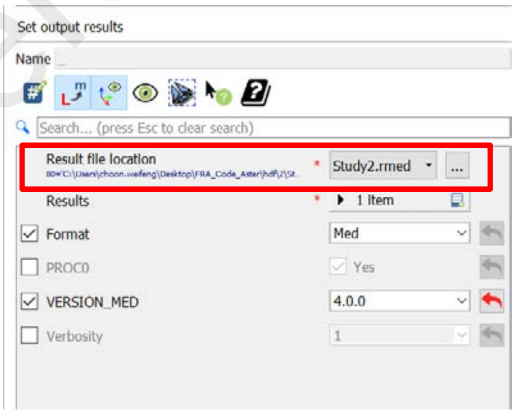

Figure 3.48: Set ouput results.

Step 9: Run analysis

The last step involves in running the analysis in a Windows PC. Choose history tab and select current case and set parameters as shown in Figure 3.49.

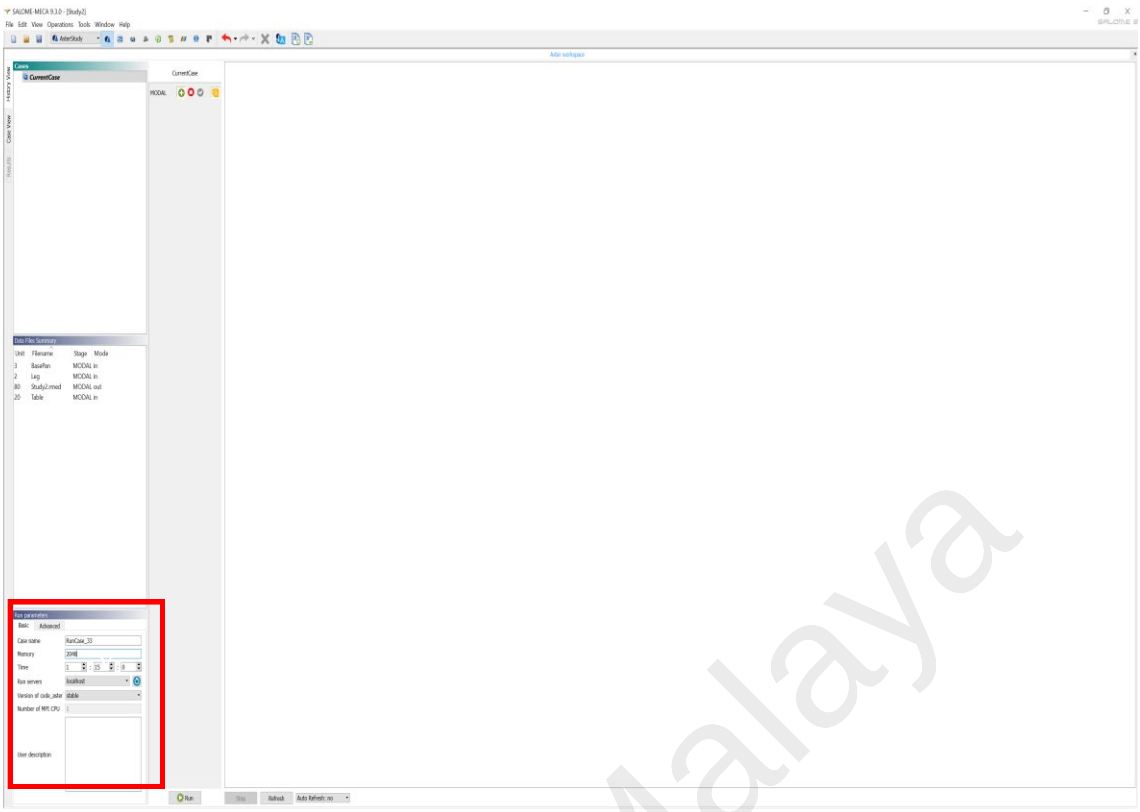

Figure 3.49: Run analysis setting.

In run parameters (Figure 3.50), define a case name, assigning RAM (simple modal analysis 2048Mb was enough) and running time (as much as possible although modal analysis does not require much time to solve).

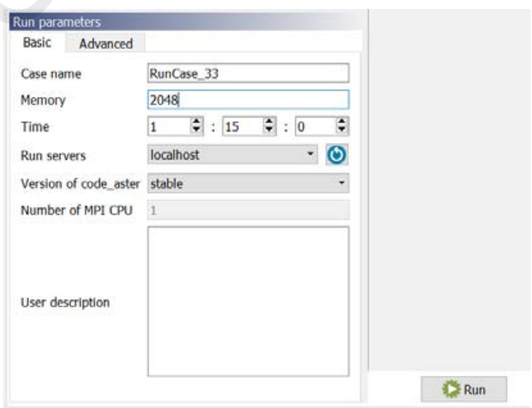

Figure 3.50: Run parameters.

3.2.2 Harmonic Response Analysis

After modal analysis was set up and the result is verified, the next step is to perform harmonic response analysis. The mesh properties and material properties are exactly similar as modal analysis since it is the same model and will not be discussed here again. Instead, this section will be focused on boundary conditions and onward.

3.2.2.1 Commercial Solver (Altair's Optistruct® 2021)

Step 1: Create excitation input point

Response analysis needed at least a source of excitation as an input. The source of excitation is a constant 1g acceleration acting on the rigid table (shaker). Thus, the center of RBE2 on the base of table is selected as an input source (in Z – direction only). SPCD card or single point constraint will represent the excitation source on single node. Since the node are tie via RBE2 with the other nodes, the whole base structure will move together, as shown in Figure 3.51.

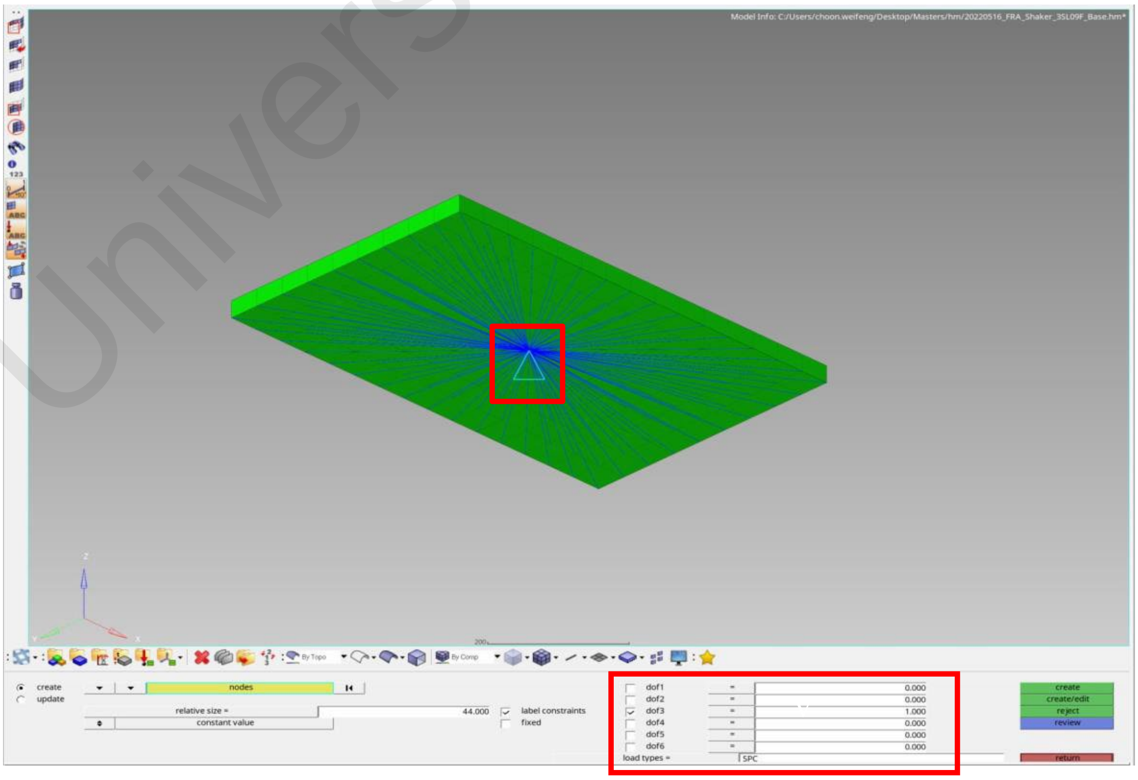

Figure 3.51: SPCD, single point constraint on the centered node.

Step 2: Excitation load profile creation

The real shaker excitation source is a constant acceleration of 1g from 5Hz to 100Hz. Thus, a TABLED card was created to key in the information with X-axis as frequency, Y-axis as 1g acceleration as shown in Figure 3.52.

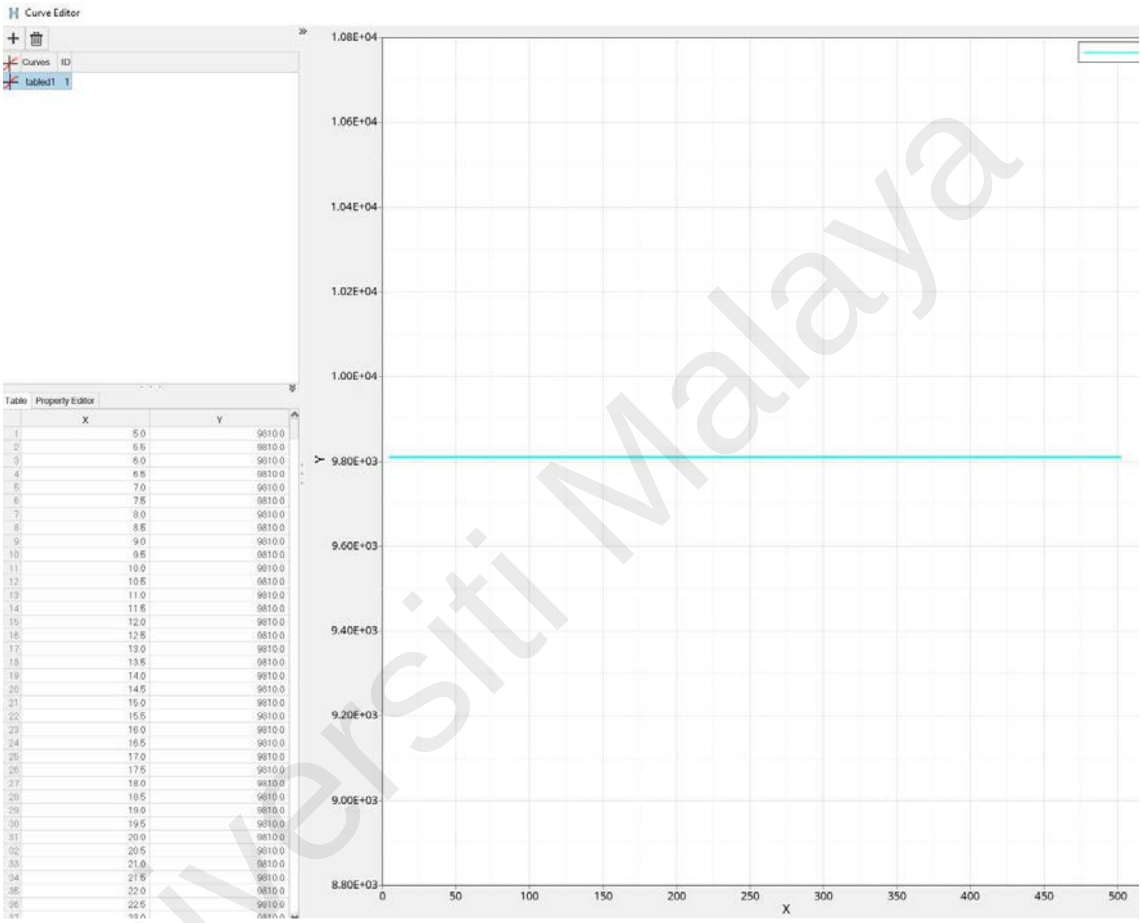

Figure 3.52: Excitation data in table format.

Step 3: Create harmonic load

Harmonic load was created under the RLOAD2 card load collector. Figure 3.53 shows the parameter setting for RLOAD2. The EXCITEID is the centered node assigned with SPCD, TB is assigned with dedicated shaker load profile, and load type is ACCE (acceleration).

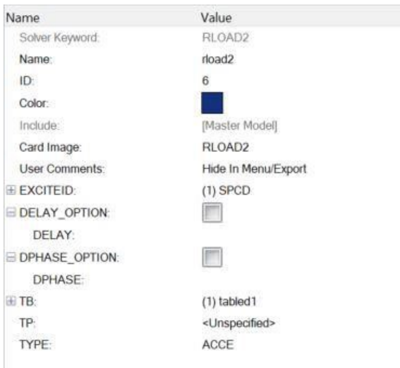

Figure 3.53: RLOAD2, with harmonic load parameters.

Step 3: Create frequency step for results

A set of frequency intervals must be specified for the output and results. FREQi card was (Figure 3.54) used to define the frequency range from 5Hz (F1) to 100Hz, in the resolution of 0.5Hz (DF), a total of 1000 increments (NDF).

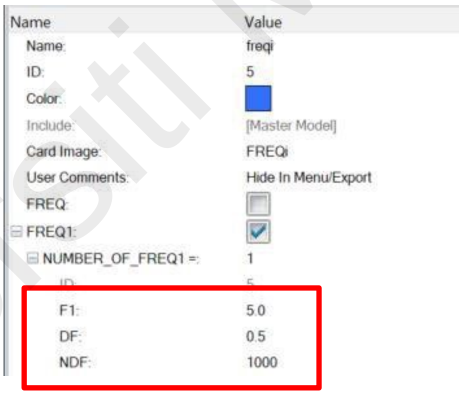

Figure 3.54: Frequency step result output definition.

Step 3: Create global output request

By default, Altair Optistruct® does not have output results unless it is specified by users. Global output request card was used to declare the output such as displacement, velocity, acceleration, stress and strain to the solver. Figure 3.55 shows the acceleration output request for the model. The acceleration is to be compare with the experiment results.

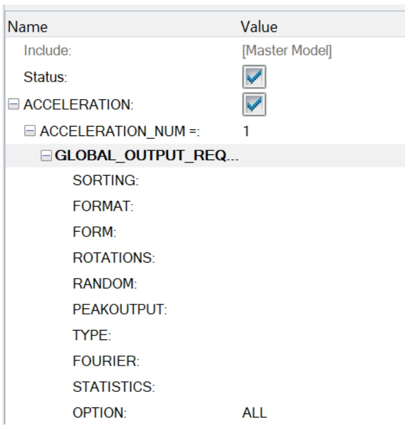

Figure 3.55: Acceleration output request.

Step 4: Create harmonic response analysis load step

Similar as previous method, a load step must be defined before solving the problem. Assign the SPC constraint, RLOAD2 excitation data, and FREQi frequency step to the harmonic response analysis card, as shown in Figure 3.56. The model ready to be solve in local Windows PC.

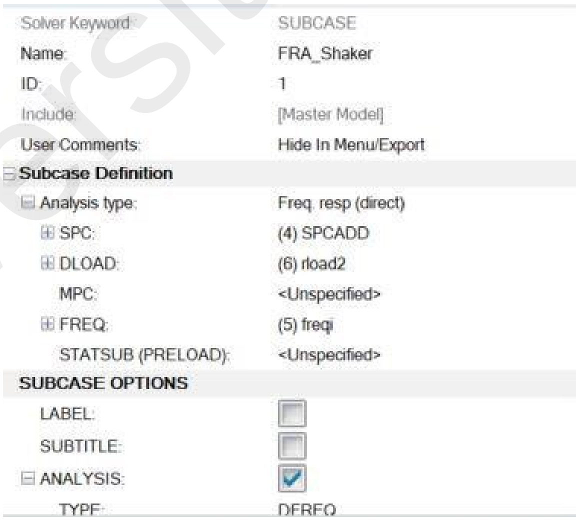

Figure 3.56: Harmonic response load step.

3.2.2.2 Open-Source Solver (Code_Aster® 2019)

For Code_Aster®, the basic idea of settings is similar. Parameters such as harmonic excitation input, stiffness matrix (harmonic excitation vector), and frequency step output, and harmonic load step creation is required to run the simulation.

Step 1: Apply load and specify nodes and direction

To apply harmonic load, one must specify the nodes and direction. The base of rigid table is selected to apply the load, with only Z direction, as shown in Figure 3.57.

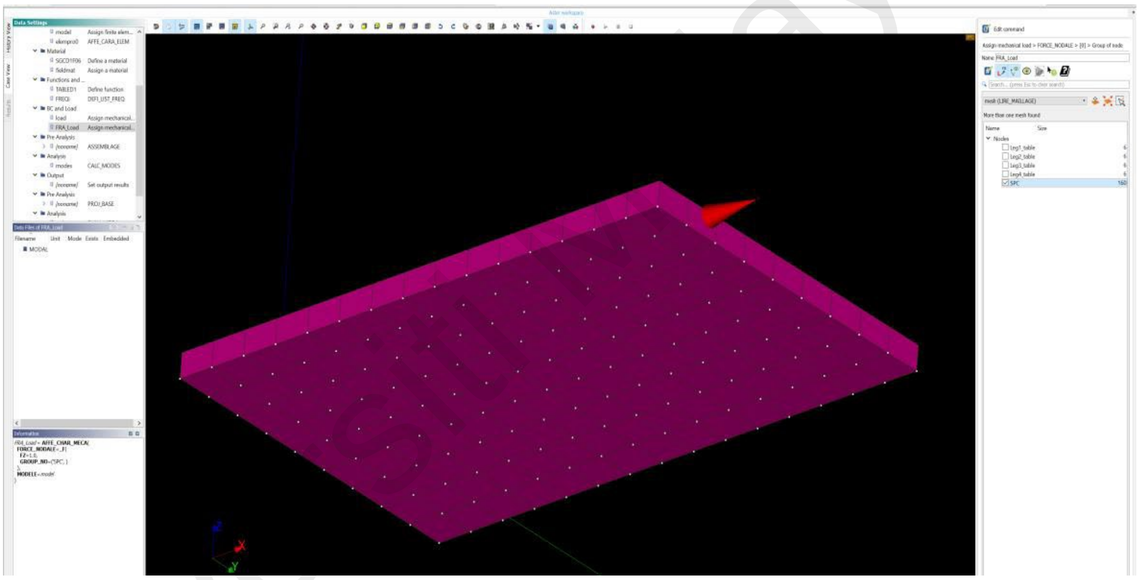

Figure 3.57: 160 nodes at the base of the table. which subjected to 4.81N harmonic load.

Figure 3.58 shows only the vertical direction are applied on the base for harmonic load (FZ). Figure 3.59 is the keyword for load assignment.

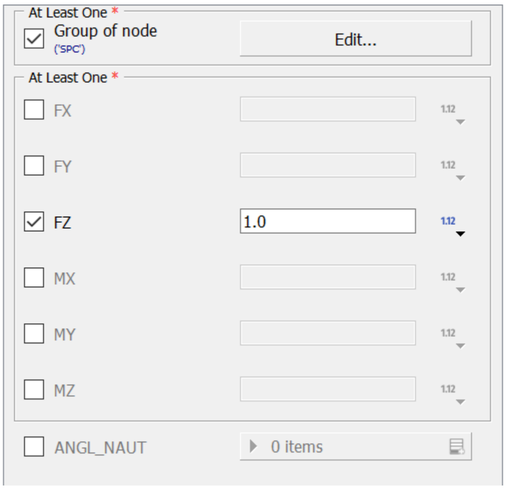

Figure 3.58: The harmonic load only acts upon Z direction.

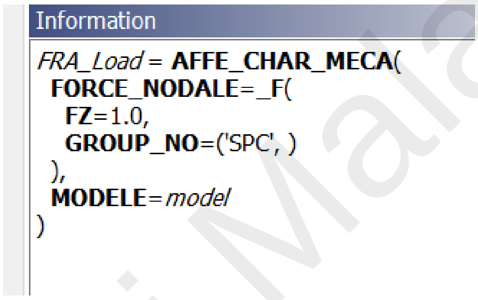

```
Information
FRA_Load = AFFE_CHAR_MECA(
  FORCE_NODALE=_F(
    FZ=1.0,
    GROUP_NO=('SPC', )
  ),
  MODELE=model
)
```

Figure 3.59: The keyword for load assignment.

Step 2: Harmonic force excitation calculation and table creation

Code_Aster® 2019 does not have acceleration excitation keyword. To apply 1G acceleration onto the rigid table, force is used instead. A simple conversion from 1G acceleration to force via newton's 2nd law:

$$F = ma \tag{3.1}$$

Where a is the acceleration, F is the force and m is the mass. By plugin in mass of rigid table and 1G acceleration (9.81m/s^2), we can acquire the harmonic force. The mass of the rigid table is calculated by the density relationship:

� = � × � ����� (3.2)

where �is the density of the material. The volume of the rectangular shaped rigid table is 0.01 cubic meter, while the density of steel is 7850kg/m3. This gives us the mass of 78.5kg. Plugin in into equation 3.1, the **force require are 770.1N.** There are as many as 160 nodes on the base of the table, thus 770.1N/160 = 4.81N of force are acting on each individual node.

To define a table function, DEFI_FONCTION keyword was used as shown in Figure 3.60and Figure 3.61.

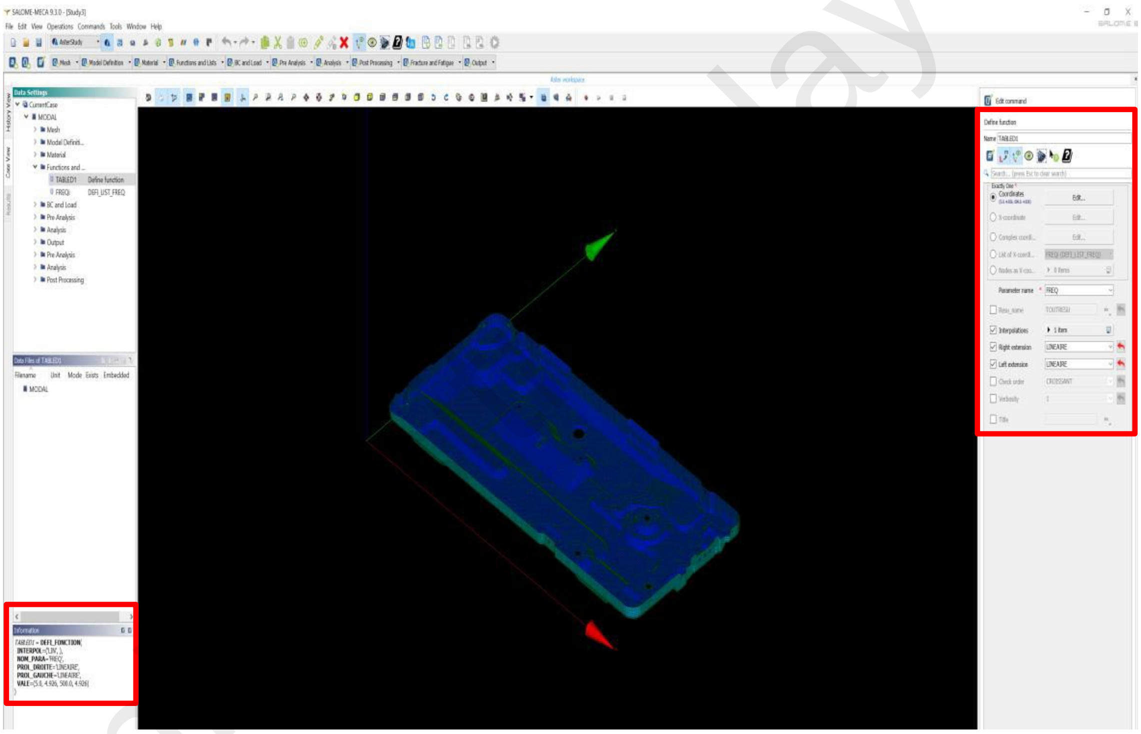

Figure 3.60: Define excitation function.

The parameters are set to be FREQ (frequency), using linear interpolation (LINEAIRE), from 5Hz to 500Hz with 4.81N of force, as shown in Figure 3.62. The keyword harmonic load table definition is shown in Figure 3.63.

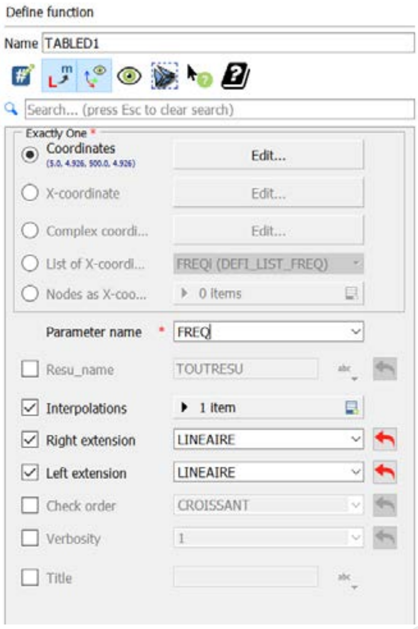

Figure 3.61: Define function parameters.

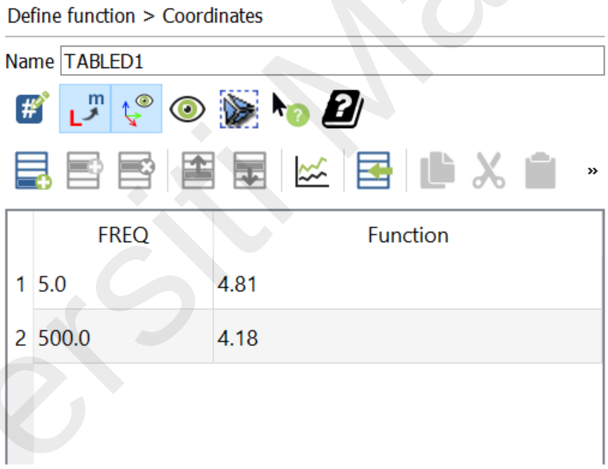

Figure 3.62: 5Hz to 500Hz, with 4.81N force.

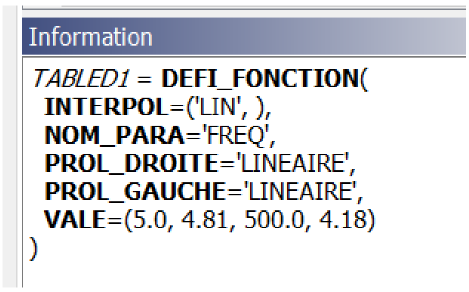

Figure 3.63: Keyword for harmonic load table definition

Step 3: Matrix assembly

Once again, Code_Aster® requires users to define the dynamic equation matrices. The mass and stiffness matrix remain the same as modal analysis, with one additional harmonic force vector matrix, by using ASSEMBLAGE keyword (Figure 3.64).

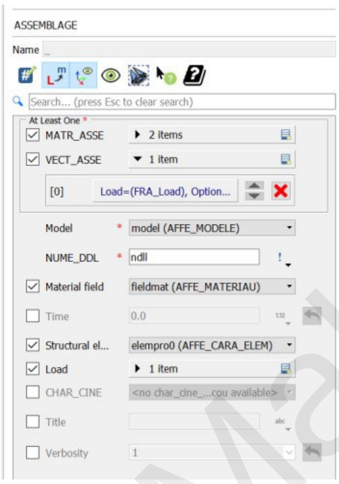

Figure 3.64: Matrix assembly parameters.

For the force matrix properties, VECT_ASSE was used. The VECTEUR is the name specified, option is using CHAR_MECA (mechanical load), select the load collector defined on step 1 for ‘Load’ input, as shown in Figure 3.65.

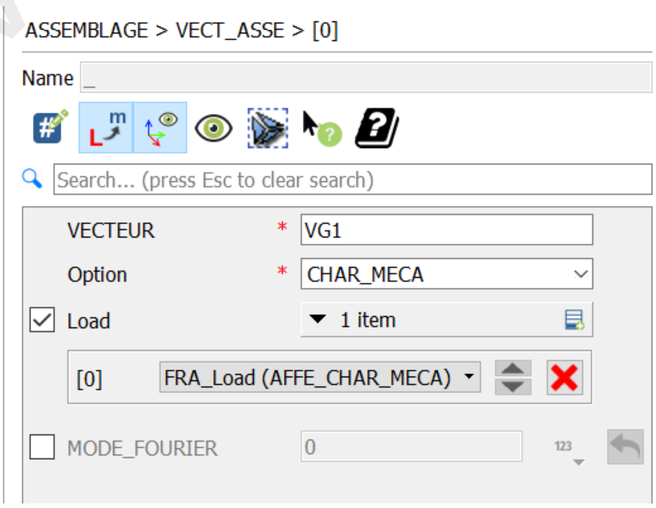

Figure 3.65: Harmonic load matrix.

The keyword for matrix assembly is shown in Figure 3.66.

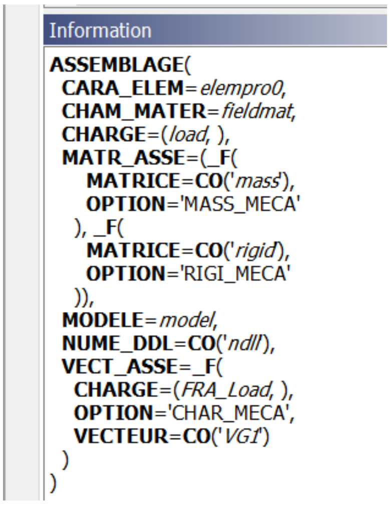

Figure 3.66: Matrix assembly keyword.

Step 4: Define harmonic load step calculation

DYNA_VIBRA keyword was used to define harmonic response load step calculation. The parameters include the list of force excitation data (created in step 2), calculation type, mass, stiffness, and force matrix, and damping coefficient, as shown in Figure 3.67.

The BASE_CALCUL is listed as GENE, which is a general calculation (direct method), TYPE_CALCUL as HARM, which is harmonic response type of calculation. MATR_MASS and MATR_RIGI are the mass and stiffness matrix as created in modal load case previously.

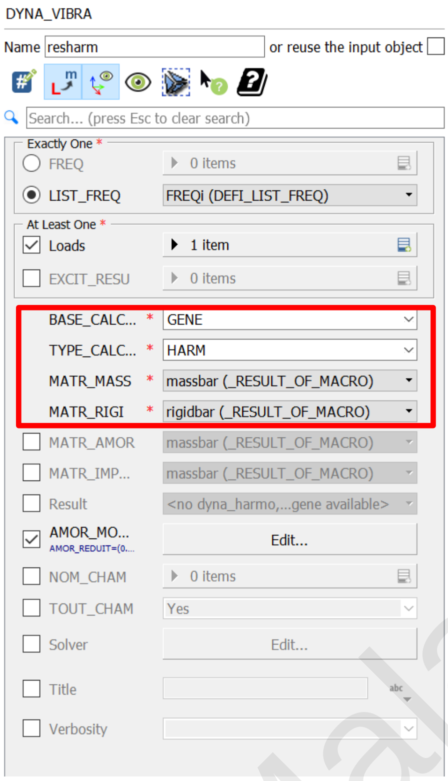

Figure 3.67: DYNA_VIBRA keyword.

For the excitation load in Figure 3.68, VECT_ASSE_GENE, the force matrix define on step 3 will be selected. Multiplier function is the tabulated data defined on step 3 (DEFI_FONCTION).

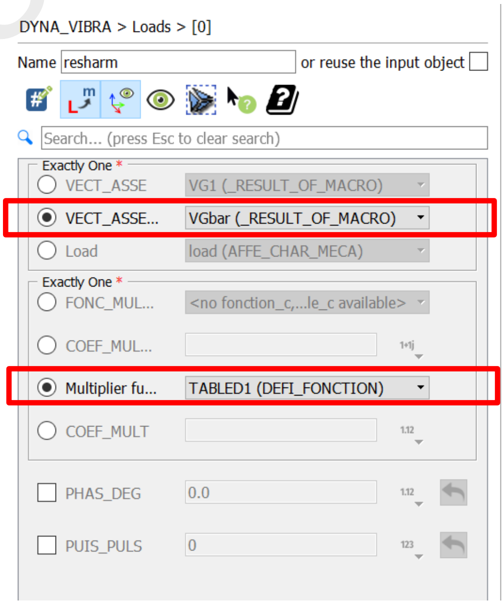

Figure 3.68: Load input parameters.

The damping coefficient of 3% (0.03) will be used in our harmonic response analysis. Code_Aster® is using AMOR_REDUIT (loss factor) for damping definition, as shown in Figure 3.69, which is the half of damping coefficient (0.015).

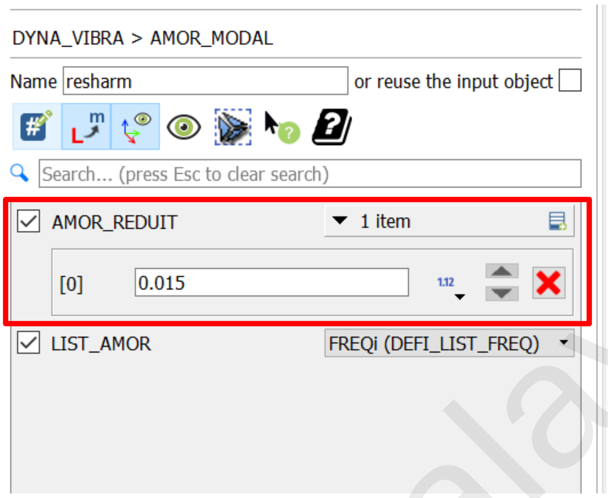

Figure 3.69: Damping definition.

Figure 3.70 shows the keyword for defining harmonic load matrix assembly.

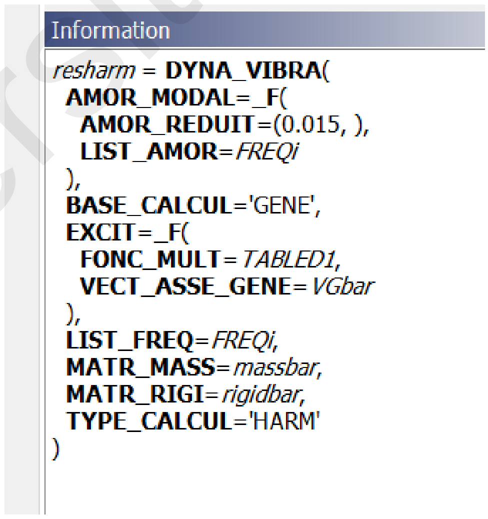

Figure 3.70: Keyword for harmonic load step.

Step 5: Define harmonic load step

By default, Code_Aster® does not output any meaningful result. User must specify which result to be calculate by using REST_GENE_PHYS keyword. Select harmonic load step

(DYNA_VIBRA) created at step 4 for RESU_GENE. For type of result to be outputted, use NON_CHAM keyword and select ACCE and DEPL (acceleration and displacement response will be calculated), as shown in Figure 3.72.

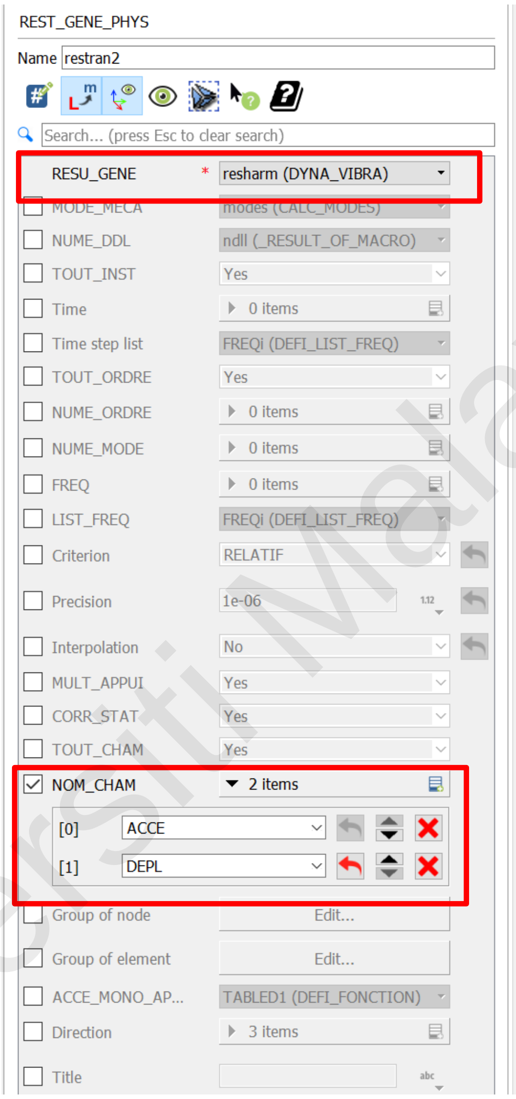

Figure 3.71: Result output.

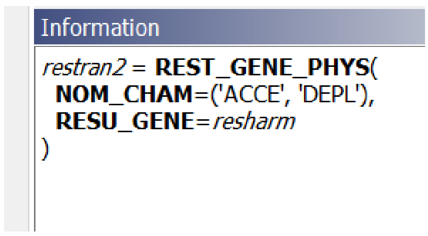

Figure 3.72: Keyword for result output.

Step 6: Define output request

For result definition, harmonic load step defined at step 7 will be selected as shown in Figure 3.73 and Figure 3.74. The model is now ready to be solve in Windows PC.

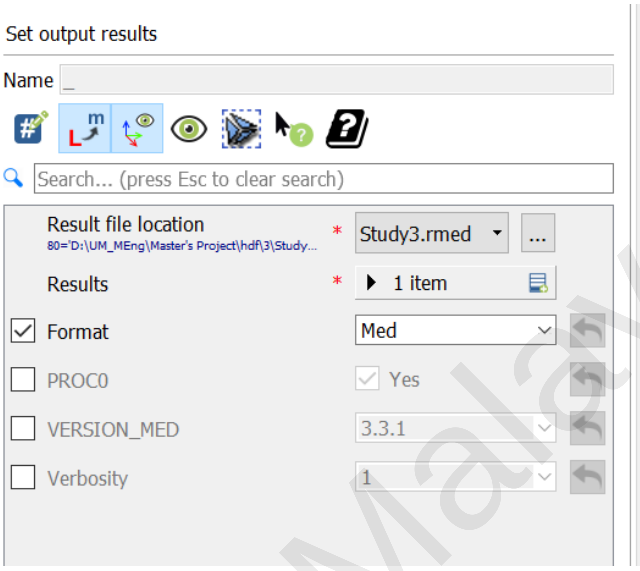

Figure 3.73: As same as modal analysis, rmed is the result file generated.

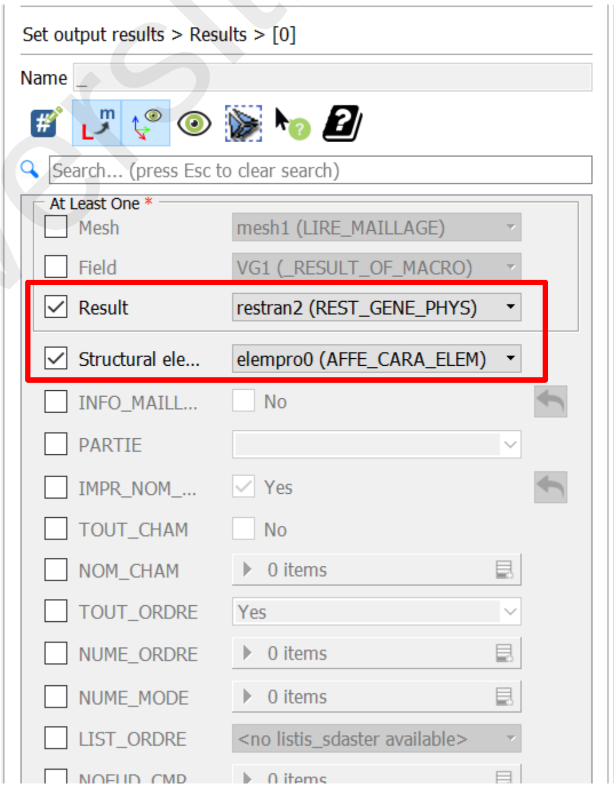

Figure 3.74: Result output file.

3.3 Commercial vs Open-Source FEA Result Extraction and Comparison

This section will be focused on how to post process the simulation result for both modal analysis and harmonic response analysis in Altair Optistruct® and in Code_Aster® 2019. To achieve objective number 2, post processing methodology is very important to ensure both result from commercial software and open source are comparable. On the commercial software (Altair's Optistruct®), the post processor is within the same software package called Altair's Hyperview®. It is a very powerful post processor that capable of many personal preferences (such as contours, lighting, CAD representation etc) on FE model results. On the other hand, Code_Aster® 2019 is relying on an open-source post processor called ParaView®. The default post processor on Salome Meca® module is not as customizable as ParaView®. Like Hyperview®, ParaView® is a powerful post processor too, but the learning curve is very steep as the support and tutorial is very limited, especially on complex model.

3.3.1 Commercial Post Processor (Altair Hyperview)

3.3.1.1 Modal Analysis

Step 1: Load the result file

After running the simulation, Altair Optistruct® will generate a result file (.h3d), use Hyperview® to open and view the file. Hyperview® default interface is shown in Figure 3.75.

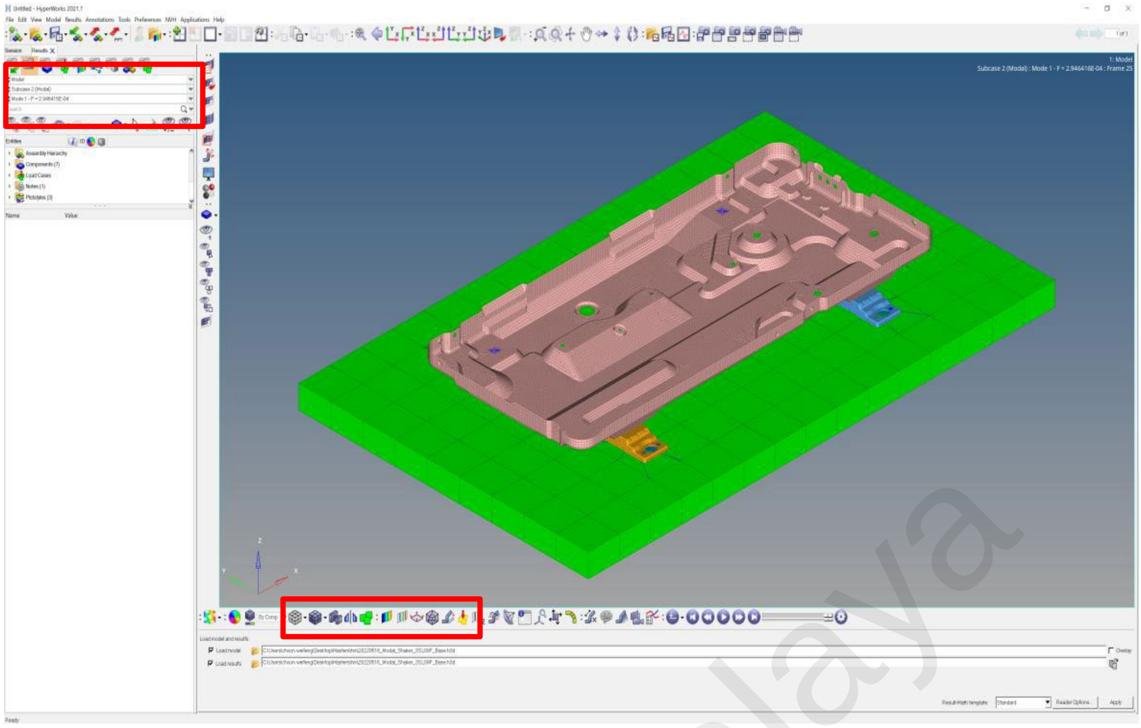

Figure 3.75: Hyperview interface.

Step 2: Load modal analysis result

Eigen mode or eigenvector result are represented in the contour form. By selecting the mode and go to work panel by clicking the contour panel, user can visualize the mode shape of the model, as indicated in Figure 3.76 and Figure 3.77. The first mode of the panel is shown in Figure 3.78, with the highest relative vector in red contour, zero movement in blue contour.

Figure 3.76: Switch between modal results.

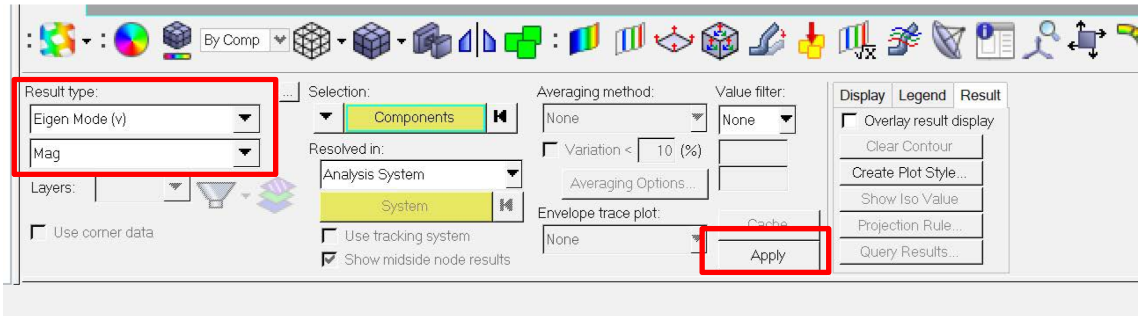

Figure 3.77: Contour panel.

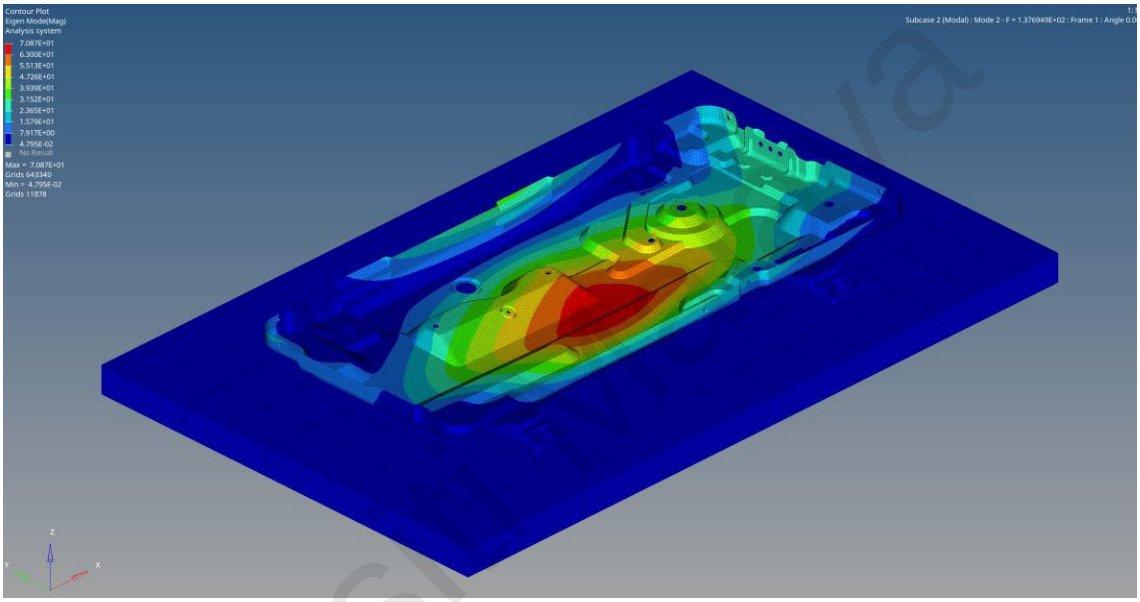

Figure 3.78: Example of a mode shape result.

Step 3: Result extraction and export

The first 7 mode (excluding rigid body mode) will be extracted and export to do analysis. The result window will be divided into 5 windows each represent a mode as shown in Figure 3.79 and Figure 3.80. The result is then output in gif format for result analysis and presentation (Figure 3.81).

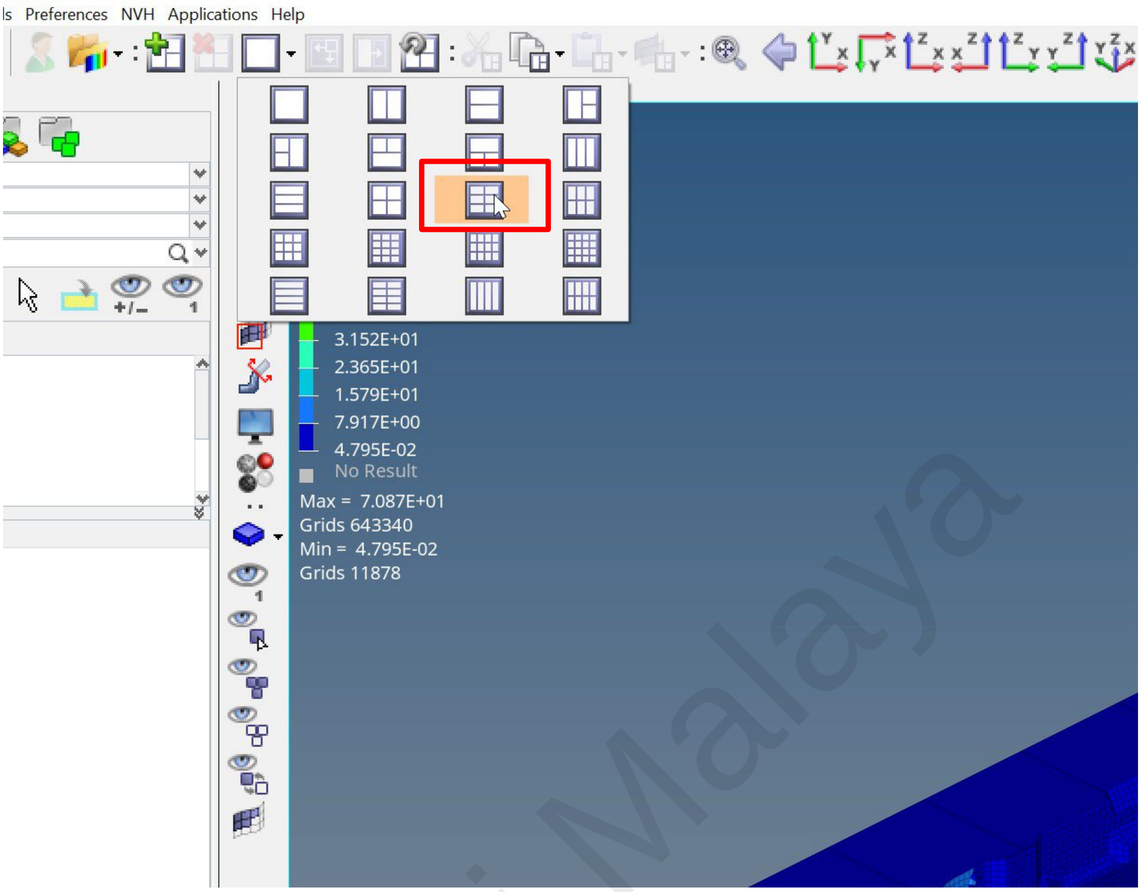

Figure 3.79: Switch to multi-window mode.

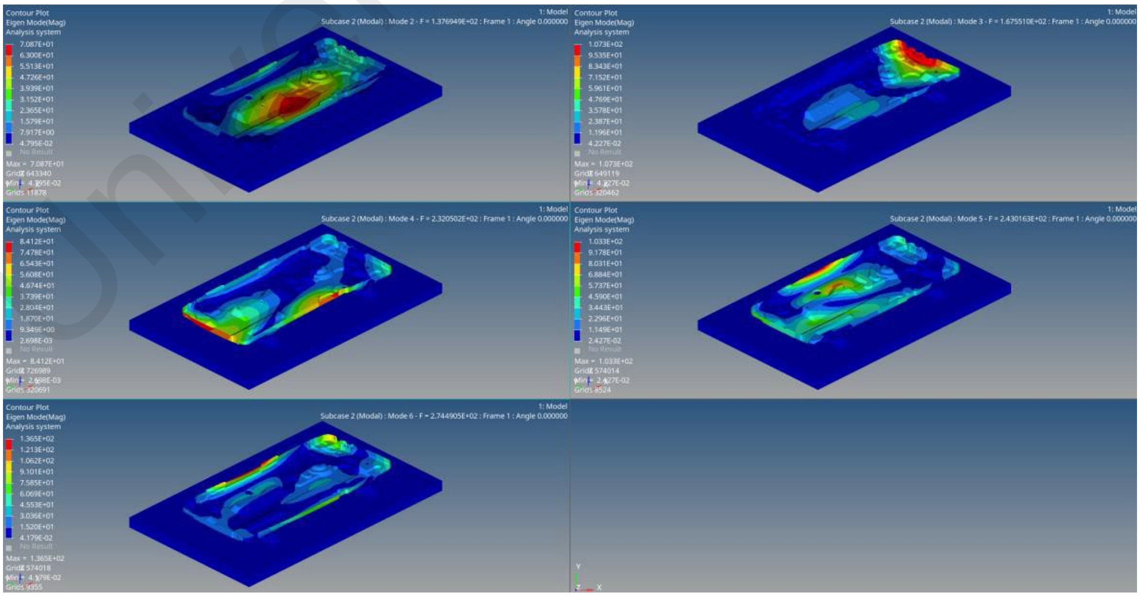

Figure 3.80: multi-window mode with different mode shapes.

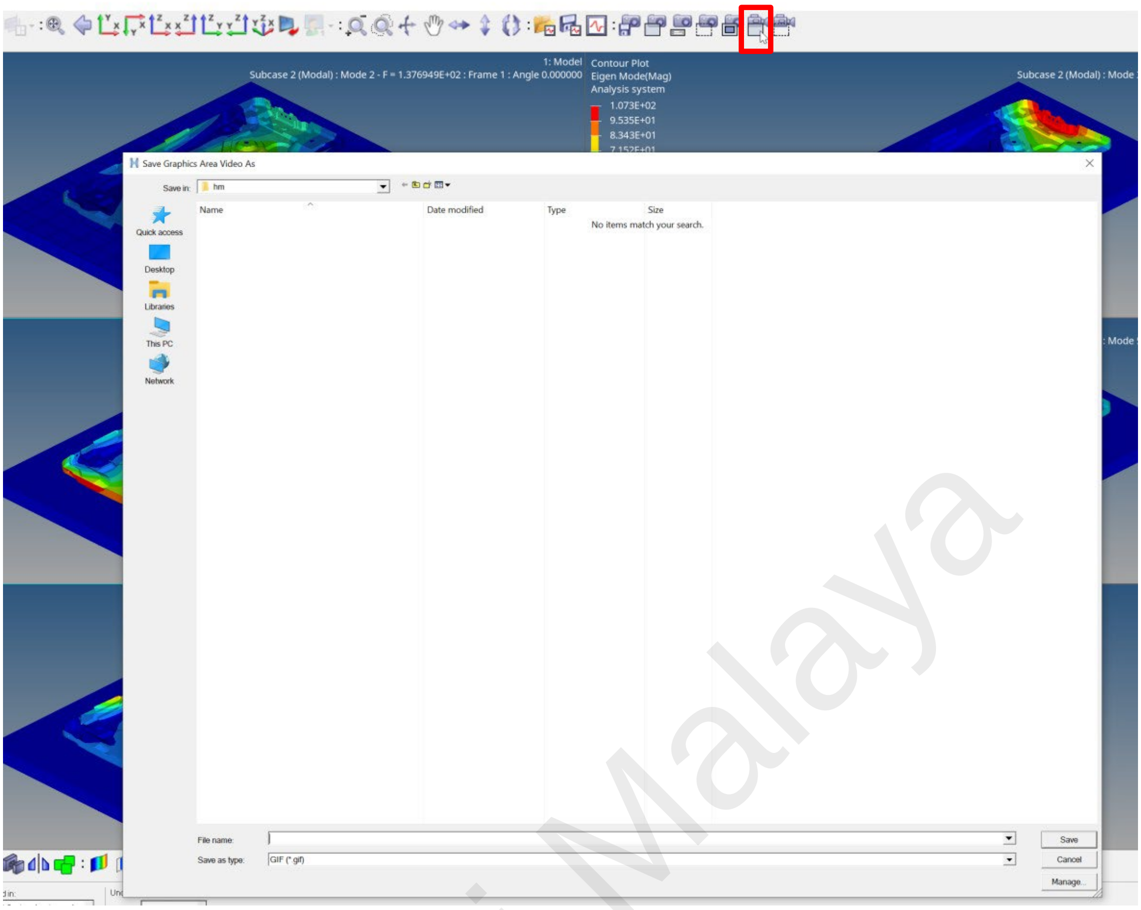

Figure 3.81: Export as GIF file and save to desired location.

3.3.1.2 Harmonic Response Analysis

Acceleration FRF plot from a single node was export and analyzed from the response analysis and compared with the experiment.

Step 1: Play the acceleration response animation from 5Hz to 500Hz

Select acceleration with Z direction at the contour panel as shown in Figure 3.82, and select time history data to play all the frequency range starting from 5Hz and end with 500Hz as shown in Figure 3.83.

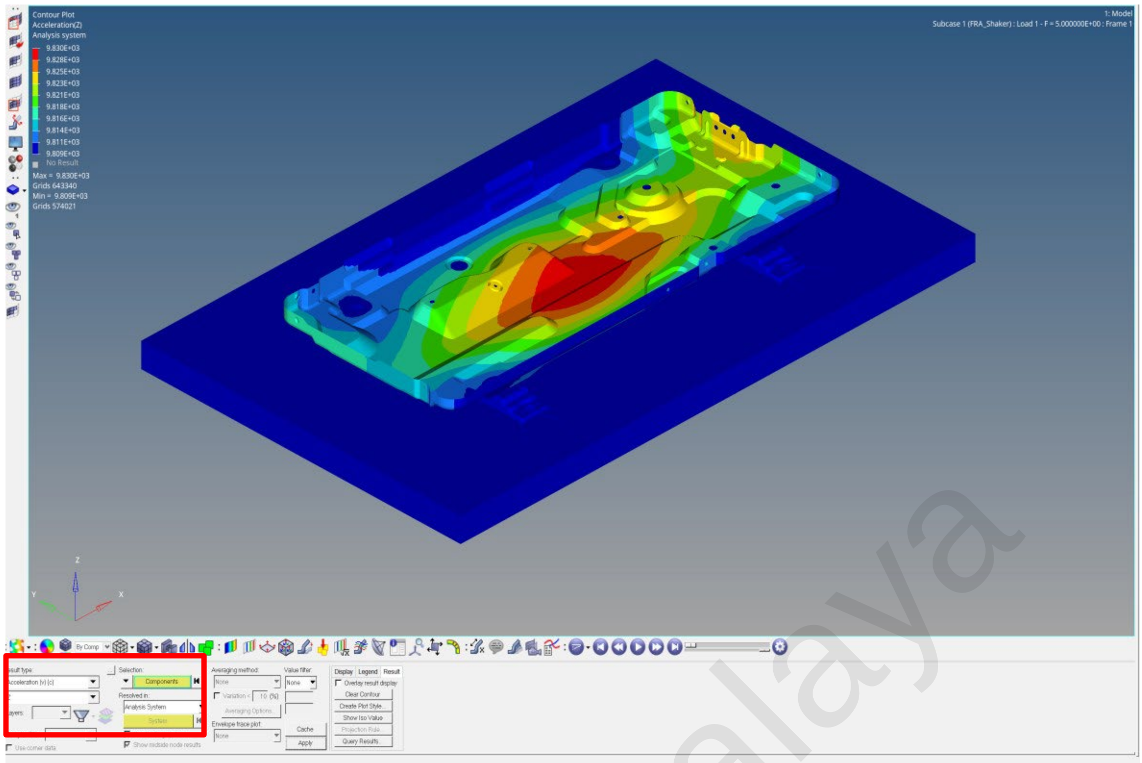

Figure 3.82: Acceleration response.

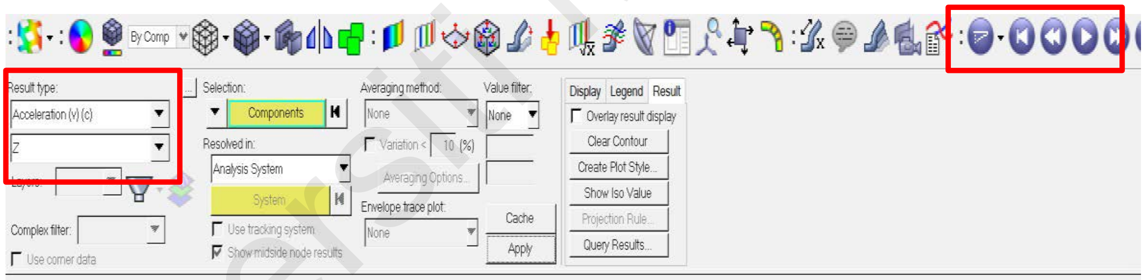

Figure 3.83: Play the acceleration animation contour.

Step 2: Select the desired node to be analyzed

Center node FRF to be selected to be compared with experiment and open-source results. Go to the plot data panel, select the centered node, and click 'create curve' as shown in Figure 3.84 and Figure 3.85.

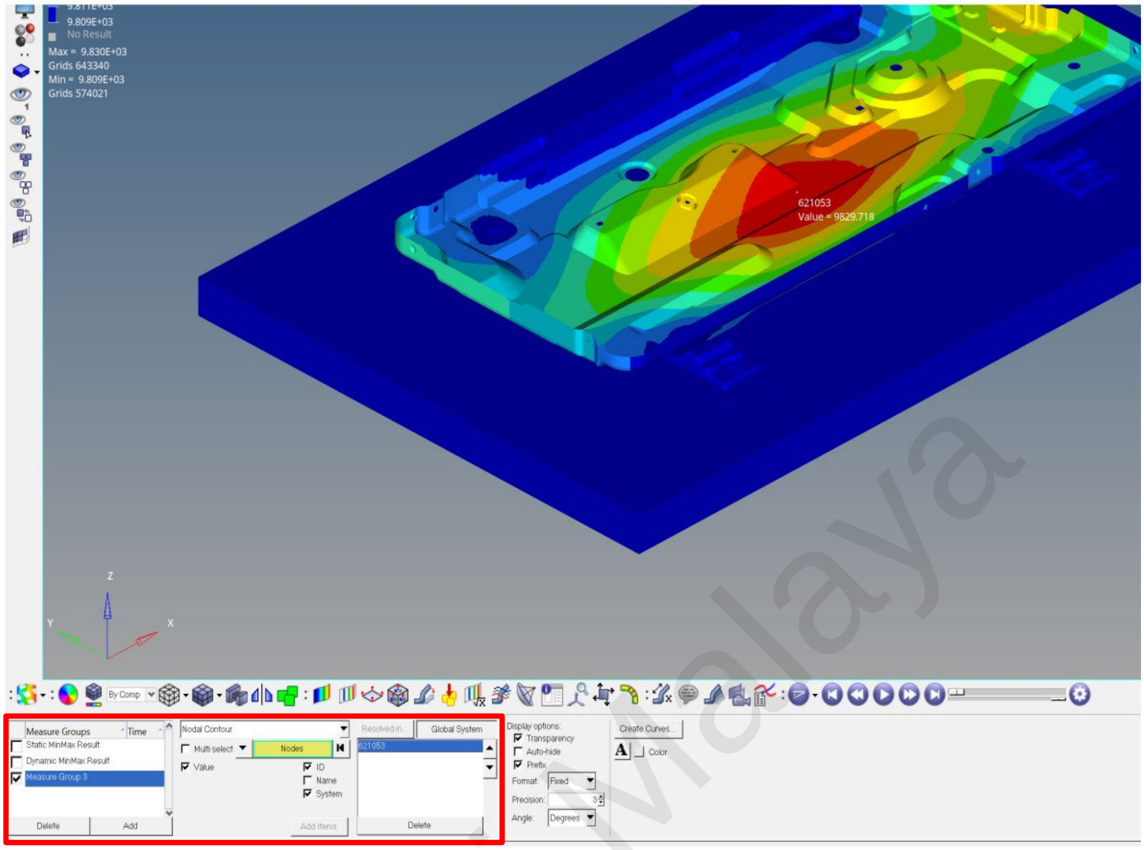

Figure 3.84: Data panel.

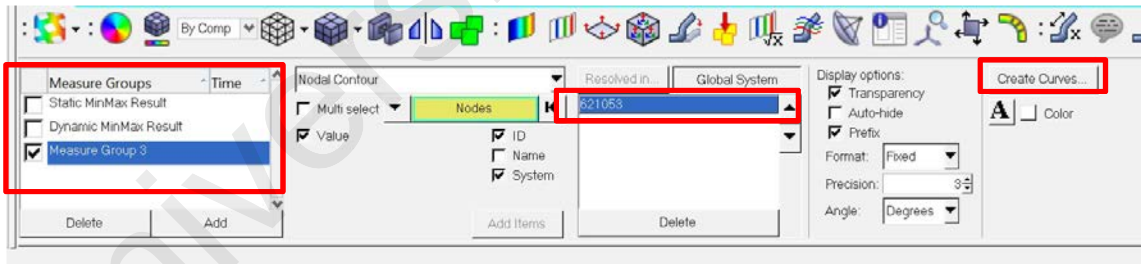

Figure 3.85: Select node and create FRF curve.

The FRF of centered node will be plotted as shown in Figure 3.86.

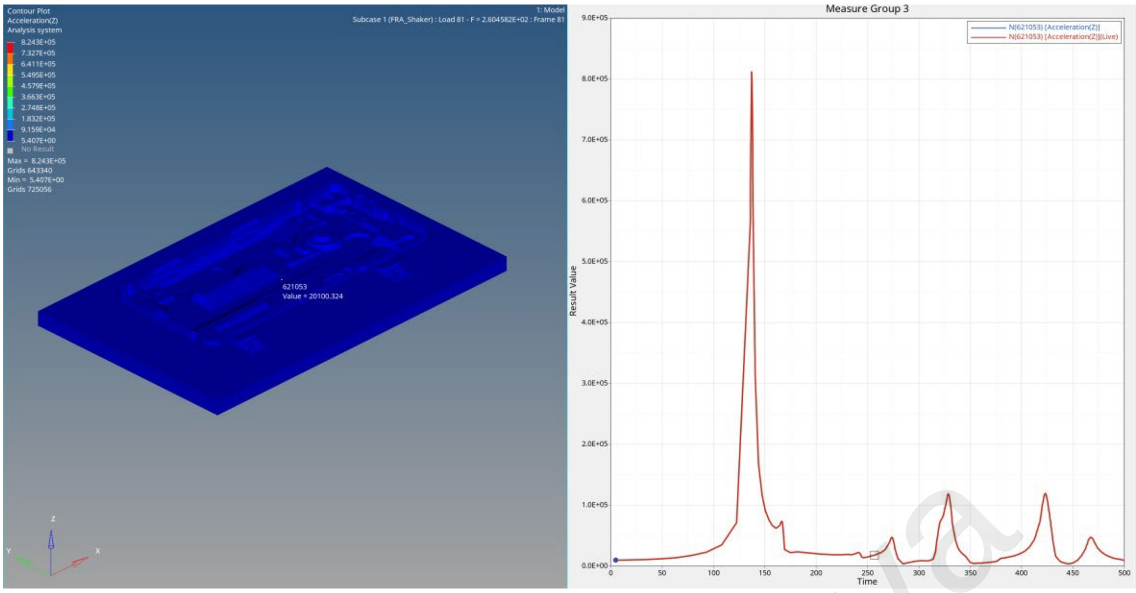

Figure 3.86: Example of the FRF.

Step 3: Export the FRF in csv format

The FRF is then exported as .csv format to be analyzed in Microsoft Excel. Figure 3.87 shows the export process from Hyperview to .csv format.

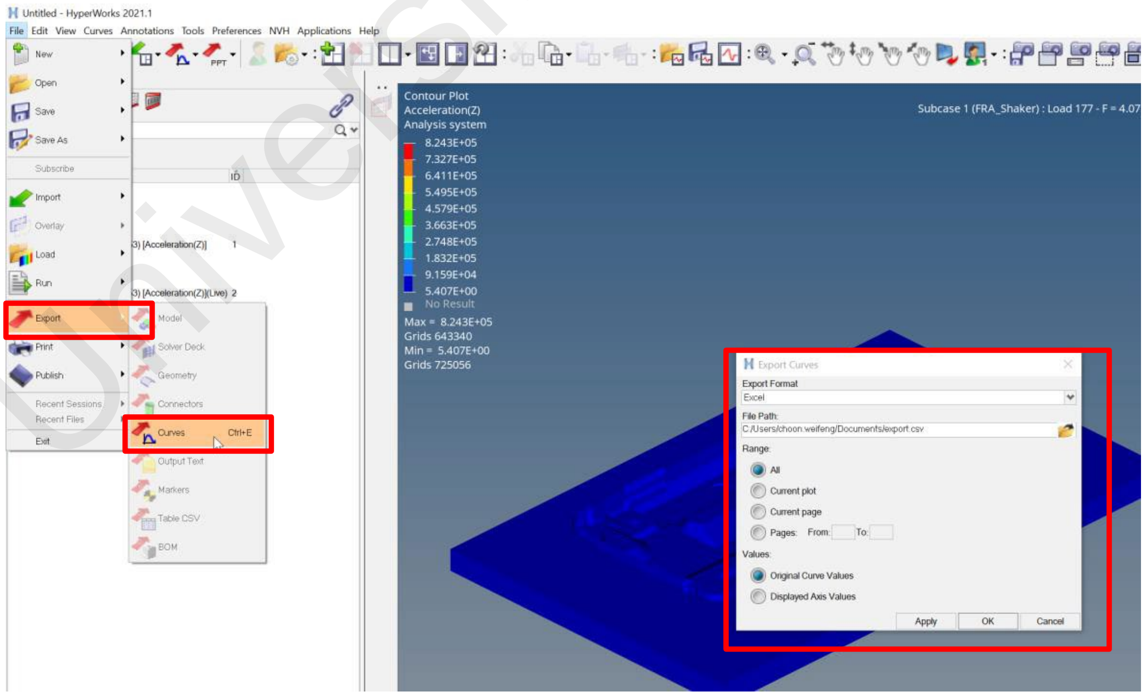

Figure 3.87: Export FRF as csv at desired location.

3.3.2 Open-Source Post Processor (ParaView)

The operation of Paraview is very different from Hyperview. The principle remains the same. Output modal result in split windows, plot acceleration FRF for center node.

3.3.2.1 Modal Analysis

Step 1: Load the result file

The result file is .rmed as created in section 3.3.1.2. Open Paraview 2019 and select the result file from the saved location.

Step 2: Load the modal result file

After opening the result file, click on generate vectors and select mode to output mode shapes. Click ‘Apply’ as shown in Figure 3.88 and Figure 3.89.

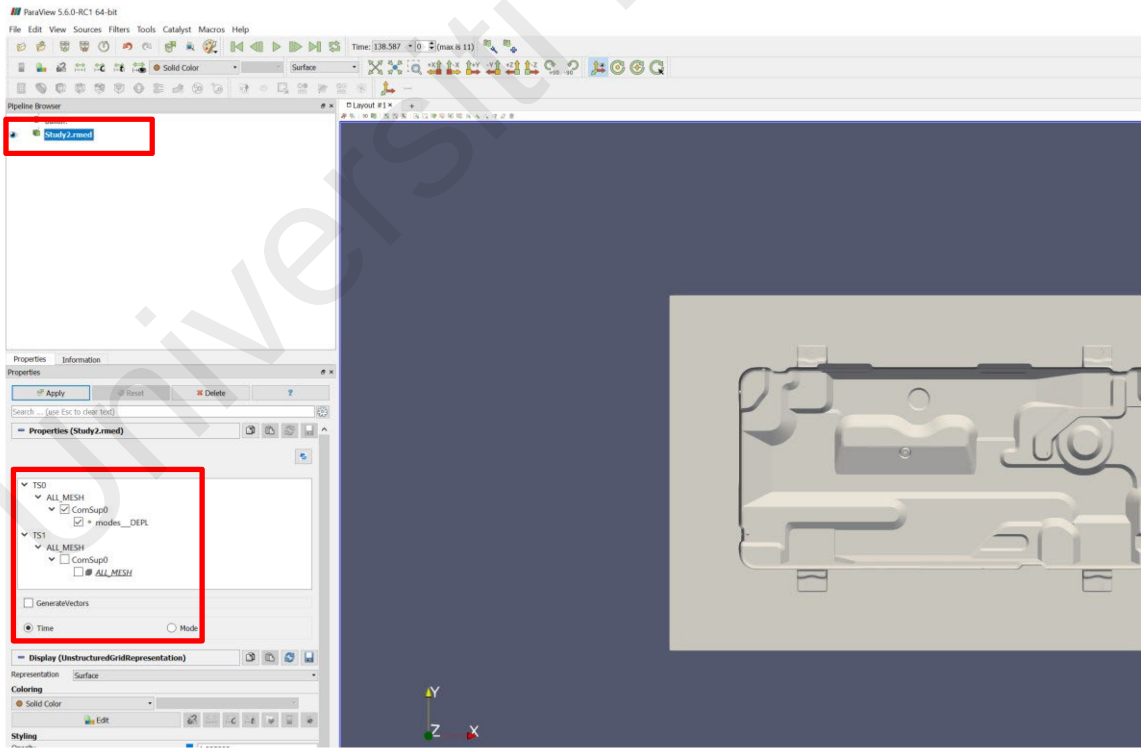

Figure 3.88: Paraview user interface.

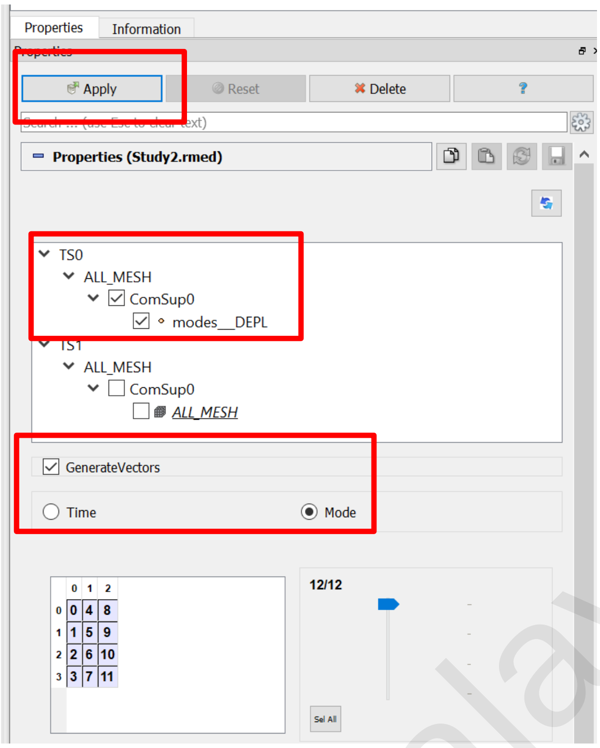

Figure 3.89: Applying mode shape result.

Step 3: Generate mode shape animation

To animate the mode shape, a Warp by Vector filter needed to be apply on the model. Figure 3.90 shows the location of Warp By Vector function in Paraview.

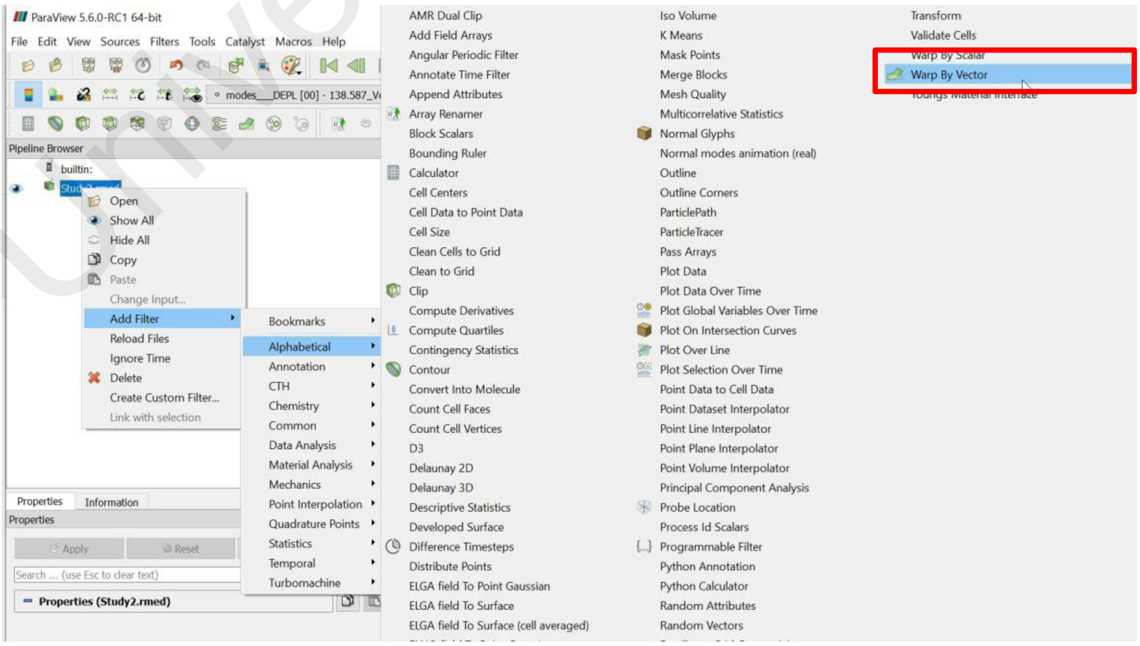

Figure 3.90: Warp by Vector filter.

Figure 3.91 shows the function of changing the contour preset to ‘jet’ to have better comparison with Altair Optistruct®.

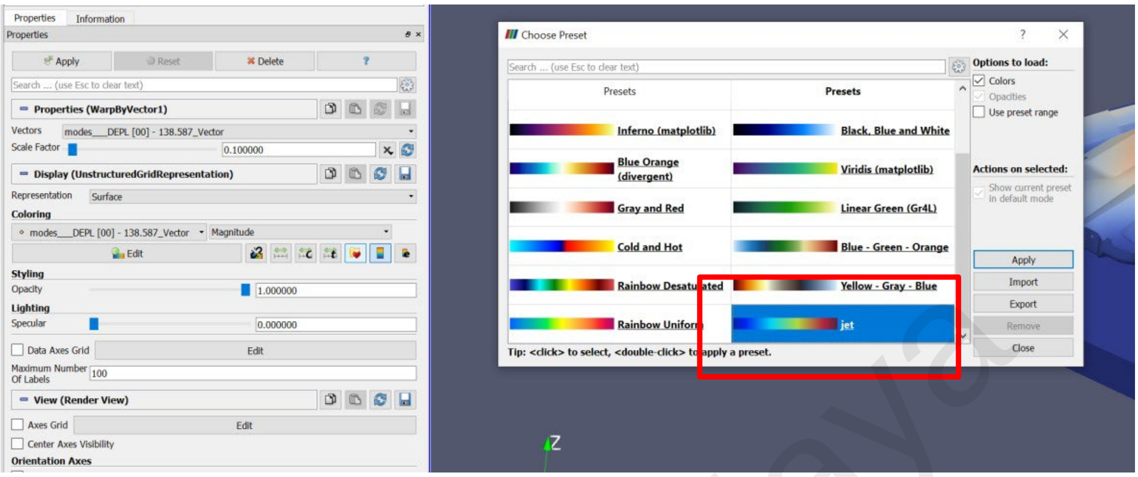

Figure 3.91: Changing contour preset.

On animation panel (Figure 3.92), change the animation replay to ‘sinusoidal’ to have repetitive the mode shape animation.

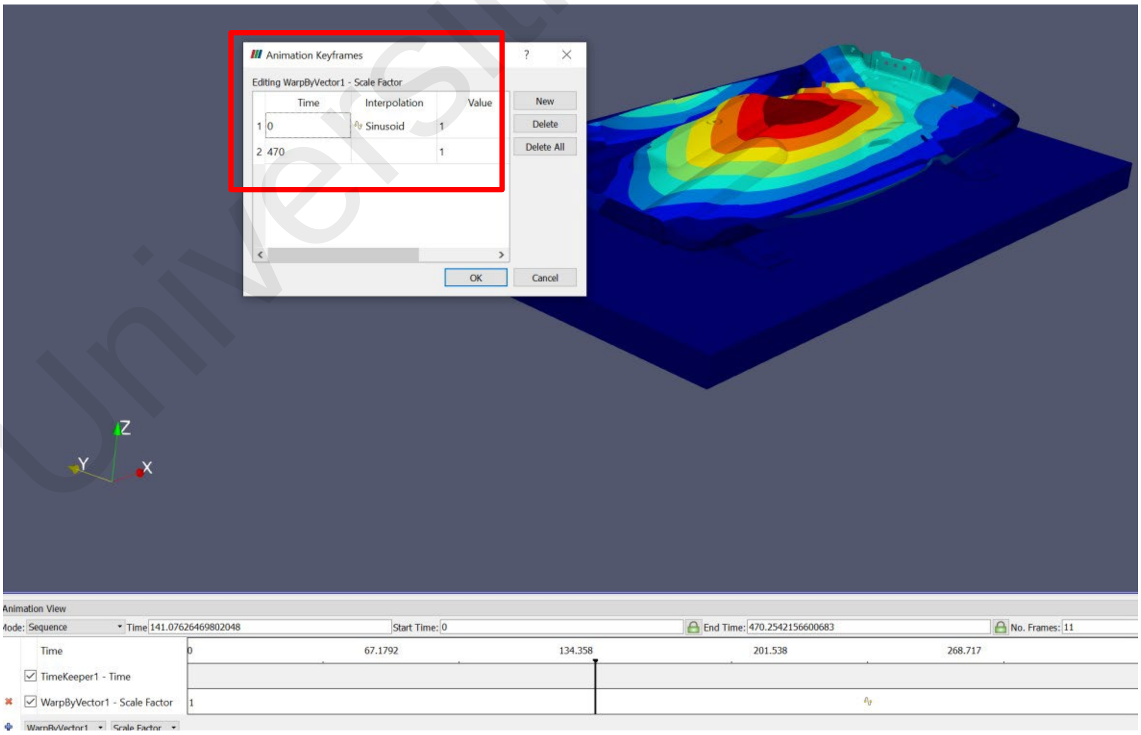

Figure 3.92: Animation keyframe.

Step 4: Export the mode shape animation as AVI

Paraview® does not have the option to save as gif file. AVI format is used instead. Go to 'File' select 'Save Animation' to export the mode shape animation onto the desired location as shown in Figure 3.93.

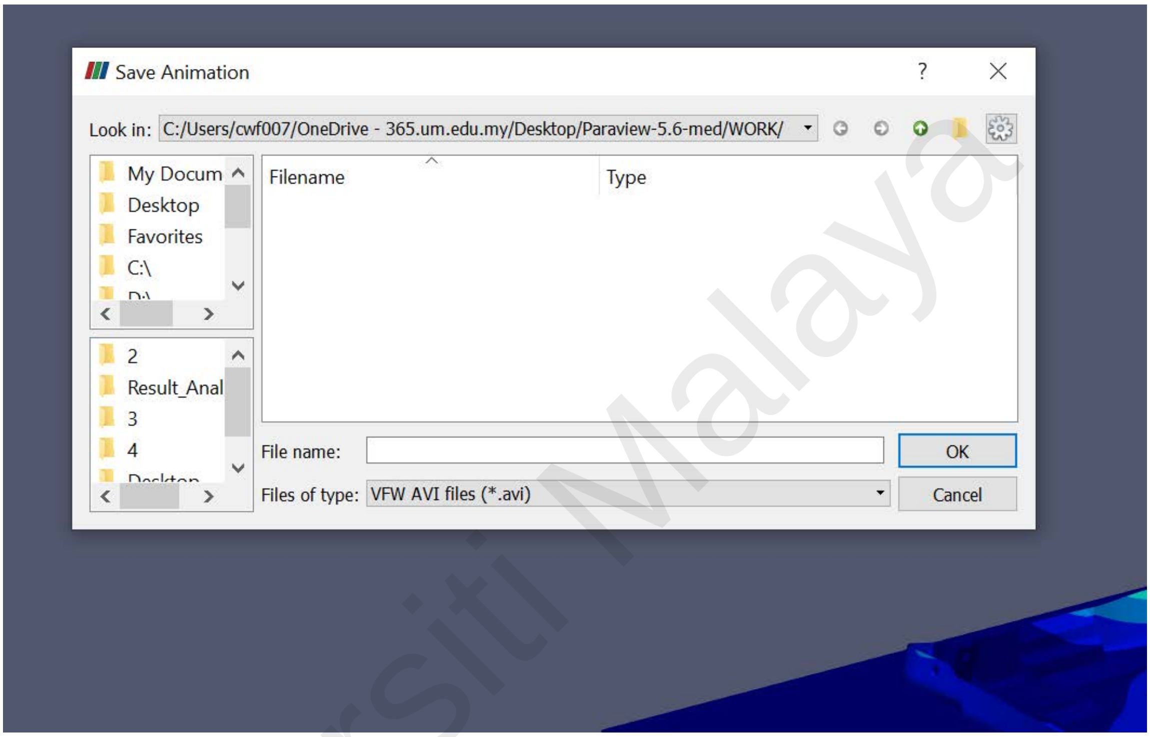

Figure 3.93: Save the animation file a desired location.

Finally, repeat the process from step 3 to step 4 for other 4 modes.

3.3.2.2 Harmonic Response Analysis

Step 1: Apply the harmonic response result file

Figure 3.94 shows the step for applying the result (acceleration and displacement) to the model, with generate vectors and time data selected. The time data here is represented asfrequency steps.

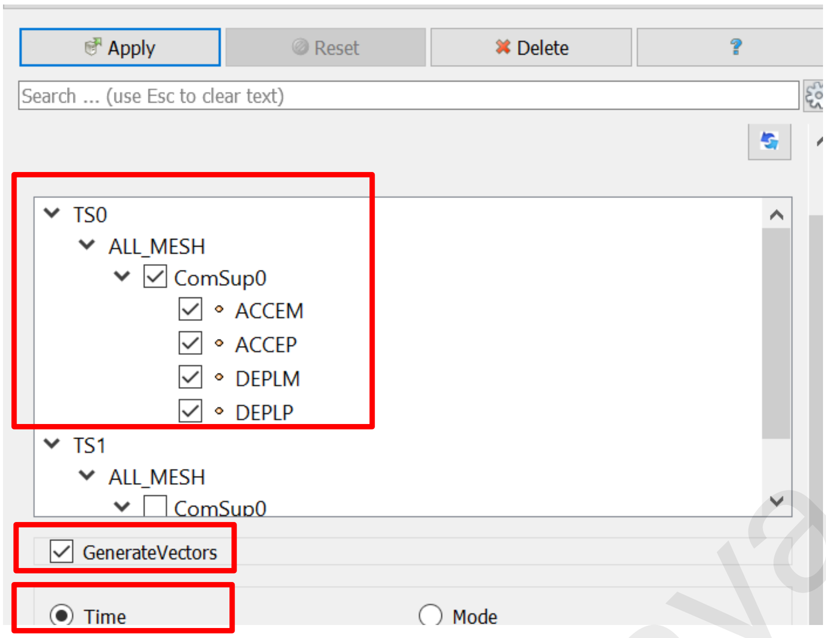

Figure 3.94: Load response results.

Step 2: Select the center node for extracting FRF data

By using interactive select point tool in Figure 3.95, nodes can be selected throughout the model.

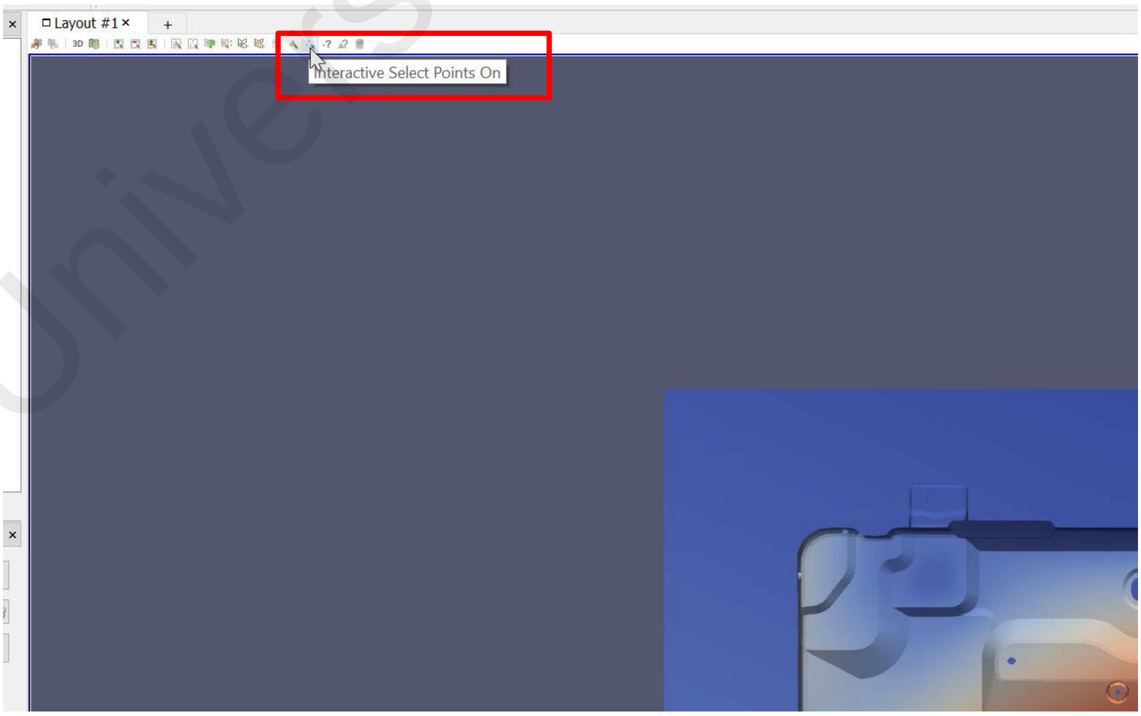

Figure 3.95: Interactive select points tool.

Select the center node (Figure 3.96), which is the accelerometer measurement location, and Altair Optistruct® output location.

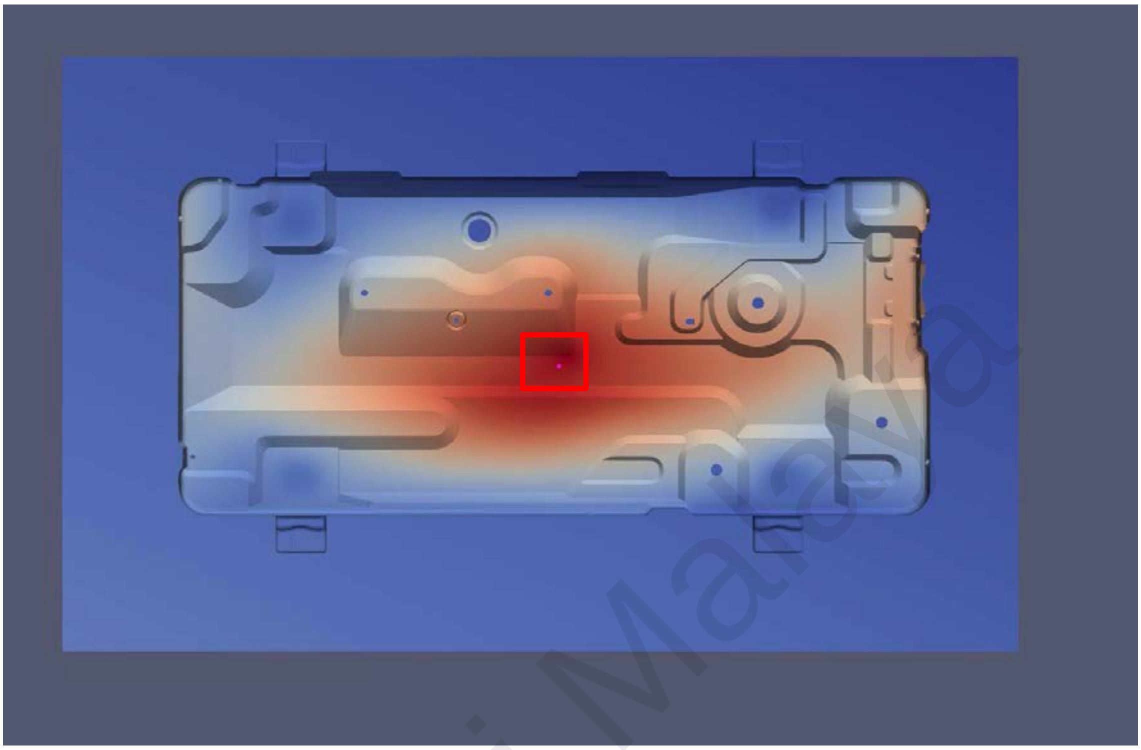

Figure 3.96: Center node.

Step 3: Apply plot selection over time filter

Figure 3.97 shows the location of the function plot selection over time filter, which allowto plot the acceleration magnitude against the frequency (the response) of the center node.Figure 3.98 shows the acceleration response of the center node.

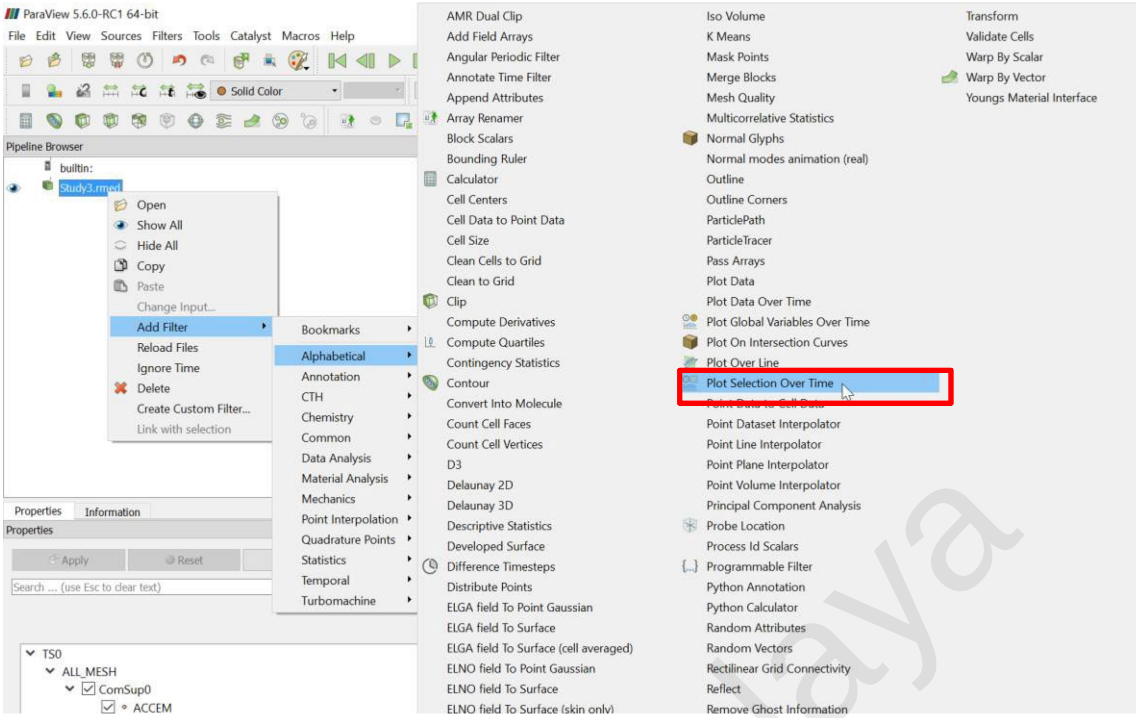

Figure 3.97: Selection over time filter.

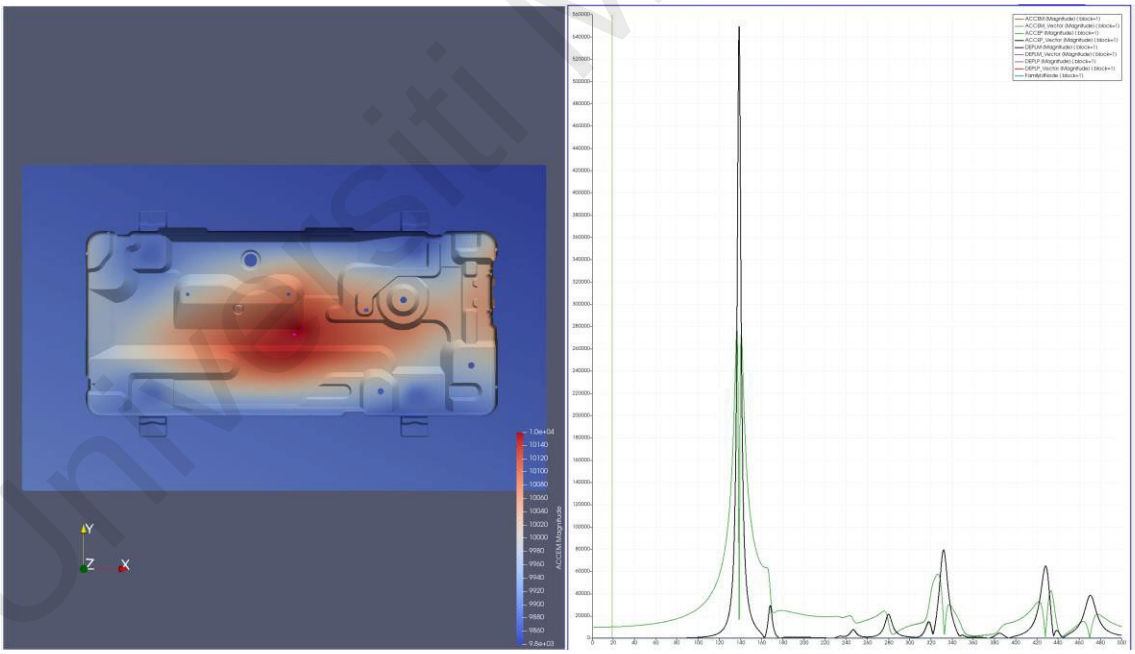

Figure 3.98: FRF data for acceleration and displacement.

Step 4: Export FRF data in CSV format

Go to file, export scene, and save the data as csv on desired location as indicated in Figure 3.99.

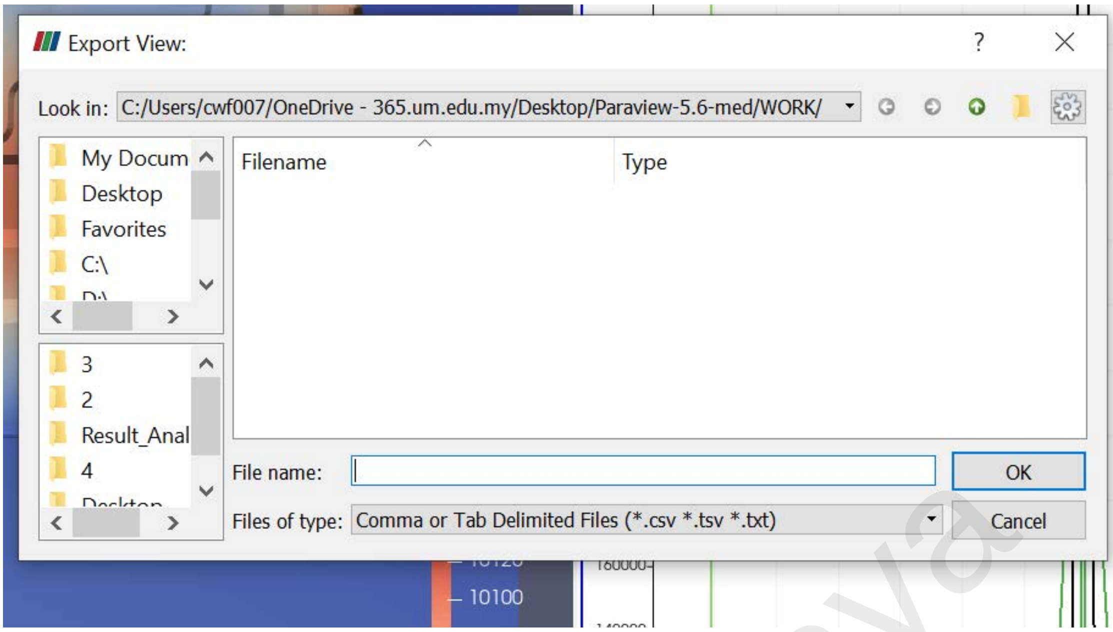

Figure 3.99: Export scene.

The response in .csv format (Figure 3.100) are ready to be compared with Altair Optistruct® andexperimental data.

	A	B	C	D	E	F	G	H	I
1	Time	ACCEM (N	ACCEM_V	ACCEP (M	ACCEP_Ve	DEPLM (M	DEPLM_Ve	DEPLP (Ma	DEPLP_Ve F
2	0.995	9874.39	9874.39	1.03743	1.03709	252.641	252.641	0.026543	0.026534
3	0.996111	9874.42	9874.42	1.06367	1.06332	252.079	252.079	0.027154	0.027145
4	0.997222	9874.44	9874.44	1.09084	1.09048	251.518	251.518	0.027785	0.027776
5	0.998333	9874.47	9874.47	1.11897	1.1186	250.959	250.959	0.028438	0.028429
6	0.999444	9874.5	9874.5	1.1481	1.14773	250.402	250.402	0.029114	0.029105
7	1.00056	9874.54	9874.54	1.1783	1.17791	249.847	249.847	0.029814	0.029804
8	1.00167	9874.57	9874.57	1.2096	1.2092	249.294	249.294	0.030538	0.030528
9	1.00278	9874.6	9874.6	1.24206	1.24165	248.743	248.743	0.031288	0.031277
10	1.00389	9874.63	9874.63	1.27573	1.27532	248.193	248.193	0.032065	0.032054
11	1.005	9874.67	9874.67	1.31068	1.31025	247.646	247.646	0.03287	0.03286
12	5	9891.53	9891.53	0.036471	0.036456	10.0222	10.0222	3.70E-05	3.69E-05
13	5.40507	9894.85	9894.85	0.034228	0.034215	8.57919	8.57919	2.97E-05	2.97E-05
14	5.81015	9898.42	9898.42	0.035008	0.034997	7.42732	7.42732	2.63E-05	2.63E-05
15	6.21522	9902.26	9902.26	0.0388	0.038791	6.49324	6.49324	2.54E-05	2.54E-05
16	6.62029	9906.36	9906.36	0.045253	0.045245	5.72532	5.72532	2.62E-05	2.61E-05
17	7.02537	9910.73	9910.73	0.053929	0.053923	5.08637	5.08637	2.77E-05	2.77E-05
18	7.43044	9915.35	9915.35	0.064501	0.064497	4.54903	4.54903	2.96E-05	2.96E-05
19	7.83552	9920.24	9920.24	0.076784	0.07678	4.09286	4.09286	3.17E-05	3.17E-05
20	8.24059	9925.4	9925.4	0.090692	0.090689	3.7023	3.7023	3.38E-05	3.38E-05
21	8.64566	9930.81	9930.81	0.106205	0.106202	3.36534	3.36534	3.60E-05	3.60E-05
22	9.05074	9936.49	9936.49	0.123342	0.123339	3.0726	3.0726	3.81E-05	3.81E-05
23	9.45581	9942.44	9942.44	0.142144	0.142141	2.81667	2.81667	4.03E-05	4.03E-05
24	9.86088	9948.65	9948.65	0.162666	0.162664	2.59163	2.59163	4.24E-05	4.24E-05
25	10.266	9955.13	9955.13	0.184972	0.18497	2.3927	2.3927	4.45E-05	4.45E-05
26	10.671	9961.88	9961.88	0.209133	0.209131	2.216	2.216	4.65E-05	4.65E-05
27	11.0761	9968.89	9968.89	0.235221	0.235219	2.05832	2.05832	4.86E-05	4.86E-05
28	11.4812	9976.18	9976.18	0.263312	0.26331	1.91704	1.91704	5.06E-05	5.06E-05
29	11.8863	9983.73	9983.73	0.293486	0.293484	1.78996	1.78996	5.26E-05	5.26E-05
30	12.2913	9991.55	9991.55	0.32582	0.325818	1.67523	1.67523	5.46E-05	5.46E-05
31	12.6964	9999.64	9999.64	0.360398	0.360396	1.57132	1.57132	5.66E-05	5.66E-05
32	13.1015	10008	10008	0.3973	0.397298	1.47689	1.47689	5.86E-05	5.86E-05
33	13.5065	10016.6	10016.6	0.436611	0.436609	1.39083	1.39083	6.06E-05	6.06E-05
34	13.9116	10025.6	10025.6	0.478415	0.478413	1.31218	1.31218	6.26E-05	6.26E-05
35	14.3167	10034.7	10034.7	0.522797	0.522795	1.24011	1.24011	6.46E-05	6.46E-05
36	14.7218	10044.2	10044.2	0.569844	0.569842	1.17391	1.17391	6.66E-05	6.66E-05
37	15.1268	10053.9	10053.9	0.619643	0.619641	1.11296	1.11296	6.86E-05	6.86E-05

Figure 3.100: Example of csv FRF data from specified node.

.

3.4 Experimental Vibration Analysis

The objective of experimental vibration analysis is to validate the FEA model for Code_Aster® to ensure that the boundary conditions, material properties, element properties and load step setting are correct. There will be two experiments to be conducted, experimental modal analysis (EMA) and harmonic response analysis. Experimental modal analysis will acquire the mode shape and natural frequencies of the base panel and to be compared with FEA results. Harmonic response analysis on other hand is to acquire the overall acceleration FRF of the base panel on center location and to be compared with FEA results. To ensure the material data and boundary condition settings in FEA is correct as well as the dynamic behavior of the component is responding well and logic, EMA will be conducted first prior to harmonic response analysis.

3.4.1 Experimental Modal Analysis (EMA)

Step 1: Specimen preparation

Prepare the base panel and rigid table. A 700mm by 400mm with 10mm thickness acrylicsheet was prepared to act as a base for the base panel. The screw hole is drilled on the acrylic sheet and the base panel was screw on top of the sheet by using M3 screw as shown in Figure 3.101 and Figure 3.102. The location of the screw is following the RBE2modeling in FEA (Figure 3.103).

Figure 3.101: M3 screw to secure the base panel on top of acrylic sheet.

Figure 3.102: M3 screw to secure the base panel on top of acrylic sheet.

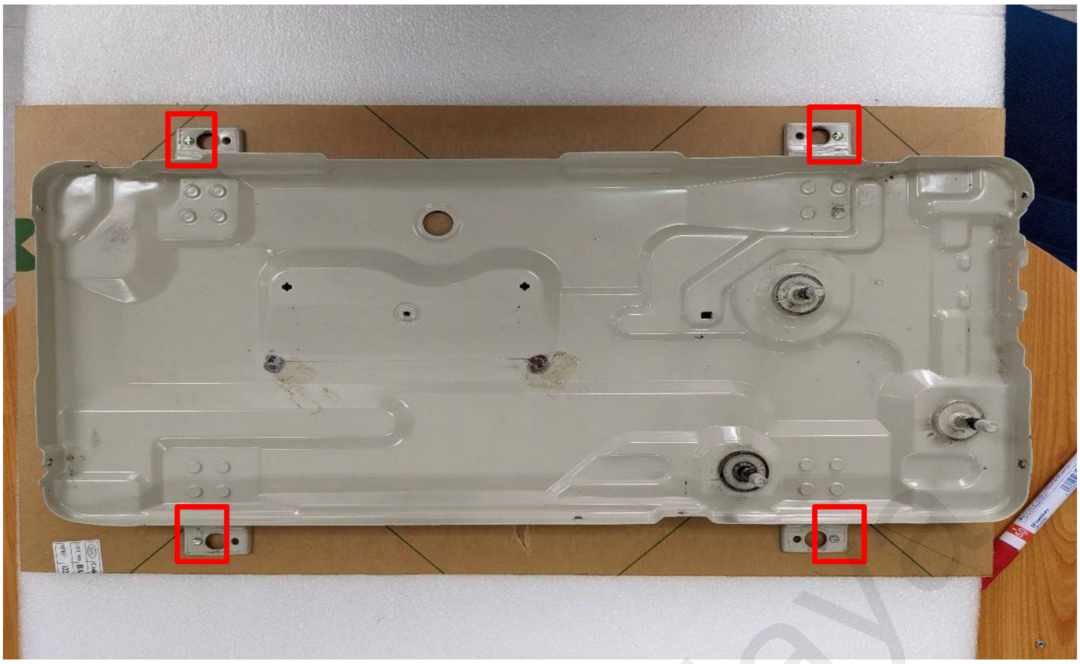

Figure 3.103: Fully secured and tightened screw location.

Step 2: Marking impact hammer and accelerometer location

21 marking will be distributed evenly across the base panel. The center node (point 11) is for accelerometer while the other points are for impact hammer impact location (rovinghammer method) as shown in Figure 3.104.

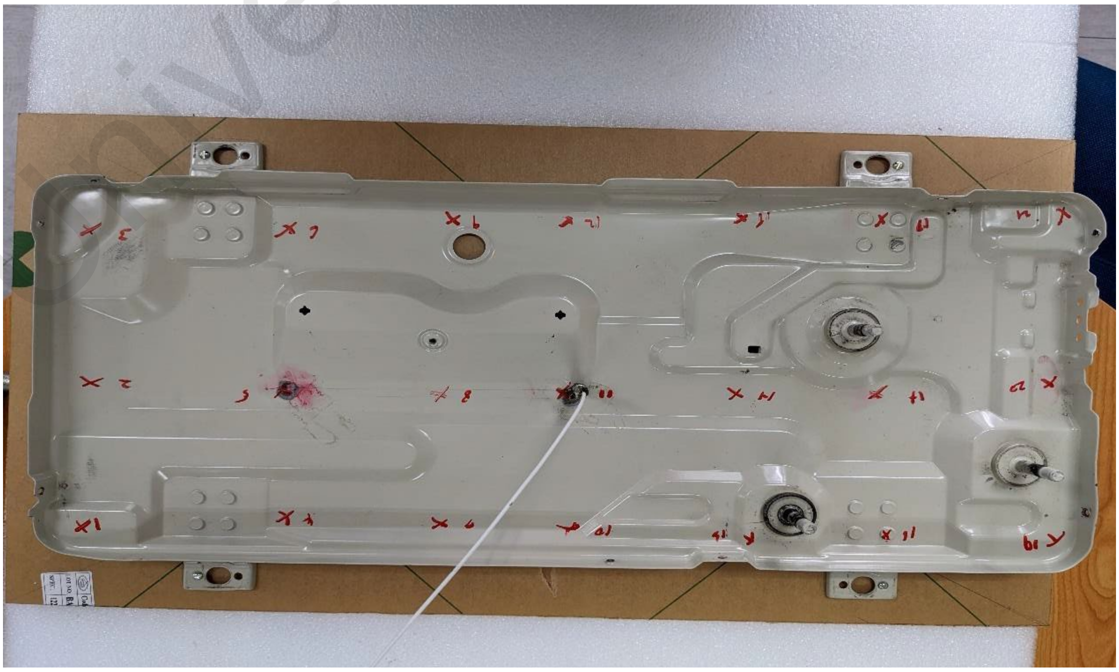

Figure 3.104: 21 points marking.

Step 3: Roving hammer and data acquisition

Connect the all the sensors to the DAQ (accelerometer and impact hammer). Start settingthe experiment parameters such as damping window to 0%, 5 times averaging, impact force indication (under 10N) etc. Start exciting the structure in vertical direction (Z – direction) on point 1 to point 21. Figure 3.105 shows the general setup of EMA.

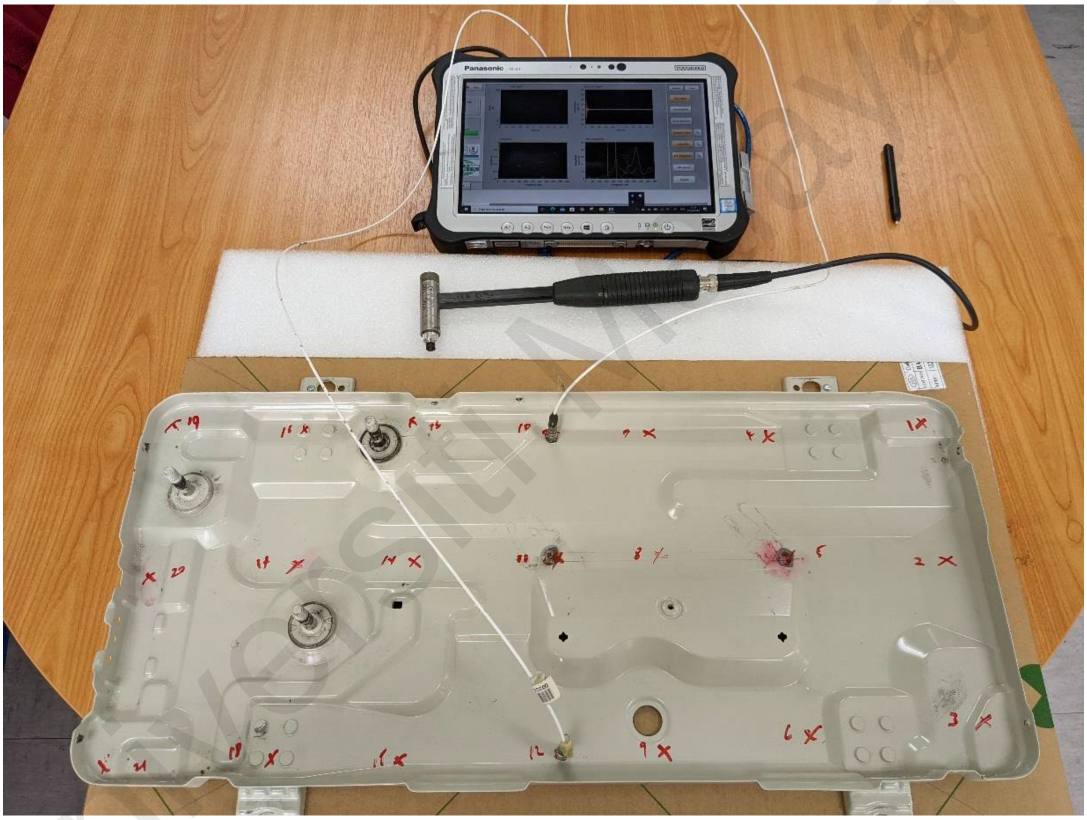

Figure 3.105: EMA setup.

Step 4: Repeat step 3 with 2 additional accelerometer location (point 10 & 12)

To capture a more detail mode shape (shape from side of the panel), accelerometer is attached to additional 2 points (10 & 12). Acquire the data with technique describe in step 3.

Step 5: Curve fitting and mode shape exporting

The collected FRF from all excitations will be extracted and analyzed in the software to perform curve fitting. After curve fitting is complete, the modes and natural frequency data can be exported to gif and Excel file. Figure 3.106 shows the example of FRF results from EMA.

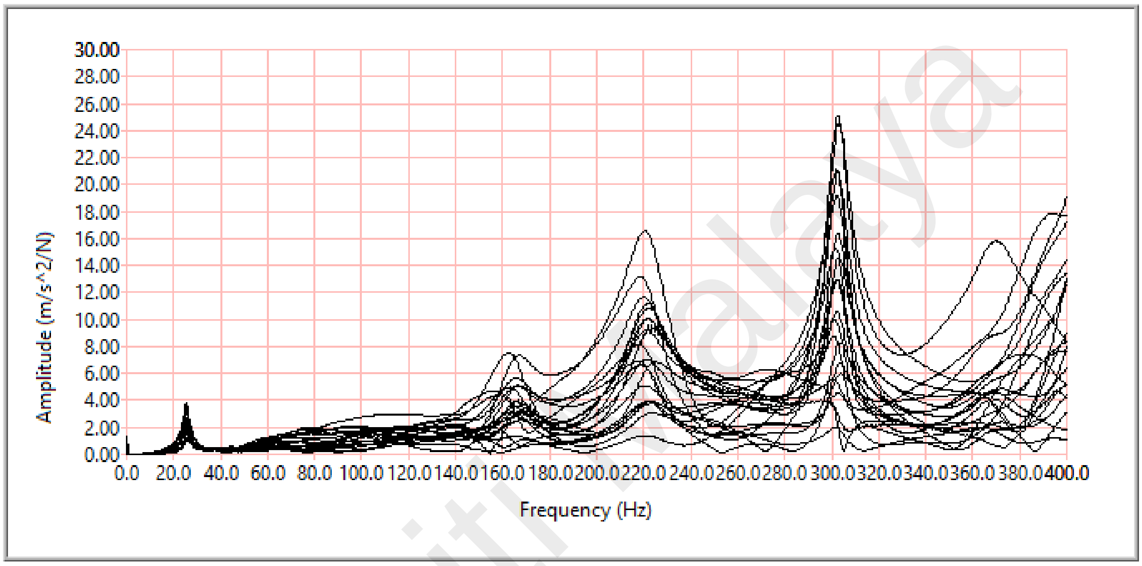

Figure 3.106: Example of an EMA FRF to be curve fit.

3.4.2 Harmonic Response Analysis

Step 1: Secure the base panel and base acrylic sheet to the shaker

The center part of the acrylic sheet is screwed to the shaker as shown in Figure 3.107.

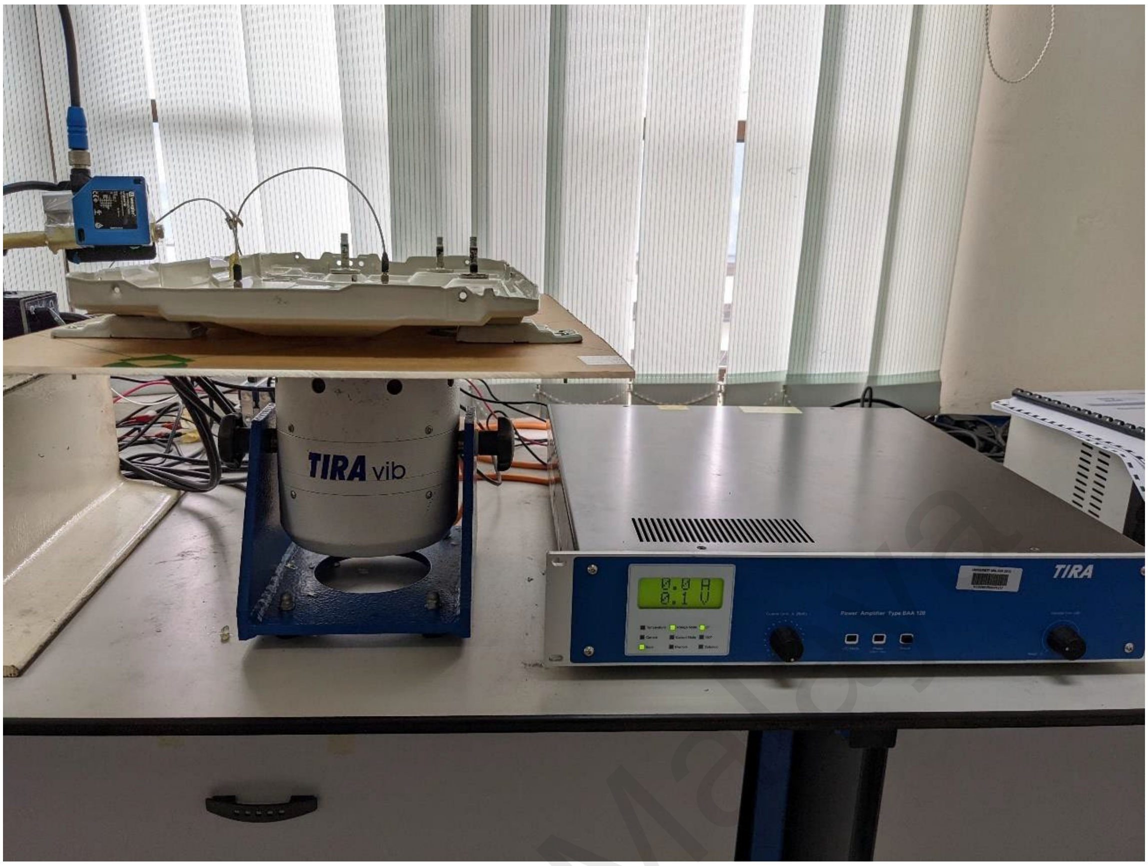

Figure 3.107: Shaker with base panel.

Step 2: Attach the accelerometer

Attach the accelerometer one to the center of base panel, one to the acrylic sheet to record the response from panel and acrylic sheet, as shown in Figure 3.108.

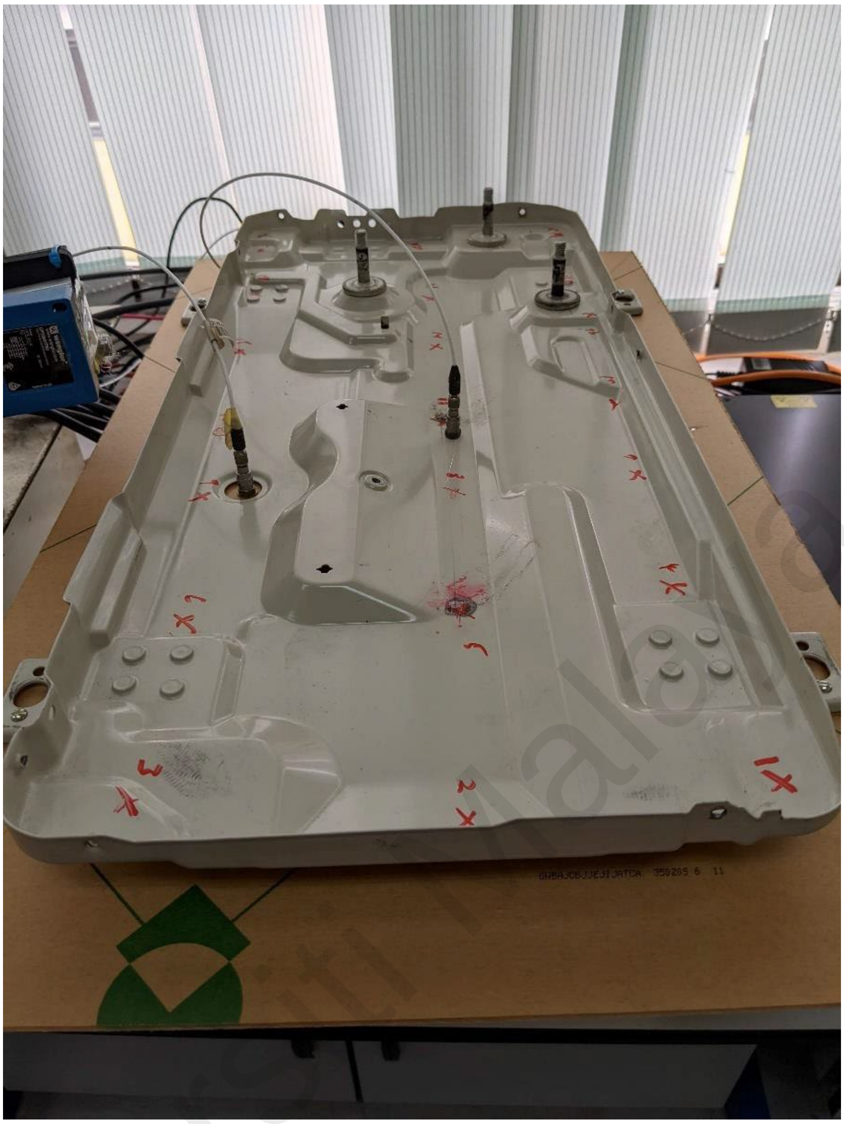

Figure 3.108: Accelerometer attachments location.

Step 3: Start the sweep measurement by controlling the shaker output.

Sine sweep excitation will be conducted from 5Hz to 250Hz with constant 1G acceleration output. Subsequently, record the accelerometer data.

Step 4: Refinement of measurement point around resonance by controlling shaker output

Since the modal result is already available, we can refine the measurement resolution at all the resonance point within 250Hz range, this will give a more accurate overall response from the structure.

Step 5: Export the data into Excel

Export the FRF data into excel and ready to be process and compared with FEA.

CHAPTER 4: RESULTS AND DISCUSSION

This chapter will elaborate the results generated from FEA and experiment by the method mentioned from previous chapter. It will dissect into three sections. The first section is the comparison of modal and response results generated from open-source and commercial FEA software, the second section will be focused on the correlation of open-source FEA results with experimental vibration (EMA) result, the third section will be the validation of FRF generated from the harmonic response analysis in FEA.

4.1 FEA Results Comparison

The objective of this section is to show that the result generated from Code_Aster® 2019 based on method in section 3.2 is correct, and to validate some of the important keyword in Code_Aster® while doing modal analysis and harmonic response analysis. The method used in Altair Optistruct® for modal analysis and harmonic response analysis are already implemented in the design workflow stage during product development. Thus, if the dynamic results generated by Code_Aster® is similar to Altair Optistruct®, Code_Aster® can be used in product development cycle with confident.

4.1.1 Modal Analysis

The comparison of first 8 flexible modes (excluding the rigid body modes) of the basepanel between Code_Aster® 2019 and Altair Optistruct® from Figure 4.1 to Figure 4.4:

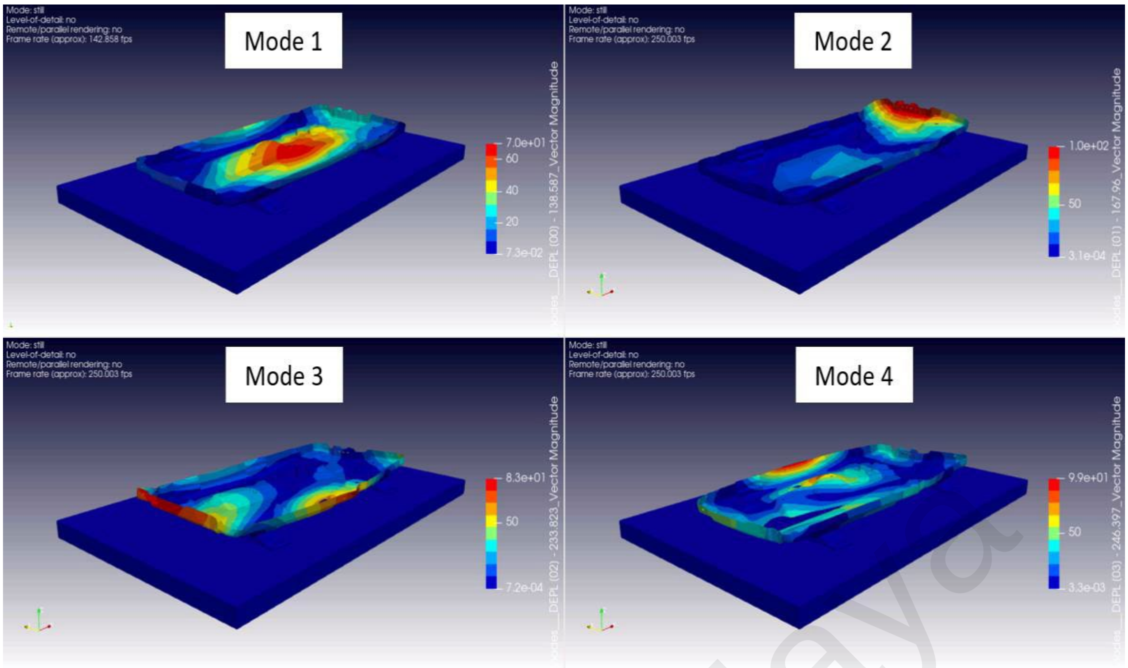

Figure 4.1: Mode shape (mode 1 – mode 4) from Code_Aster® 2019.

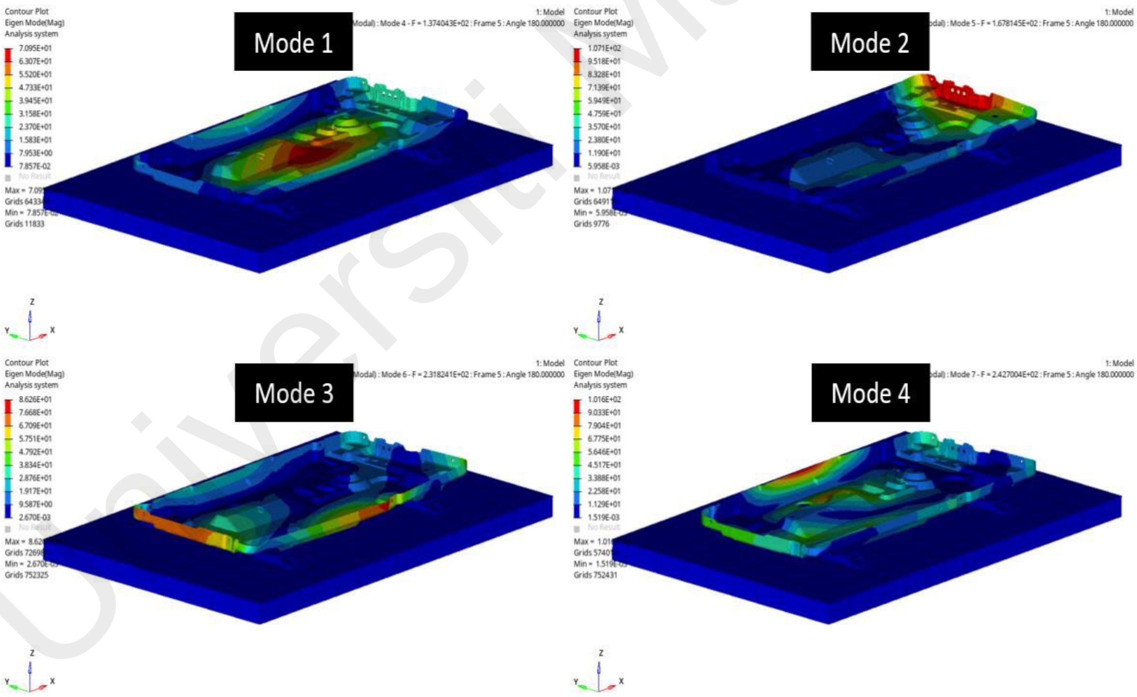

Figure 4.2: Mode shape (mode 1 – mode 4) from Altair's Optistruct®.

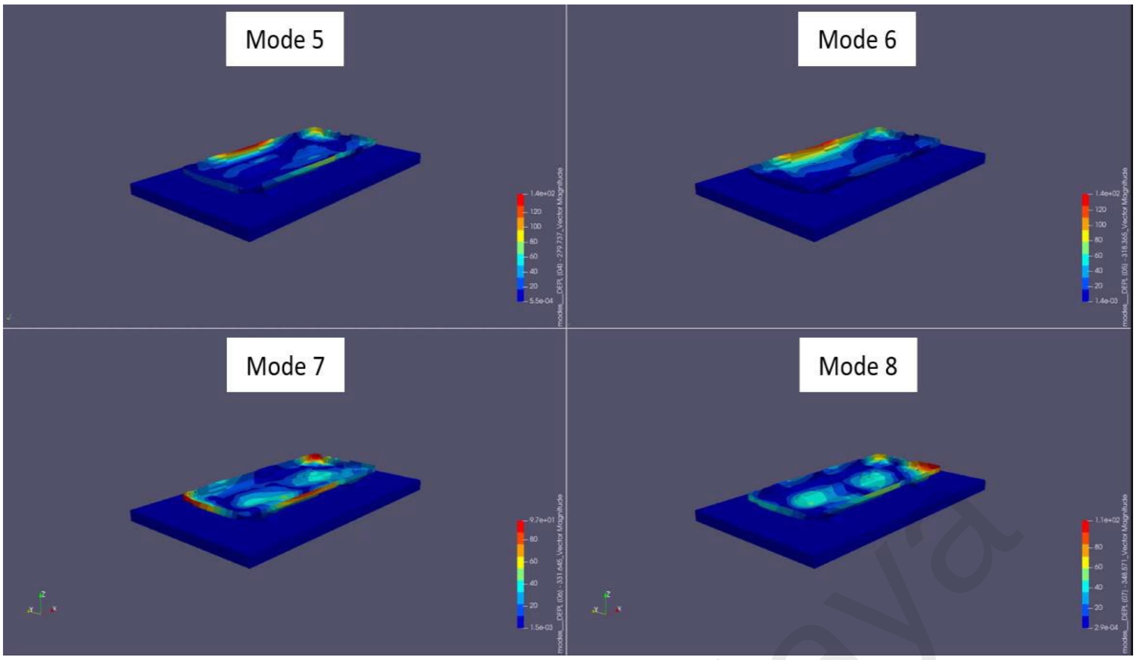

Figure 4.3: Mode shape (mode 5 – mode 8) from Code_Aster® 2019.

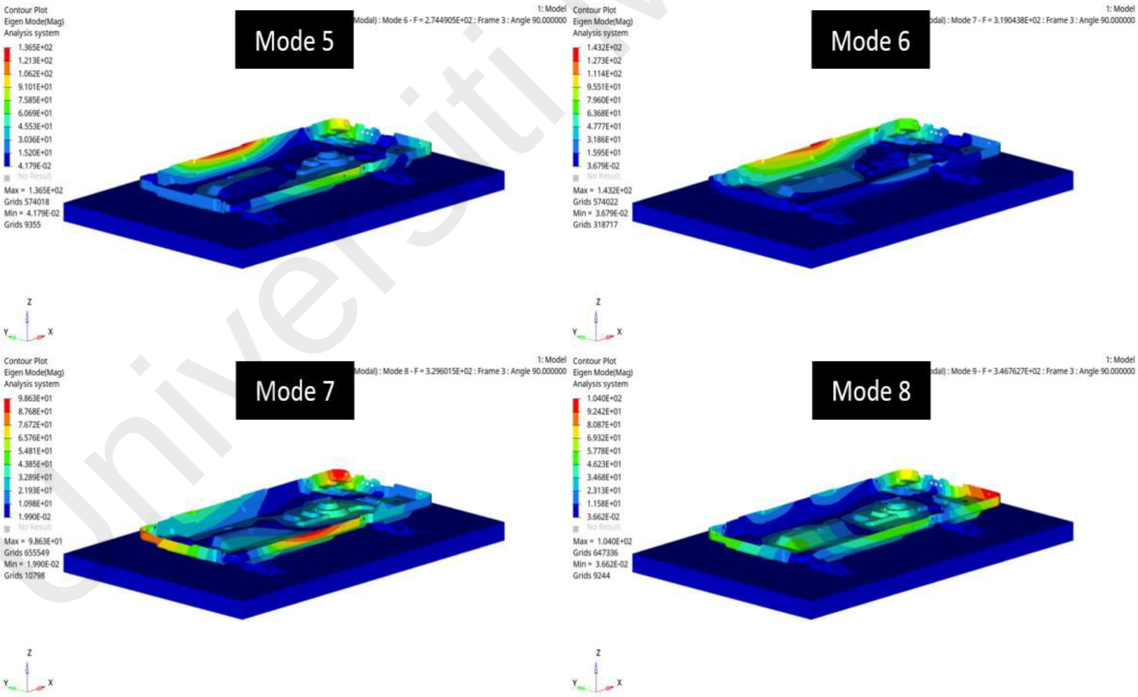

Figure 4.4: Mode shape (mode 5 – mode 8) from Altair's Optistruct®.

From the observation, the mode shape is very similar between the two solvers. The frequency difference between the solvers is as following (Table 4.1):

Table 4.1: Percentage difference between results from two solvers.

Mode	OS	CA	Delta, Δ
1	137.4Hz	138.6Hz	0.87%
2	167.8Hz	167.9Hz	0.06%
3	231.8Hz	233.8Hz	0.86%
4	242.7Hz	246.4Hz	1.52%
5	274.5Hz	279.7Hz	1.89%
6	319.0Hz	318.4Hz	0.02%
7	329.6Hz	331.6Hz	0.61%
8	346.8Hz	348.6Hz	0.52%

As predicted the frequency difference between the results from two solver is very low, with maximum error of only 1.89%.

By comparing the differences in vector of the mode shape through MAC plot shown in Figure 4.5, both solvers give exactly the same results, from mode 1 to mode 8.

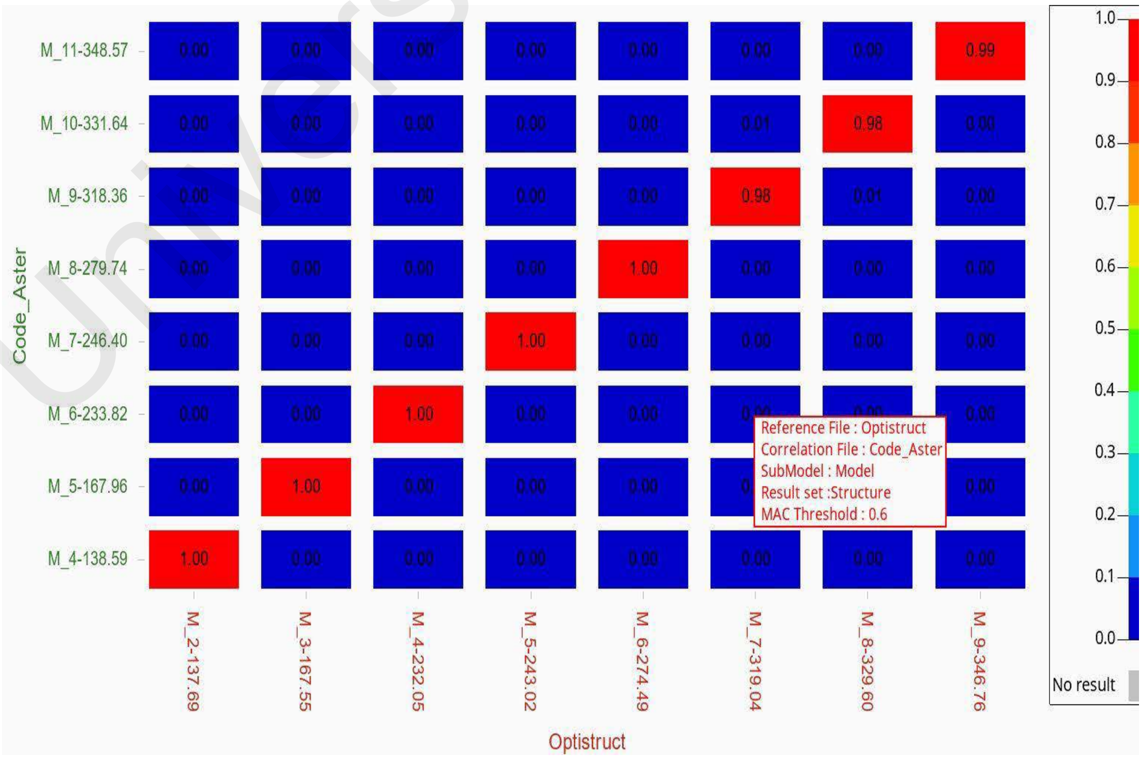

Figure 4.5: MAC correlation between mode shapes from both solvers.

4.1.2 Harmonic Response Analysis

The harmonic response from both solvers is extracted throughout the frequency band of 5Hz to 500Hz. Based on modal analysis from previous section, there is a mode at around 137Hz (first flexible mode) which the center location of the base panel is vibrating. When subjected to the shaker load with constant 1G acceleration, the acceleration and displacement FRF at the center node from both solvers shows that there is a very high peak on around 137Hz, as predicted. Figure 4.6 and Figure 4.7 shows the overlapping of acceleration and displacement response respectively from both solver in log scale.

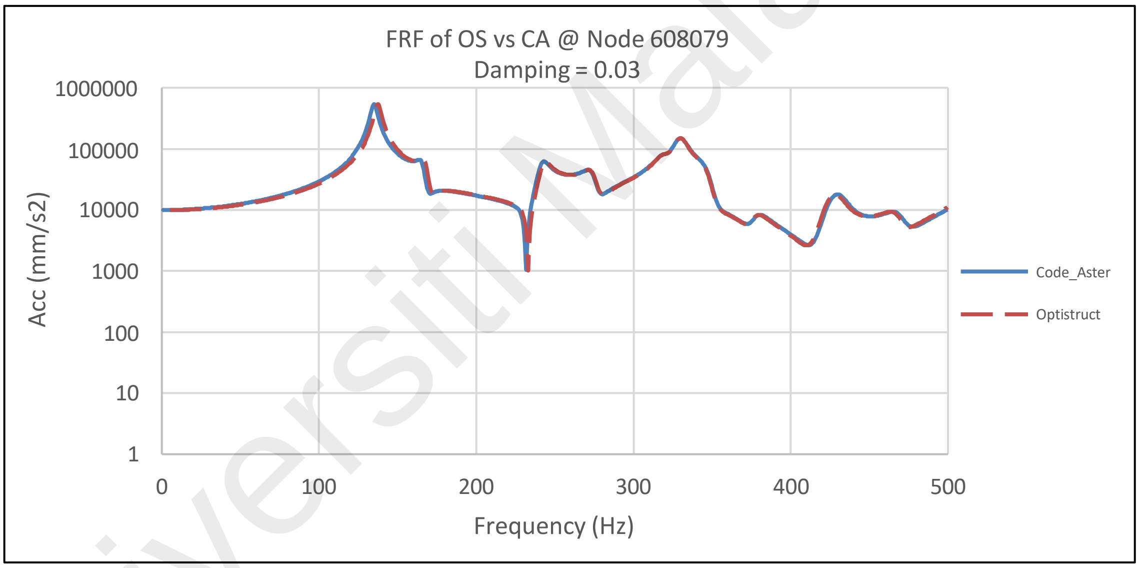

Figure 4.6: Acceleration FRF (log scale) from both solvers.

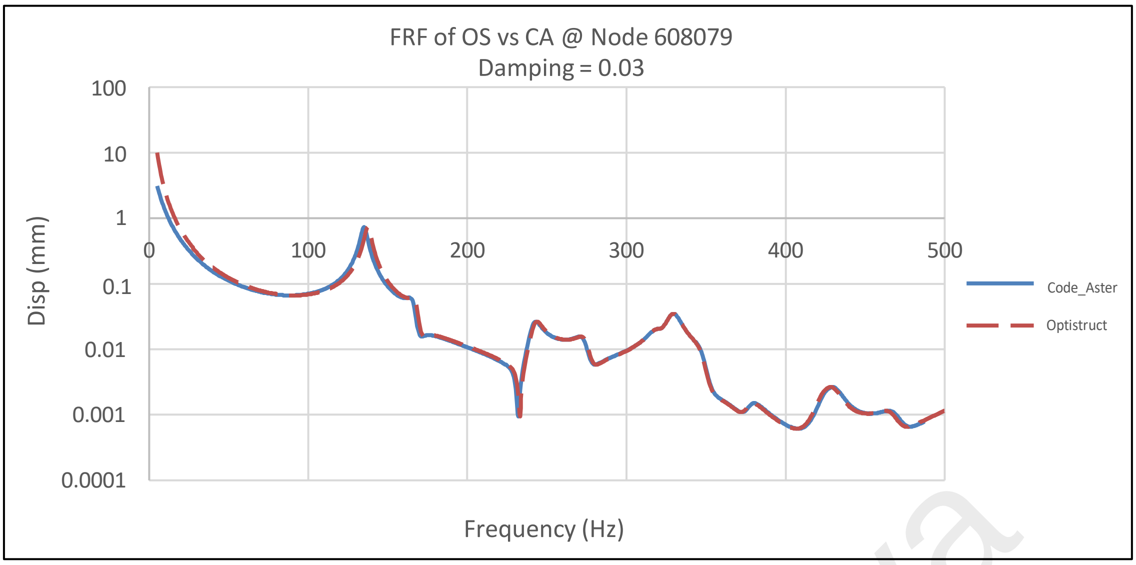

Figure 4.7: Displacement FRF (log scale) from both solvers.

The acceleration response contour from both solver is shown in Figure 4.8 and Figure 4.9.

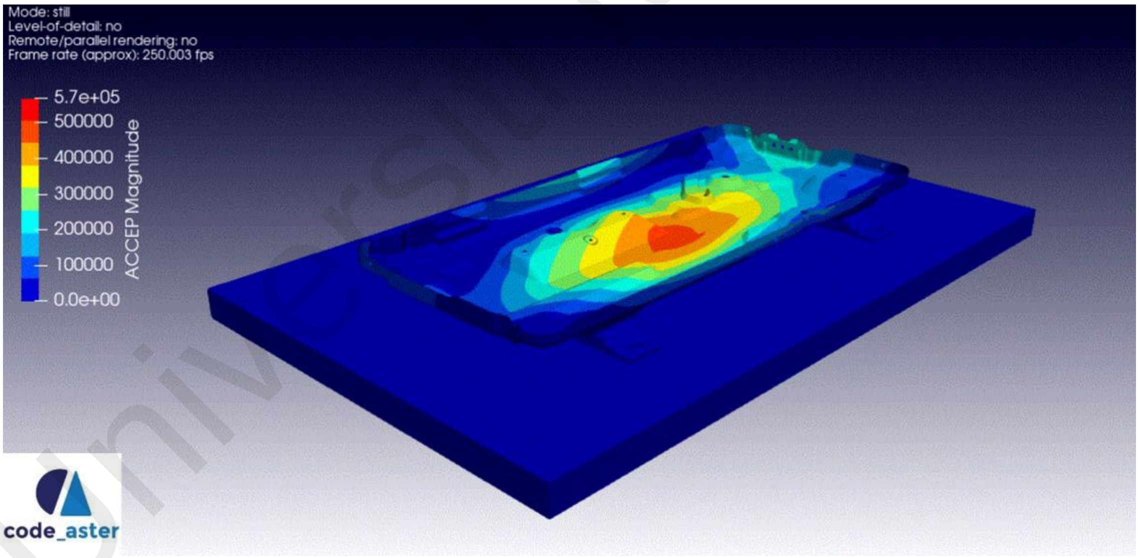

Figure 4.8: Harmonic response from Code_Aster® 2019 near 137Hz.

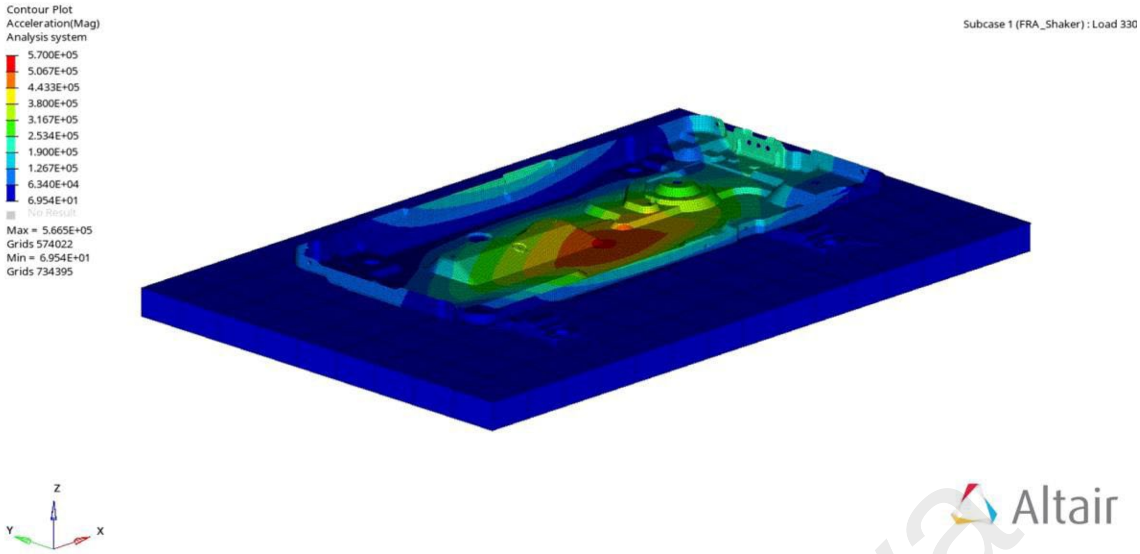

Figure 4.9: Harmonic response from Altair's Optistruct near 137Hz.

The response from both solvers is identical, thus the methodology (settings and keyword) used in Code_Aster® 2019 is correct. Objective number 1 has been achieved.

4.2 FEA Results (Normal Mode) Validation with Experimental Modal Analysis

As mentioned in section 3.4.1, three sets of roving hammer data have been acquired, with three different positions for accelerometer, which is point 11, point 10 and point 12 (center, upper center, and lower center). The FRF is shown in Figure 4.10, Figure 4.11and Figure 4.12 respectively.

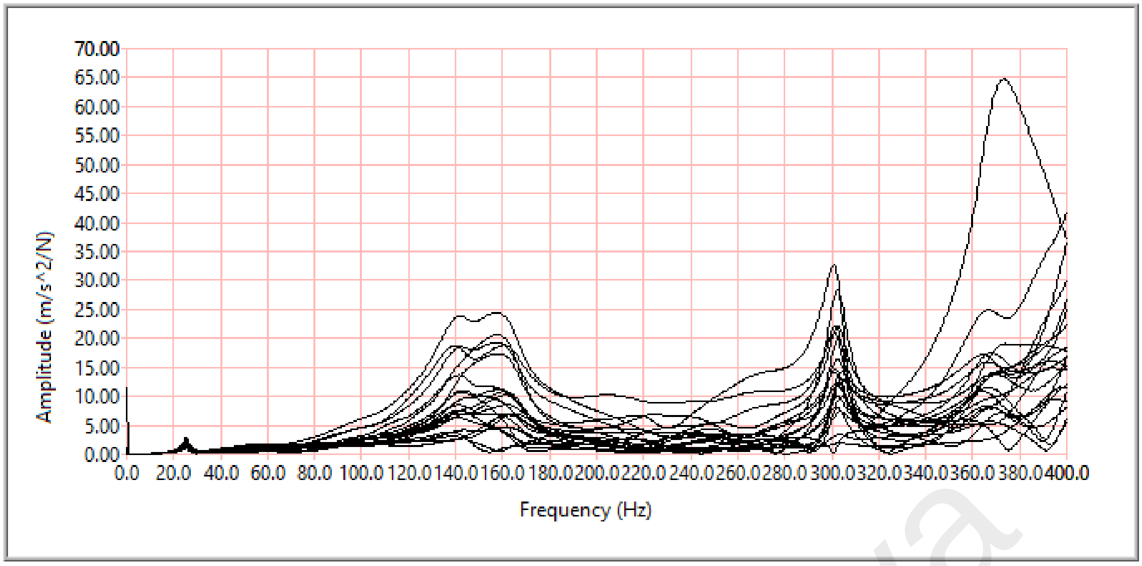

Figure 4.10: Point 11 accelerometer FRF.

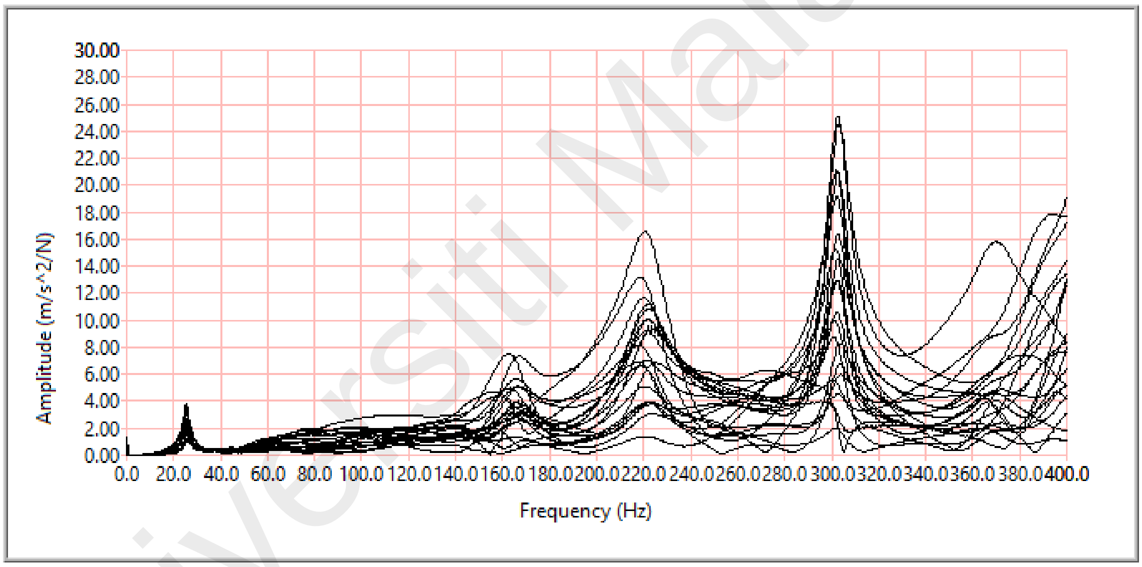

Figure 4.11: Point 10 accelerometer FRF.

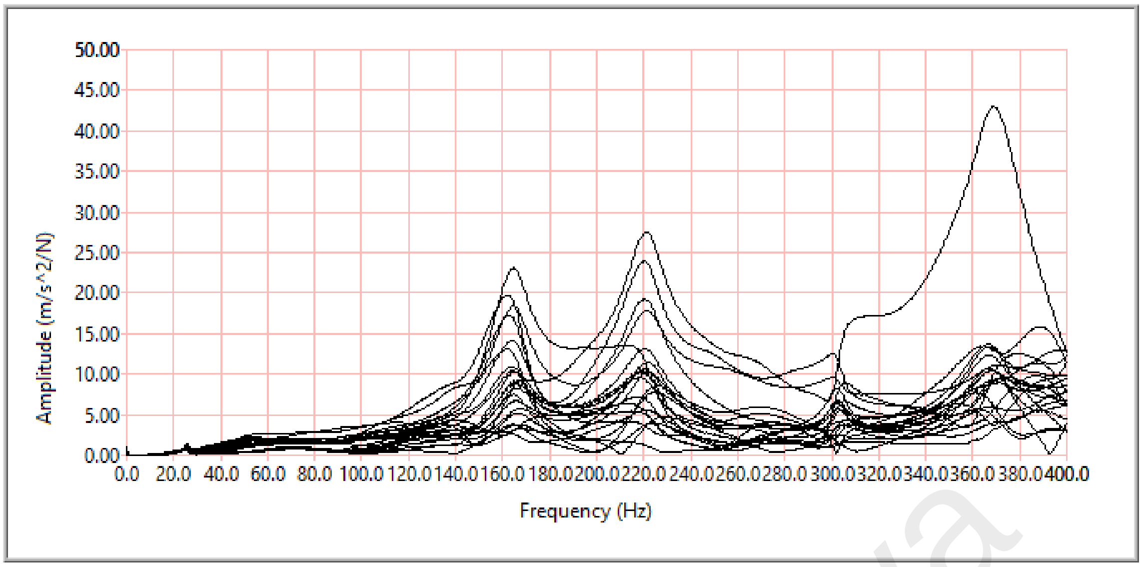

Figure 4.12: Point 12 accelerometer FRF.

Curve fitting algorithm is applied to all the FRF to extract the stable mode shape and natural frequency with damping coefficient and ready to be compared with the FEA results. Figure below show the comparison of mode shape from Code_Aster® 2019 and EMA. Figure 4.13 to Figure 4.17 shows the similarity of mode shapes between Code_Aster® and EMA, from mode 1 to mode 7 (exclusion from mode 4 and mode 6).

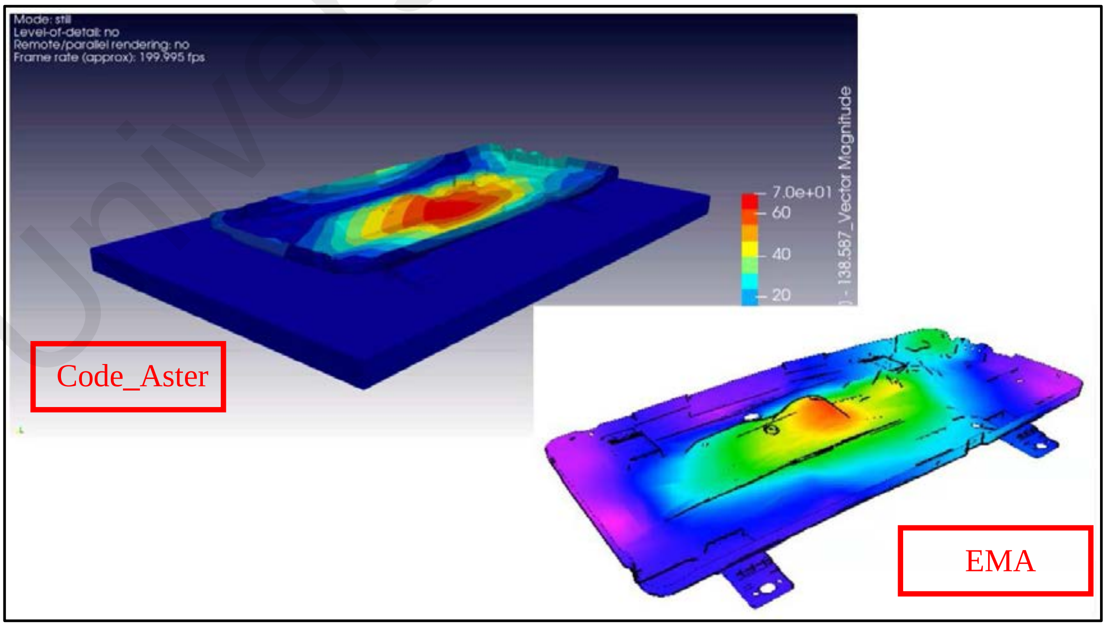

Figure 4.13: Mode 1 comparison between Code_Aster® and EMA.

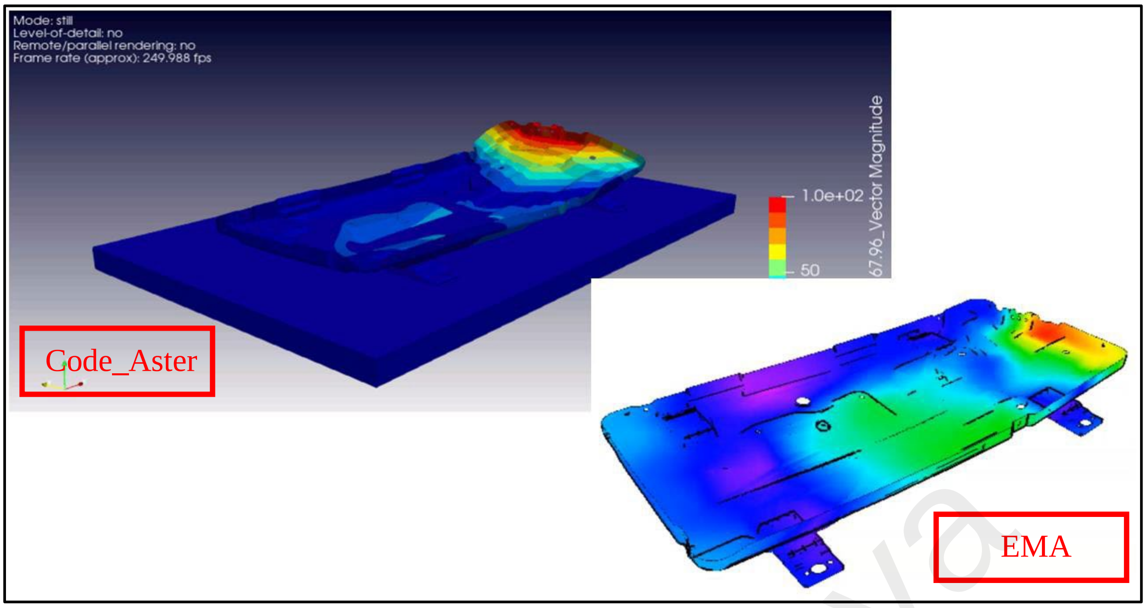

Figure 4.14: Mode 2 comparison between Code_Aster® and EMA.

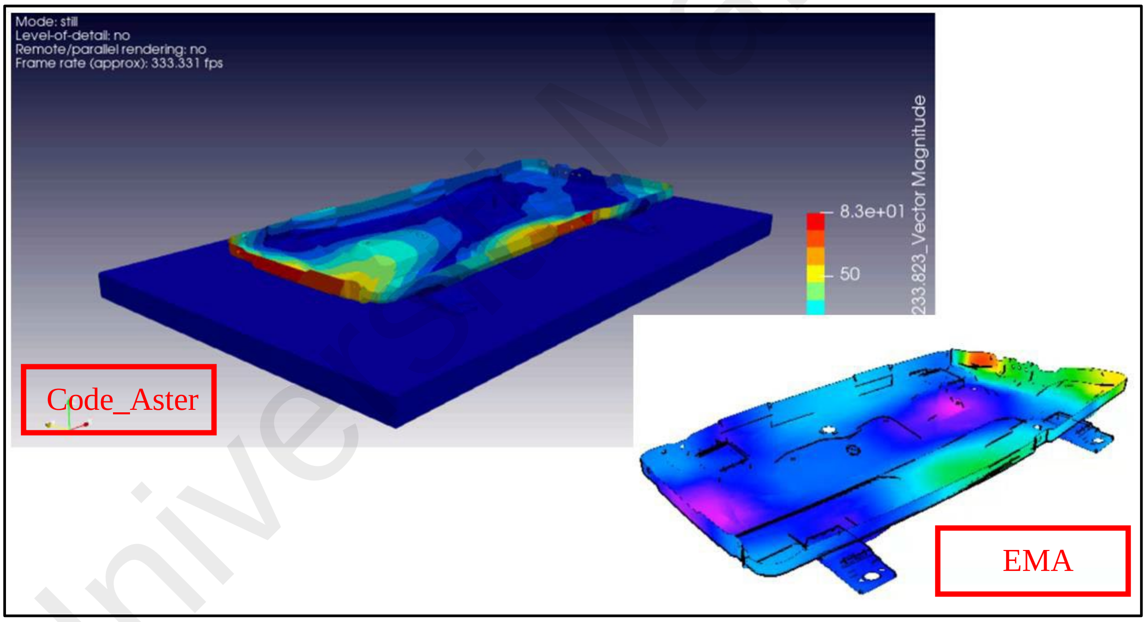

Figure 4.15: Mode 3 comparison between Code_Aster® and EMA.

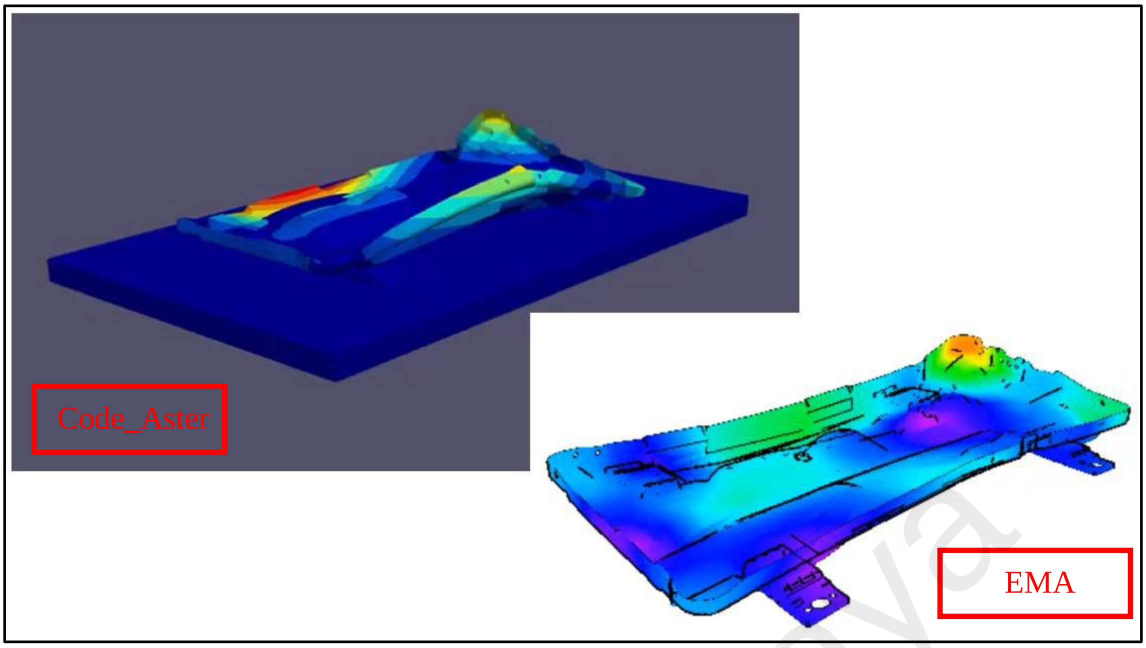

Figure 4.16: Mode 5 comparison between Code_Aster® and EMA.

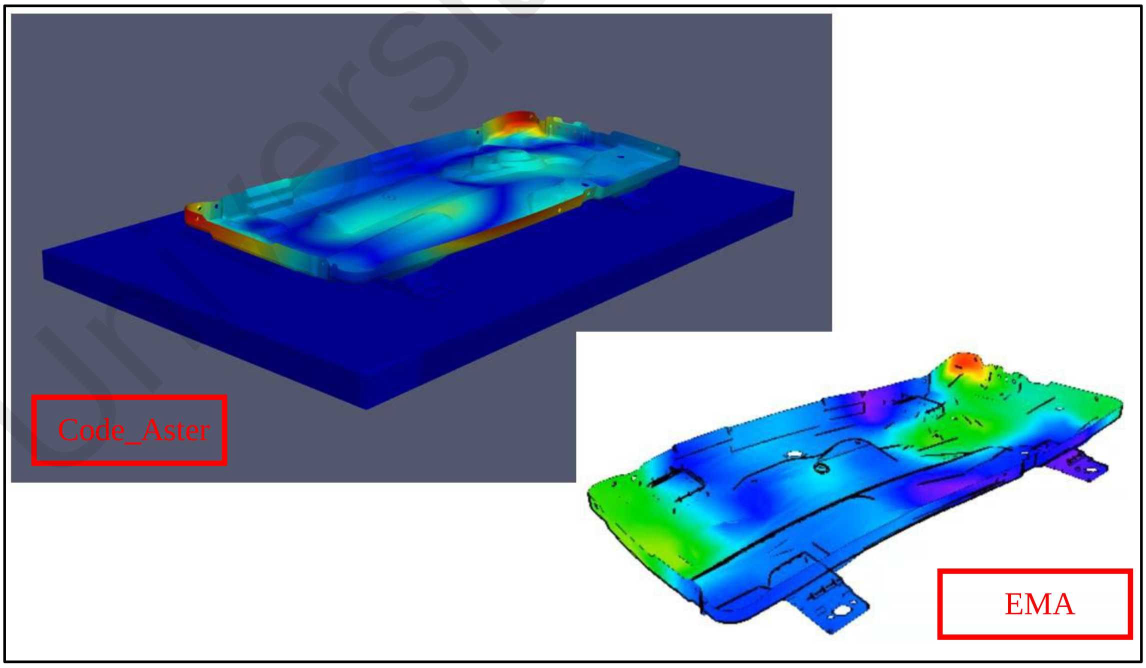

Figure 4.17: Mode 7 comparison between Code_Aster® and EMA.

Table 4.2: Frequency difference between Code_Aster 2019 and EMA.

Mode	EMA	CA	Delta, Δ
1	139.7Hz	138.6Hz	0.79%
2	165.5Hz	167.9Hz	1.45%
3	221.7Hz	233.8Hz	5.46%
4	-	246.4Hz	-
5	248.5Hz	279.7Hz	12.6%
6	-	318.4Hz	-
7	302.6Hz	331.6Hz	9.58%
8	-	348.6Hz	-

Table 4.2 shows the frequency difference between EMA and Code_Aster®. The maximumerror between EMA and Code_Aster® is about only 12.6%. The correlation is very good especially on the first 3 modes, with very similar mode shapes on both sides. In EMA, mode 4, mode 6 and mode 8 is missing might be due to insufficient excitation DOF (different direction of hammer excitation) and insufficient accelerometer data acquisition location. Including X and Y direction for impact hammer excitation and increase the accelerometer data acquisition location for example on the side skirting of the panel during the experiment will improve the result but will take longer time to setup and process.

Table 4.3: MAC correlation between Code_Aster® 2019 and EMA.

EMA	Code_Aster: Mode 1	Mode 2	Mode 3	Mode 5	Mode 7
Mode 7	0.005167	0.004595	0.00802	0.019083	0.818966
Mode 5	0.206333	0.049752	0.586132	0.681332	0.10879
Mode 3	0.125897	0.246553	0.51876	0.38931	0.021397
Mode 2	0.086464	0.593418	0.014724	0.016698	0.09694
Mode 1	0.83911	0.15992	0.122139	0.05466	0.00018

The similarity of mode shape vector between Code_Aster® and EMA were compared using MAC plot. As shown in Table 4.3, the similarity of mode shape in mode 1 and mode 7 is very high (>0.8) while the other 3 mode is lower than 0.8. From the mode shape animation, mode 2, 3, 5 having local mode at the side skirting of the panel, which the accelerometer does not measure. The other reason might be due to over stiffness of FEA modeling cause by the usage of RBE2 on connection between leg and panel and with the rigid table, the connection point is infinitely stiff, this will affect the overall mode shape of the structure. From the observation of the mode shape 2, 3, and 4, in simulation, the base leg and the area of welding between the leg and base panel is not moving at all (overly stiff), due to the usage of RBE2 connection. In EMA, the leg has slight vertical movement, which is true since the real boundary condition is not infinitely stiff. Improvement in FEA modeling technique such as modeling the screw component using 3D element or weld element for welding location with actual welding and screw properties can help with reducing the error and improving the MAC correlation.

4.3 FEA Results (FRA) Validation with Vibration Signature Data Acquisition

This section will be discussing the comparison of FRF between Code_Aster® and experiment, by the method described in section 3.3.2.2 and 3.4.2 respectively. The response at center node of the panel from sweep analysis is as following (Figure 4.18):

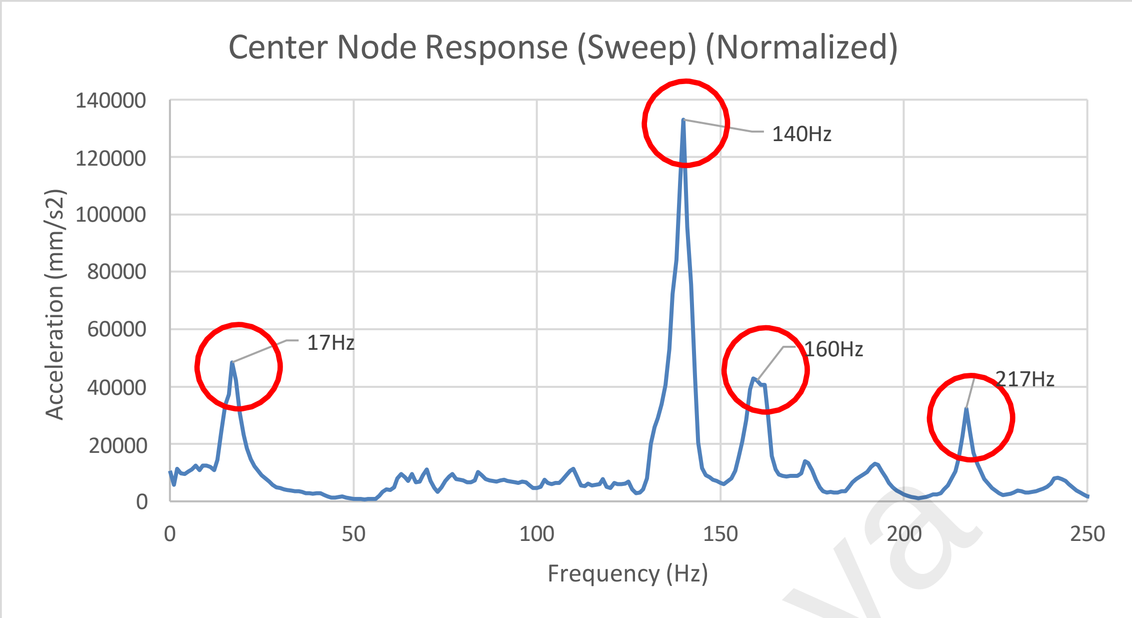

Figure 4.18: Response from experimental sweep analysis.

From the sweep analysis, the accelerometer is picking up some background noise from the component and shaker especially from 50Hz to 120Hz. Mode 1 (140Hz), 2 (160Hz) and 3 (217Hz) is shown as peaks, which is similar to those found in EMA FRF. The is anadditional response at 17Hz, which is missing from both FEA and EMA, might be due torigid body mode from the acrylic table.

By refining the measuring resolution around the resonance point and every 10Hz on non-resonance point, the background noise can be eliminated and the peak profile is more profound than before. The amplitude from the peak had also increased since the measurement from sweep analysis is not detailed enough to capture the true maximum value. The 4 peaks are still visible from Figure 4.19 for refine measurement around peak.

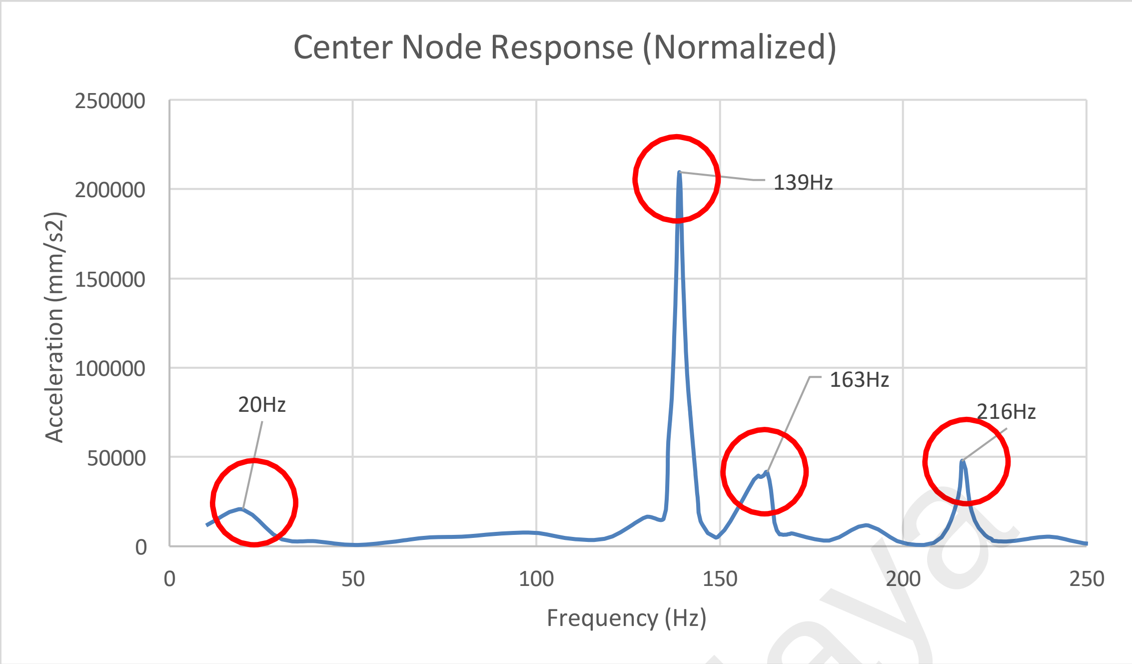

Figure 4.19: Experimental response from refine measurement at peak.

Figure 4.20 show the center node response results from Code_Aster®. By comparing Code_Aster® result with experiment, the magnitude is higher especially on 137Hz resonance. Since the FEA is using constant damping of 3%, it might be insufficient to dampen the response at 137Hz. The overall acceleration response spectrum especially atthe resonance is similar to the experiment, but with smoother data since FEA results does not contain any background noise.

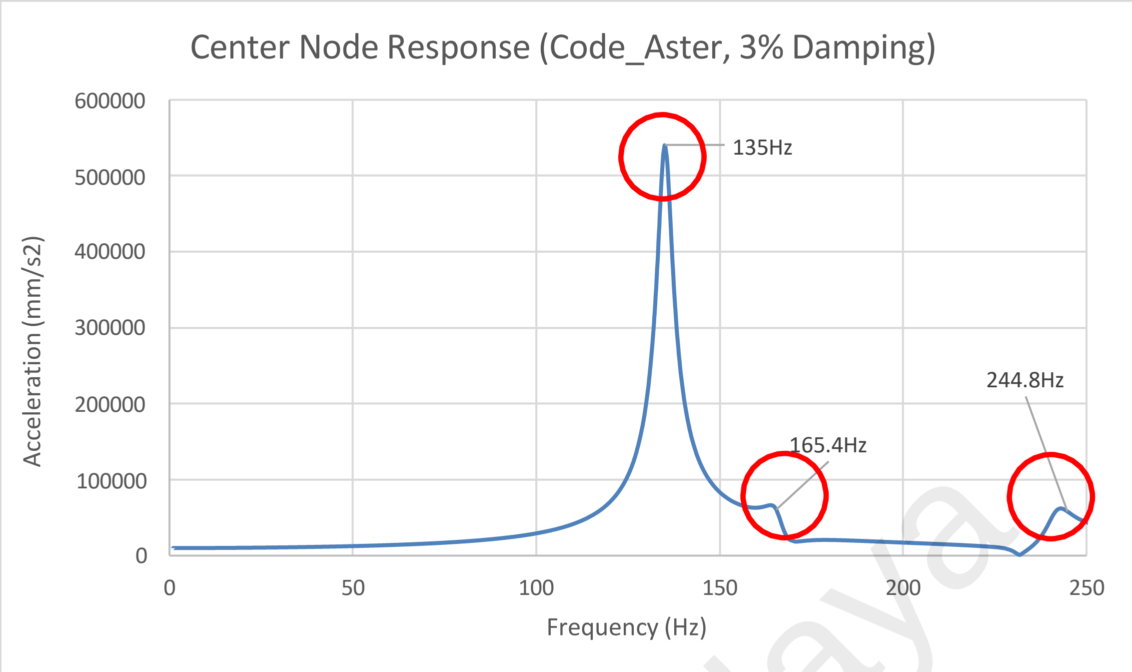

Figure 4.20: Response from Code_Aster®.

In Code_Aster®, direct method is unable to input frequency related damping data into the model, modal method can be used in the future as accuracy improvement to solve for a more accurate response. Damping coefficient extracted from EMA (Table 4.4) will be use, instead of constant 3% (general data for steel) that used in this project, so that the magnitude of the response will be similar to the experiment.

Table 4.4: Damping coefficient for each mode from EMA.

Mode	Frequency	Damping
1	139.7Hz	5.25%
2	165.5Hz	7.90%
3	221.7Hz	4.36%
4	-	-
5	248.5Hz	6.41%

CHAPTER 5: CONCLUSION AND RECOMMENDATION

5.1 Conclusion

With appropriate methodology, the three objectives of the projects have been achieved. The finite element modeling methodology and technique for vibration analysis (normal mode analysis and harmonic response analysis) in Code_Aster® 2019 has been explored and validated. The rigid body element (RBE2), the material properties keyword, element properties keyword and boundary condition setup proven to be appropriate and correct in Code_Aster® 2019.

For normal mode analysis, the mode shape and natural frequency are identical between two solvers, as the maximum difference in natural frequency was only 1.89%, and the MAC correlation are having 1.0 across all 8 modes. While applying 3% damping coefficient to the base panel, there is no difference in acceleration and displacement response between the two solvers (the response spectrum of same nodes is overlapping between solvers) from the harmonic response analysis by using direct method.

The maximum error between EMA and Code_Aster® 2019 results was only 12.6% at mode 5. With the correct mode shape and natural frequencies, harmonic response function will be similar as it is calculated based on the dynamic properties of the structure. Since Code_Aster® 2019 does not have the option or keyword for acceleration harmonic input, the mass of the structure must be calculated to convert acceleration into force input. Nevertheless, Code_Aster® results also shows good matching on all resonance peaks with the experimental response spectrum. Improvement can be made on the simulation model such as replacing RBE2 to 3D element with screw and weld properties for reducing overall stiffness and input the correct damping factor from EMA into the model, better accuracy can be achieved while comparing the response magnitude.

This study shows that Code_Aster® is a very powerful yet capable solver with high reliability on vibration analysis (normal mode with harmonic response analysis) and it issuitable for the usage in actual product development cycle.

5.2 Future Recommendations

On the successful of this project, there are still many ways that the methodology can be improve while helping to shorten the product cycle development time in DRDM. Firstly, full model (outdoor unit) transportation simulation can be developed by continuing using the method shown in this project, as shown in Figure 5.1. The methodology can be extended throughout for the whole product range from DRDM like indoor unit with different horsepower, rooftop unit, or air handling unit (AHU) etc. Secondly, the efficiency of the method can be improved to shorten simulation time such as implementation of the pre to post process of FEA on in house HPC, by utilizing all the available cores and computing power with parallelism capabilities from Code_Aster®. Thirdly, the repeating process such as material and element property assignment, which taking a lot of time can be shorten by implementing Python scripting to automate some of the input for keyword in the command file of Code_Aster® as suggested by the study of EDF (EDF, 2021). Finally, accuracy improvement on the FEA results can be done by implementing a more precise and accurate input for such as material data, boundary conditions and correct damping factor.

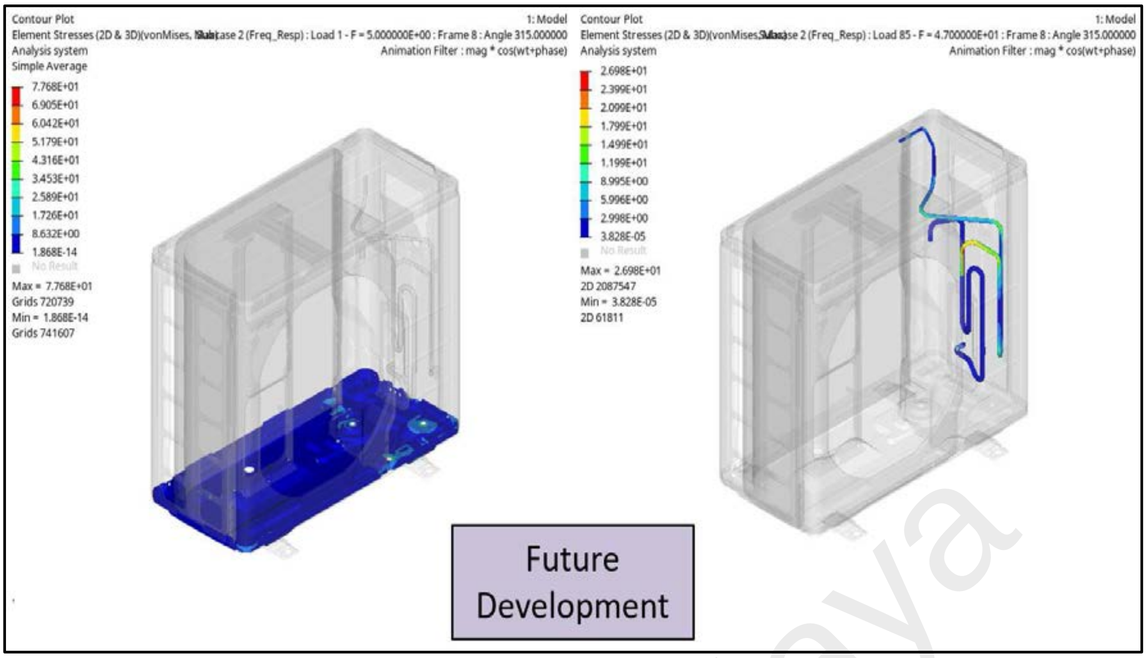

Figure 5.1: Full unit transportation simulation by using Code_Aster® (future FEA method development).

5.3 Sustainability

When using vibration FEA itself, the development time and cost of the product cycle has been greatly reduced (already factored the manpower and costs of simulation software). Code_Aster® is just a bonus since it is fully open-source and does not require any licensing fees. The scalable capability of Code_Aster® is a huge up point especially for large model problem since it can utilize the computing power from all the available cores on HPC, this greatly reduce the costs (time and licensing fees), the only limitation is only from the hardware itself.

Vibration FEA is not limited only to transportation problem, it can be used to troubleshoot resonance problem, acoustic problem or predevelopment prototyping structural integrity check. If the results from vibration FEA is accurate and reliable, it can helps engineer to solve thousands of development and predevelopment issues. All by using Code_Aster®, the free and powerful FEA solver.

The methodology described here can be pass on to other CAE engineers so that they can learn to use and understand the principal of open-source software. CAE engineers can also give training to development engineer or testing engineer on the knowledge of vibration FEA and Code_Aster®, so that they are capable to do simple vibration FEA using Code_Aster®. By sustaining the simulation culture in DRDM, it will help on development cycle and countless research project in both short term and long run especially in a R&D center.

5.4 Complexity

The learning curve of Code_Aster® is very steep. Since it does not have a user-friendly UI and the user manual are direct translated from French, it is very hard for user to master the skills compared to commercial software. There is also lack of software support team, which when the user facing a bug or unsolved issue, they can only post the problem on Code_Aster® official forum and waiting the other users to provide aid. The keyword of Code_Aster® is mainly construct from French; it is sometimes very hard to interpret the function of that keyword. It is a little bit buggy on the interface for Code_Aster® 2019 Windows version, as it is the first full version release for Windows machine. However, the original version for Linux OS is very stable. User is recommended to have some knowledge of FEA in theory and commercial solver before using Code_Aster®.

5.5 Lifelong learning

The open-source vibration FEA methodology from this project can be serve as a lifelong learning for CAE engineers and even design engineers. The knowledge on finite element modeling, material behavior, dynamic behavior and troubleshooting for vibration problem is a vital skill for engineers. The development and pioneering in open-source FEA solver methodology will help DRDM to save costs, especially in annual software licensing fees. The steep learning curve of an open-soft FEA software serve to further strengthen the skillset and theoretical knowledge, whether it's on mechanics of material, vibration theory and application (experiment and simulation), finite element method, of a CAE engineer. This project definitely opens up the possibility of using open-source solver for various structural problem apart from vibration such as linear static, explicit dynamic, buckling, and even optimization. Much to be explore and learn by using Code_Aster®.

REFERENCES

Antonutti, R., Peyrard, C., Incecik, A., Ingram, D., & Johanning, L. (2018). Dynamic mooring simulation with Code_Aster with application to a floating wind turbine. *Ocean Engineering, 151*, 366-377. doi:https://doi.org/10.1016/j.oceaneng.2017.11.018

Bai-Mao, L., Van-Xuan, T., Xiang-Hong, H., & Qian, L. (2015). Critical Plane Orientation Under Biaxial Fatigue Loading Conditions. *Procedia Engineering, 133*, 72-83. doi:https://doi.org/10.1016/j.proeng.2015.12.625

Brandt, A. (2011). *Noise and Vibration Analysis*. John Wiley & Sons Ltd, The Atrium, Southern Gate, Chichester, West Sussex, PO19 8SQ, United Kingdom: John Wiley & Sons, Ltd.

DePalma, A. (Producer). (2011). FEA: Only as Good as the Operator. Retrieved from https://www.asme.org/topics-resources/content/fea-only-as-good-as-the-operator

DRDM. Retrieved from https://www.daikinmalaysia.com/drdm/company-profile/

DRDM. (2019). Vibration Test. In *TP/RD/F-03.003(00)* (pp. 3). DRDM: DRDM.

Durand, C. (2007). Free Software for Computatinal Mechanics: EDF's Choice. Retrieved from https://www.code-aster.org/UPLOAD/DOC/Presentation/2007_nafems.pdf. from NAFEMS https://www.code-aster.org/UPLOAD/DOC/Presentation/2007_nafems.pdf

EDF. Code_Aster. In www.code-aster.org (Ed.), (pp. 2): EDF.

EDF. (2021a). Code_Aster Documentation. Retrieved from https://www.code-aster.org/spip.php?rubrique19

EDF. (2021b). Development in Code_Aster. Retrieved from https://www.code-aster.org/UPLOAD/DOC/Formations/09-command.pdf. from EDF https://www.code-aster.org/UPLOAD/DOC/Formations/09-command.pdf

EDF. (2021c). Licenses, Code_Aster. Retrieved from https://www.code- aster.org/spip.php?article306

EDF. (2021d). Modal Analysis. Retrieved from https://www.code-aster.org/UPLOAD/DOC/Formations/01-modal-analysis.pdf. from EDF https://www.code-aster.org/UPLOAD/DOC/Formations/01-modal-analysis.pdf

EDF. (2021e). Presentation of the reference machine. Retrieved from https://www.code-aster.org/spip.php?article252. https://www.code-aster.org/spip.php?article252

EDF. (2021f). Square plate meshed in shell elements: modal computation. Retrieved from https://www.code-aster.org/spip.php?article252. https://www.code-aster.org/spip.php?article252

EDF. (2021). Methods Python of access to the objects Aster. Retrieved from https://www.code-aster.org/doc/default/en/man_u/u1/u1.03.02.pdf. from EDF https://www.code-aster.org/doc/default/en/man_u/u1/u1.03.02.pdf

Formulation of the Equations of Motion. (2010). In M. Petyt (Ed.), *Introduction to Finite Element Vibration Analysis* (2 ed., pp. 1-18). Cambridge: Cambridge University Press.

FreeBSD. (2021). Why you should use a BSD style license for your Open Source Project. Retrieved from https://freebsd.org/doc/en_US.ISO8859-1/articles/bsdl-gpl/article.html#:~:text=In%20contrast%20to%20the%20GPL,project's%20or%20company's%20needs%20change. https://freebsd.org/doc/en_US.ISO8859-1/articles/bsdl-gpl/article.html#:~:text=In%20contrast%20to%20the%20GPL,project's%20or%20company's%20needs%20change.

G. Banwell, S. M., S. Rothberg, J. Roberts. (2012). Using experimental modal analysis to validate a finite element model of a tennis racket. *Procedia Engineering, 34*.

GNU. (2021a). The GNU General Public License. Retrieved from https://www.gnu.org/licenses/licenses.html#GPL

GNU. (2021b). Overview of the GNU System. Retrieved from https://www.gnu.org/gnu/gnu-history.html. from GNU https://www.gnu.org/gnu/gnu-history.html

Gülbahçe, E., & Çelik, M. (2021). Experimental modal analysis for the plate structures with roving inertial shaker method approach. *Journal of Low Frequency Noise, Vibration and Active Control, 41*(1), 27-40. doi:10.1177/14613484211039323

Gupta, B. V. R. (1985). Finite Element Free Vibration Analysis of Damped Stiffened Panels. *Computers & Structures, 24, No.3*, 485-486.

Han, L. I. U., Dominique, G., & Jiesheng, M. I. N. (2019). CODE_ASTER – AN EDF OPEN-SOURCE SOFTWARE TO SOLVE ADVANCED STRUCTURAL PROBLEMS. *The Proceedings of the International Conference on Nuclear Engineering (ICONE), 2019.27*, 1811. doi:10.1299/jsmeicone.2019.27.1811

J.P.Aubry. (2021). *Beginning with Code_Aster, A Practical Intro to FEM using Code_Aster and Gmsh.*

Jimin He, Z.-F. F. (2011). *Modal Analysis*. Oxford, England: Butterworth-Heinemann.

M P, P., Yaacob, S., Abdul Majid, M. S., & Krishnan, P. (2013). *Steel Plate Damage Diagnosis using Probabilistic Neural Network.*

M. Sergio, T. A. (2015). *Pleasure Vessel Vibration and Noise Finite Element Analysis*. Paper presented at the 6th Beta CAE International Conference, Thessaloniki, Greece. https://www.beta-cae.com/events/c6pdf/7A_3_DAPPOLONIA.pdf

M.H. Fouladi, Z. X. P., K.H. Yap. (2014). An Integrated Finite Element Approach To Model Brazing of Copper Tubes. *Journal of Engineering Science and Technology*(EURECA 2014 Special Issue April), 11.

Moaveni, S. (2015). *Finite Element Analysis, Theory and Application with ANSYS* (Fourth ed.): Pearson Education Limited.

N.S Gokhale, S. S. D., S.V Bedekar, A.N. Thite. (2008). *Practical Finite Element Analysis* [1st]. In Altair (Ed.), (pp. 445).

Paige, C. C. (1980). Accuracy and effectiveness of the Lanczos algorithm for the symmetric eigenproblem. *Linear Algebra and its Applications*, *34*, 235-258. doi:https://doi.org/10.1016/0024-3795(80)90167-6

Pástor, M., Binda, M., & Harčarik, T. (2012). Modal Assurance Criterion. *Procedia Engineering*, *48*, 543–548. doi:10.1016/j.proeng.2012.09.551

Petyt, M. (2003). *Introduction to Finite ELement Vibration Analysis*. In C. U. Press (Ed.), (pp. 574).

Rao, S. S. (2011). *Mechanical Vibration* (5th ed.). 1 Lake Street, Upper Saddle River, NJ 07458: Prentice Hall.

RedHat. (2019). What is the Linux kernel? Retrieved from https://www.redhat.com/en/topics/linux/what-is-the-linux-kernel. https://www.redhat.com/en/topics/linux/what-is-the-linux-kernel

S.H. Lee, S. M. R., W.B. Jeong. (2012). Vibration analysis of compressor piping system with fluid pulsation. *Journal of Mechanical Science and Technology*, *26*(12), 7. doi:10.1007/s12206-012-0891-8

Sabet, F. A., Koric, S., Idkaidek, A., & Jasiuk, I. (2021). High-Performance Computing Comparison of Implicit and Explicit Nonlinear Finite Element Simulations of Trabecular Bone. *Computer Methods and Programs in Biomedicine*, *200*, 2. doi:https://doi.org/10.1016/j.cmpb.2020.105870

Shen, Y. (2021). *Reduced order models for geometrically nonlinear vibrations of thin structures.* (PhD). Institut Polytechnique De Paris,

Stallman, R. (1983). New Unix Implementation. Retrieved from https://groups.google.com/g/net.unix-wizards/c/8twfRPM79u0/m/1xlglzrWrU0J,%20Sept.%201983. https://groups.google.com/g/net.unix-wizards/c/8twfRPM79u0/m/1xlglzrWrU0J,%20Sept.%201983.

top500.org. (2021). OPERATING SYSTEM FAMILY / LINUX. Retrieved from https://www.top500.org/statistics/details/osfam/1/. https://www.top500.org/statistics/details/osfam/1/

V. Chonhenchob, S. P. S., J.J. Singh, S. Sittipod, D. Swasdee, S. Pratheepthinthong. (2010). Measurement and analysis of truck and rail vibration levels in Thailand. doi:10.1002/pts.881

Venugopal, D., Pinninti, R. R., & Komaraiah, M. (2014). HARMONIC ANALYSIS OF ROTARY COMPRESSOR USING FEA. *4621*.

Ye, N., Su, C., & Yang, Y. (2021). Free and Forced Vibration Analysis in Abaqus Based on the Polygonal Scaled Boundary Finite Element Method. *Advances in Civil Engineering, 2021*, 7664870. doi:10.1155/2021/7664870